

Supplement of Atmos. Chem. Phys., 20, 15037–15060, 2020
<https://doi.org/10.5194/acp-20-15037-2020-supplement>
© Author(s) 2020. This work is distributed under
the Creative Commons Attribution 4.0 License.



Supplement of

The potential role of organics in new particle formation and initial growth in the remote tropical upper troposphere

Agnieszka Kupc et al.

Correspondence to: Agnieszka Kupc (agnieszka.kupc@univie.ac.at)

The copyright of individual parts of the supplement might differ from the CC BY 4.0 License.

S1. The MAIA box model: binary neutral and ion-assisted nucleation

The Model of Aerosols and Ions in the Atmosphere (MAIA; Lovejoy et al., 2004; Kazil et al., 2007) describes the oxidation of SO_2 to gaseous H_2SO_4 , the nucleation of neutral and negative $\text{H}_2\text{SO}_4\text{-H}_2\text{O}$ clusters, aerosol growth by sulfuric acid condensation/evaporation, and particle coagulation. The production rate of H_2SO_4 is calculated assuming that the reaction of SO_2+OH is the rate limiting step of the oxidation of SO_2 to form H_2SO_4 (Lovejoy et al., 1996). Nucleation is described with laboratory thermochemical data for H_2SO_4 and H_2O uptake and loss by small neutral and negative clusters (Curtius et al., 2001; Lovejoy and Curtius 2001; Froyd and Lovejoy, 2003; Hanson and Lovejoy, 2006). The thermochemical data for uptake and loss of H_2SO_4 and H_2O by large sulfuric acid aerosol ($\gg 5$ sulfuric acid molecules) originate from the liquid drop model and H_2SO_4 and H_2O vapor pressures over bulk solutions. These were calculated with a computer code (provided by S. L. Clegg, personal communication, 2007) which adopts experimental data from Giaque et al. (1960) and Clegg et al. (1994). The thermochemical data for intermediate sized particles are a smooth interpolation of the data for small and large aerosol particles. The model uses 20 linear bins in which H_2SO_4 content increases by 1 molecule per bin, and 50 geometric bins in which H_2SO_4 content increases by a factor of 1.45 per bin, covering a dry (312.15 K, 10% RH) particle diameter range of $\sim 0.5\text{--}800$ nm.

The model operates along trajectories with changing pressure, temperature and relative humidity (Kazil et al., 2007, Weigel et al., 2011) in the temperature range 180-320 K and the relative humidity range 1-101 %, which includes upper troposphere conditions. MAIA parametrizes the OH diurnal cycle as a half-sine centered around noon with a prescribed noon OH concentration, while setting the nighttime OH concentration to 0. The length of the daytime period is calculated from the day of year and location. The MAIA simulations are initialized with the SO_2 gas phase mixing ratio, an Aitken and an accumulation mode of given geometric mean diameter, geometric standard deviation, and surface area concentration. Atmospheric ionization rates due to galactic cosmic rays are calculated as a function of latitude, altitude, and solar cycle phase by a model of energetic particle transport in the Earth's atmosphere (O'Brien, 2005). The transformation between geographic and geomagnetic coordinates is calculated with GEOPACK (<http://geo.phys.spbu.ru/~tsyganenko/modeling.html>) and the International Geomagnetic Reference Field 12 coefficients (<https://www.ngdc.noaa.gov/AGA/vmod/igrf.html>).

S1.1 MAIA input data

Measured, estimated, and calculated inputs needed to initialize the MAIA box model are given in Table S1. MAIA was configured to use Aitken and accumulation mode geometric mean diameters, standard deviation, and aerosol surface area concentrations corresponding to these two modes. Each input in Table S1 represents the initial conditions present at the start of the simulation (t_0) and includes pre-existing background aerosol; these background particles compete with newly formed particles for condensable vapors. Hence, condensing vapor in the gas phase can contribute both to the formation of new particles and growth of the pre-existing background aerosol.

We expect the output of MAIA model to be sensitive to the temperature dependence of nucleation rates, SO_2 mixing ratio, OH concentration, and the pre-existing background aerosol into which the convective outflow is mixed.

The variability of the simulated aerosol size distribution to various initial conditions was examined by conducting several sensitivity simulations (Table S1) on SO₂, OH, size distribution (background aerosol).

MAIA does not explicitly account for the mixing of highly scavenged air detraining from convective outflow with surrounding, upper tropospheric (UT) air with a more aged aerosol (e.g., Weigel et al., 2011). We have undertaken sensitivity studies that vary the pre-existing background aerosol used as initial input parameter (Table S1). We assume volume mixing ratios of SO₂ between 1 and 100 ppt, which are based on ATom 4 observations for SO₂ and literature data for NH₃ and organic precursors.

Upper tropospheric OH concentrations over the remote Pacific Ocean range between 1-4.3x10⁶ molecule cm⁻³ as determined from in situ measurements during ATom, and are consistent with literature values (e.g. Seinfeld and Pandis, 2006). We set the OH concentration for a solar zenith angle of 0° to 3x10⁶ molecule cm⁻³ and parameterized the OH diurnal cycle. In MAIA OH is parameterized as a half-sine centred around noon where the mixing ratio of nighttime OH concentration is assumed to be 0 (Kazil et al., 2007; Weigel et al., 2011). The length of the daytime period is calculated for the date, altitude, latitude, and longitude of the back trajectories. The OH concentration along the trajectory and the resulting production rate of H₂SO₄ are then calculated. We ignore possible enhanced OH due to cloud reflectivity in the vicinity of convective outflow. MAIA box model simulation results are presented in Table S4.

S2. TOMAS model: smoothing of the simulated size distribution

We follow a top hat method for transferring mass between size sections during condensation/evaporation, as described by Stevens et al. (1996) and Hodshire et al. (2019). After a top hat representation of the distribution is constructed for each bin, then these are translated according to the analytic solution. The translated top hats are then remapped to the bins. However, it may happen that a bin will empty out into an adjacent larger bin, creating oscillations of number/mass within the diameter space. To reduce the noise created by these oscillations, we transfer mass between adjacent bins in post-processing by moving number to make the mass: number ratio in each bin equal to the geometric mean of the bin mass:number limits. This method conserves total number and mass. The bin emptying will not go away with a shorter timestep, and it is a common feature of 2-moment microphysics schemes that use a top-hat or moving-center approach for condensational growth. We do not smooth MAIA output.

An example of the smoothed and not-smoothed TOMAS size distribution and the corresponding NME values are presented in Fig.S14.

Table S1. Ranges of parameters used for sensitivity studies in MAIA box model. Values varied to match the observed size distribution in *italic*).

Parameter		Initial value used
Abbreviation	Unit	MAIA
SO ₂ *	pptv	<i>1-100</i>
H ₂ SO ₄	molecule cm ⁻³	<i>1 x10³</i>
OH at solar zenith angle of 0°	molecule cm ⁻³	<i>1x10⁶, 3x10⁶, 4.3x10⁶</i>
OH at night		<i>0</i>
Ionisation rate** (ion pair production rate)	cm ⁻³ s ⁻¹	<i>95-115</i>
Time since CI	hours	<i>0.4-10.5</i>
Background pre-existing aerosol: surface area (S _{area}) of the Aitken and accumulation mode	μm ² cm ⁻³	<i>S_{area}, S_{area}x2, S_{area}/2, S_{area}=0</i>
Geometric mean diameter	nm	<i>Vary from case to case</i>

* SO₂ measured on ATom 4 only

** at STP: 273.15 K and 1013 hPa

Table S2. Number of simulated cases (out of total 32) for which the temperature along the trajectory was within and out-of-the temperature range of the nucleation scheme used in TOMAS model.

Scheme	T regime, K	No of cases within T regime of the scheme	% of cases within T regime of the scheme	No of cases below min. T of the scheme
VEHK	230.15 - 305.15	14	44	18
NAPA	240 - 300	7	22	25
RIC	270 - 310	0	0	32
DUN	208 - 292	32	100	0

VEHK: neutral binary nucleation using Vehkamäki et al. (2002) scheme

RIC: neutral nucleation with biogenic oxidation products (Riccobono et al., 2014), updated by temperature dependence according to Yu et al. (2017)

NAPA: neutral ternary nucleation (Napari et al., 2002)

DUN: ion-induced and neutral nucleation scheme (Dunne et al., 2016) with both neutral and ion-induced binary and neutral and ion-induced ternary pathways

Table S3. Number of identified cases of recent NPF associated with CI for the Atlantic between 30° N and 30° S latitude that meet the following criteria: T <260 K, CI >95%, and modal peak diameter <12 nm.

ATom mission	Number of cases meeting criteria listed above		
	Trajectory age <1 day	Trajectory age 1-2 days	Trajectory age 2-3 days
1	6	5	1
2	18	38	41
3	20	29	48
4	16	5	17
Total	60	77	67

Table S4. Summary of the best NME results for each of the simulated cases and nucleation schemes undertaken at OH equal 3×10^6 molec cm^{-3} along with corresponding figure number presenting detailed results. Simulation runs where other initial conditions were varied are also indicated. Best NME values of all schemes are in bold and shaded.

Model run ID	Corresponding figure	Time since CI, hrs	Best NME for each of the nucleation schemes simulated											Studies on additionally varied model input parameters (e.g. OH, SD, F_{orgnuc})	
			TOMAS												MAIA
ATom2 cases			VEHK	VEHK +org _{gr}	RIC	NAPA	NAPAt	NAPA +org _{gr}	NAPAt +org _{gr}	DUN NH ₃ =0	DunNH ₃ =0 +org _{gr}	DUN	DUN +org _{gr}	BIN _{n+ch}	
sd486	Fig. 6	7.3	0.48	0.41	0.02	0.42	0.39	0.38	0.17	0.37	0.30	0.34	0.04	0.73	Figure S46-54
sd390	Fig. S12	1	0.90	0.61	0.26	0.32	0.90	0.31	0.30	0.92	0.92	0.49	0.34		
sd391	Fig. S13	0.66	0.94	0.93	0.21	0.47	0.94	0.3	0.89	0.94	0.94	0.87	0.83		
sd400	Fig. S14	1.17	0.78	0.29	0.05	0.36	0.78	0.29	0.29	0.89	0.85	0.48	0.10		
sd404	Fig. S15	3.5	0.63	0.15	0.06	0.33	0.34	0.15	0.15	0.90	0.86	0.27	0.07		
sd446	Fig. S16	7.85	0.84	0.43	0.21	0.70	0.70	0.41	0.09	0.65	0.55	0.60	0.14		
sd448	Fig. S17	9.08	0.47	0.4	0.10	0.4	0.47	0.3	0.21	0.34	0.38	0.28	0.27		Figure S59-62
sd452	Fig. S18	6.55	0.58	0.15	0.11	0.42	0.43	0.13	0.13	0.63	0.34	0.33	0.17		
sd461	Fig. S19	2.83	0.72	0.32	0.08	0.45	0.36	0.32	0.19	0.69	0.13	0.30	0.09	0.85	Figure S55-56
sd470	Fig. S20	4.5	0.31	0.36	0.28	0.31	0.31	0.31	0.17	0.72	0.70	0.31	0.15		
sd477	Fig. S21	10.5	0.35	0.32	0.05	0.45	0.29	0.32	0.02	0.61	0.45	0.29	0.11		Figure S63-65
sd491	Fig. S22	0.4	0.96	0.91	0.08	0.88	0.95	0.25	0.64	0.96	0.96	0.90	0.59	0.99	Figure S57-60
sd496	Fig. S23	1.48	0.77	0.36	0.07	0.42	0.73	0.24	0.08	0.96	0.95	0.36	0.13		
sd498	Fig. S24	1.95	0.33	0.11	0.06	0.32	0.32	0.02	0.06	0.92	0.92	0.25	0.14		
sd530	Fig. S25	3.72	0.57	0.25	0.13	0.57	0.57	0.25	0.25	0.73	0.74	0.73	0.74		
sd533	Fig. S26	2.9	0.76	0.16	0.03	0.76	0.76	0.13	0.13	0.84	0.53	0.84	0.53		
sd535	Fig. S27	1.88	0.66	0.36	0.06	0.65	0.65	0.36	0.36	0.91	0.86	0.91	0.86		
sd537	Fig. S28	1.7	0.62	0.34	0.09	0.42	0.61	0.22	0.28	0.92	0.86	0.41	0.05	0.84	
sd540	Fig. S29	3.4	0.44	0.17	0.12	0.19	0.25	0.15	0.09	0.23	0.34	0.21	0.09		
sd543	Fig. S30	0.81	0.92	0.92	0.39	0.43	0.92	0.41	0.68	0.92	0.92	0.92	0.92		
ATom4 cases															
sd22	Fig. S31	2.84	0.76	0.75	0.39	0.44	0.75	0.39	0.66	0.76	0.75	0.76	0.75		
sd32	Fig. S32	6.55	0.76	0.76	0.34	0.45	0.64	0.39	0.36	0.76	0.76	0.75	0.71		
sd72	Fig. S33	11.04	0.84	0.62	0.31	0.35	0.50	0.33	0.34	0.63	0.62	0.63	0.62		
sd75	Fig. S34	11.99	0.79	0.79	0.28	0.41	0.70	0.41	0.34	0.79	0.79	0.78	0.78		
sd78	Fig. S35	13.76	0.76	0.76	0.38	0.43	0.47	0.37	0.20	0.76	0.76	0.74	0.74		
sd82	Fig. S36	14.57	0.67	0.67	0.27	0.44	0.54	0.21	0.32	0.67	0.67	0.67	0.85		
sd132	Fig. S37	12.99	0.63	0.62	0.27	0.33	0.31	0.28	0.27	0.62	0.62	0.37	0.28		
sd134	Fig. S38	13.55	0.61	0.60	0.22	0.26	0.26	0.26	0.27	0.60	0.60	0.31	0.27		
sd179	Fig. S39	17.23	0.32	0.36	0.02	0.32	0.32	0.36	0.10	0.86	0.85	0.33	0.09		
sd183	Fig. S40	19.39	0.75	0.17	1.84	0.37	0.34	0.15	0.15	0.47	0.28	0.31	0.19		
sd186	Fig. S41	22.36	0.24	0.50	4.25	0.24	0.23	0.50	0.27	0.53	0.52	0.22	0.08		
sd188	Fig. S42	23.27	0.66	0.69	2.12	0.65	0.25	0.69	0.44	0.19	0.65	0.19	0.18		
Number of cases with best NME					21	0	0	4	6	0	0		5		

VEHK: neutral binary nucleation using Vehkamäki et al. (2002) scheme

org_{gr}: with organics added for initial growth

RIC: neutral nucleation with biogenic oxidation products (Riccobono et al., 2014), updated by temperature dependence according to Yu et al. (2017)

NAPA: neutral ternary nucleation (Napari et al., 2002)

NAPAt: neutral ternary nucleation (Napari et al., 2002), with a tuning factor of 10^{-5}

DUN: ion-induced and neutral nucleation scheme (Dunne et al., 2016) with both neutral and ion-induced binary and neutral and ion-induced ternary pathways

DUN_{NH₃=0}: ion-induced binary nucleation scheme (Dunne et al., 2016)

BIN_{n+ch}: neutral and ion-induced binary nucleation scheme (MAIA; Lovejoy et al., 2004; Kazil et al., 2007)

Table S5. Summary of the measured aerosol surface area for each of the studied cases. The highest surface area values for each case are shaded.

ATom2 Case identifier	Surface area, $\mu\text{m}^2 \text{cm}^{-3}$			
	Nucleation mode 3-12nm	7-12nm	Aitken mode 12-60nm	Accumulation mode >60nm
sd486	4.71	1.90	1.00	0.37
sd390	2.89	0.89	1.87	0.81
sd391	2.74	0.64	1.54	1.36
sd400	1.14	0.25	1.88	1.44
sd404	2.47	0.76	1.98	0.84
sd446	2.18	0.91	3.44	1.66
sd448	2.05	0.68	2.95	1.17
sd452	2.63	0.90	2.91	1.20
sd461	1.37	0.36	2.39	0.95
sd470	0.95	0.47	3.35	1.01
sd477	3.33	1.21	2.04	0.59
sd491	2.79	0.48	1.29	0.74
sd496	4.22	1.32	1.79	0.75
sd498	3.05	0.82	2.13	0.80
sd530	0.89	0.37	1.95	3.32
sd533	2.13	0.95	1.88	3.33
sd535	2.23	1.10	1.61	2.49
sd537	2.25	0.95	1.40	0.88
sd540	0.53	0.07	0.90	0.63
sd543	2.71	1.43	1.99	1.62
ATom4 cases				
sd22	0.44	0.33	1.05	1.41
sd32	0.50	0.37	0.90	1.12
sd72	0.37	0.31	1.40	1.75
sd75	0.86	0.62	1.11	1.36
sd78	0.31	0.22	0.94	1.56
sd82	0.37	0.31	1.69	2.23
sd132	0.09	0.06	1.13	1.76
sd134	0.14	0.09	1.94	2.03
sd179	0.84	0.56	0.38	0.28
sd183	0.17	0.08	0.52	0.40
sd186	0.05	0.02	0.445	0.436
sd188	0.07	0.02	0.26	0.22
TOTAL number of cases with highest surface area in each size range	11	0	10	11

Table S6. Comparison between measured SO₂ (ATom 4) and simulated SO₂ mixing ratios corresponding to for best NME values in the RIC simulations (TOMAS model).

ATom4 case number	SO ₂ measured, pptv	RIC		
		SO ₂ simulated, pptv	Organics	NME
sd22	nd	61.6	100	0.39
sd32	nd	7	100	0.34
sd72	8.12	14.4	48.3	0.31
sd75	6.32	11.3	100	0.28
sd78	4.33	23.4	8.9	0.38
sd82	5.65	11.3	100	0.27
sd132	3.58	2.1	18.3	0.27
sd134	6.90	1	100	0.22
sd179	11.29	1.6	8.9	0.02
sd183	11.20	1	1	1.84
sd186	8.47	1	100	4.25
sd188	8.97	1	100	2.12

nd -no data

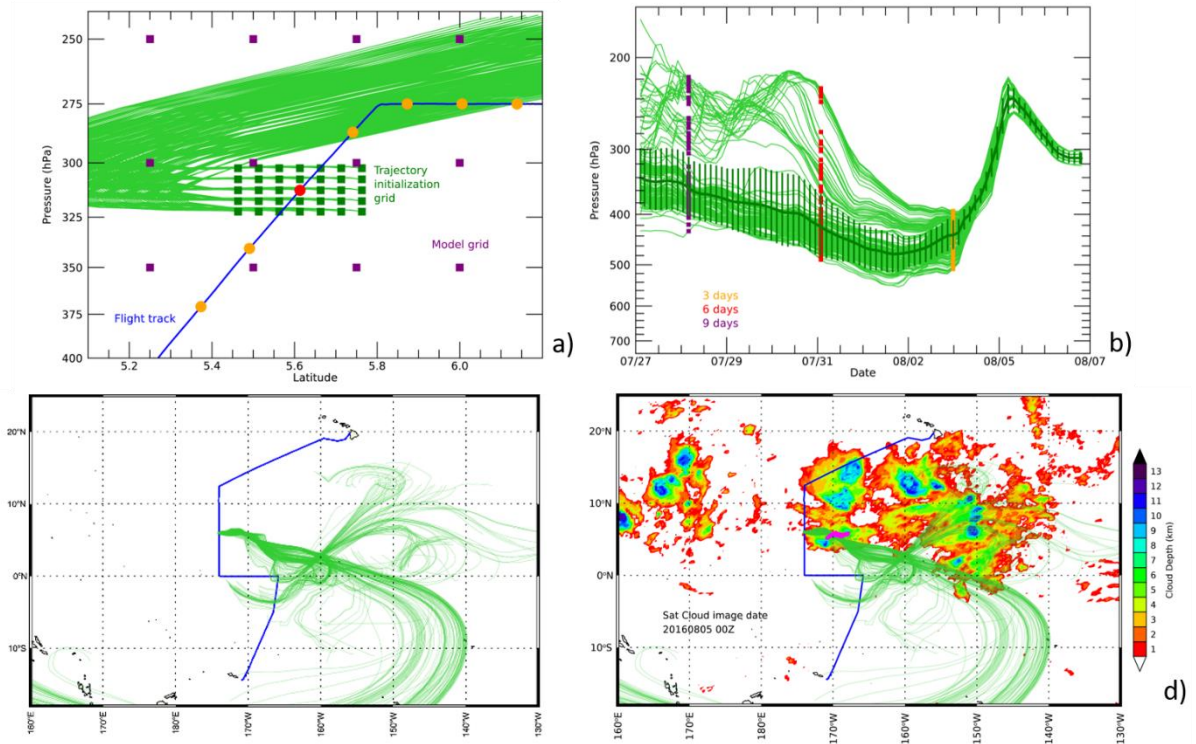


Figure S1: Example of trajectory calculations and analysis: a) Pressure cross-section of the DC-8 flight track (blue line) showing an exemplary cluster of 245 back-trajectories initialized within a grid (grey squares; $0.3^\circ \times 0.3^\circ \times 20$ hPa) centered around the DC-8 location every minute of flight (filled circles). The model reanalysis grid is shown by black squares. b) Pressure as a function of back-trajectory time. The back-trajectory time step is 3 hours, based on the reanalysis data. Uncertainty in the back-trajectory locations is represented by the 3-D spread in the trajectory cluster. The vertical uncertainty is estimated as the standard deviation in pressure (hPa) of the trajectory cluster at each time. c) Flight track and a cluster of back trajectories initiated at a certain minute of the flight. d) Back trajectories and cloud depths. The convective influence (CI) probability is the fraction of the 245 trajectories within each cluster that passed through a convective system with cloud depth >5 km. Magenta dots represent the point of CI with a trajectory distance tolerance of 0.15° (~10-15 km) from the cloud and for which the RH with respect to liquid water (RH_w) of the trajectory was >50 %.

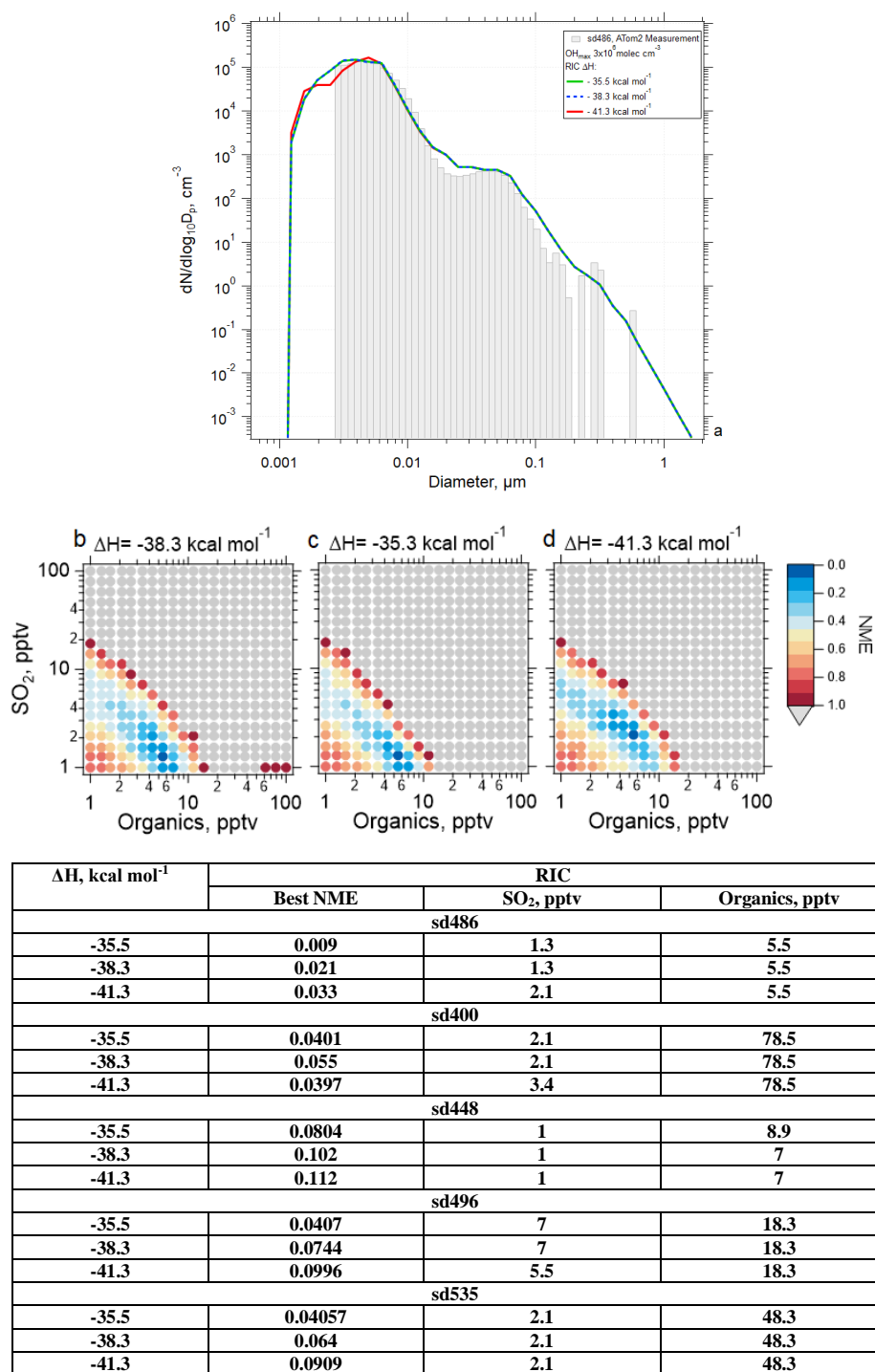


Figure S2: The impact of the change of enthalpy (ΔH) by $\pm 3 \text{ kcal mole}^{-1}$ in the RIC scheme and case study sd486. (ATom 2, 2017-02-04, 03:05:31-03:06:30 UTC) where measurements were made 7.3 hours following convective influence, and temperature along the trajectory varied between 218 and 226 K. (a) Observed (shaded bars) and simulated (lines) aerosol size distributions for three values of ΔH (b-d) NME between the modeled and measured size distribution for the RIC scheme with varying organics mixing ratios. The color of the circle indicates the value of NME corresponding to a particular initial mixing ratio of SO₂, or organics that varied between 0 and 100 pptv. Blue represents the best agreement, red poorer agreement, and grey the worst (NME >1). There were 400 sensitivity tests for this scheme. The table presents the NME results for five different cases, one of them corresponds to the size distributions in panel (a) and associated initial mixing ratios of gas-phase precursors.

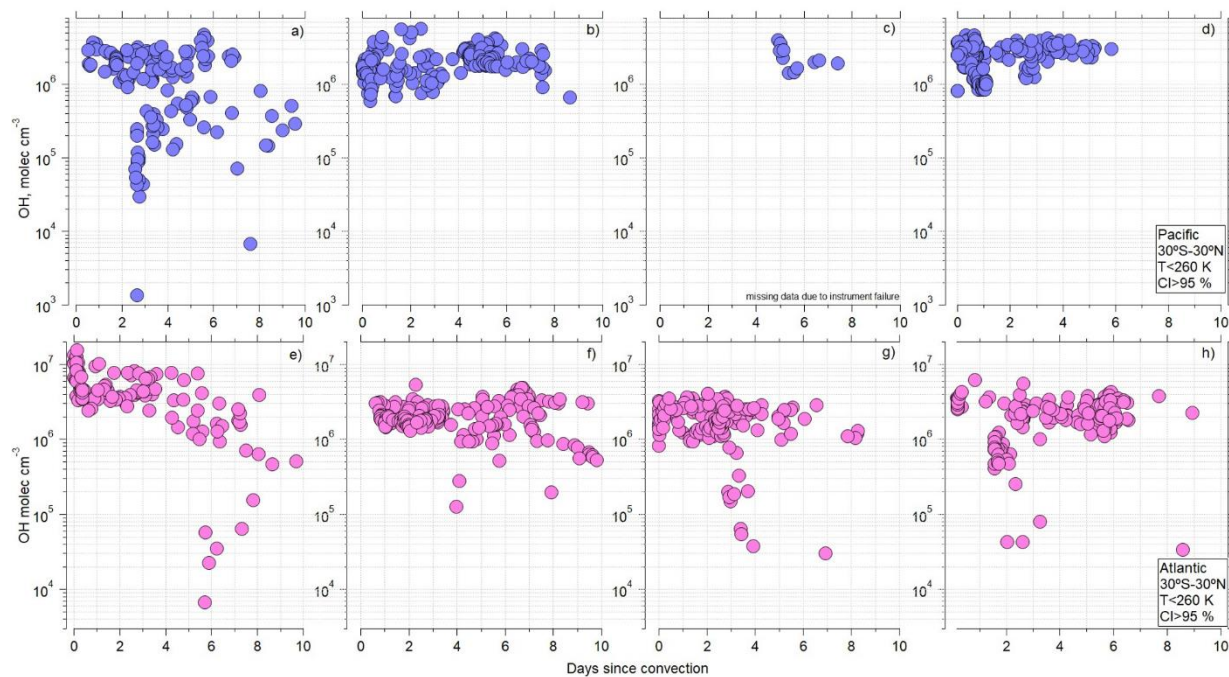


Figure S3: Measured hydroxyl radical (OH) concentration as a function of time since convective influence for ATom 1-4, over the Pacific (a-d) and the Atlantic (e-h) (30° S - 30° N), where temperature <260 K and probability of CI is >95%. If these conditions are met and an aerosol number mode with a modal peak diameter <12 nm is present within one day since CI, we consider the case for analysis by box modeling.

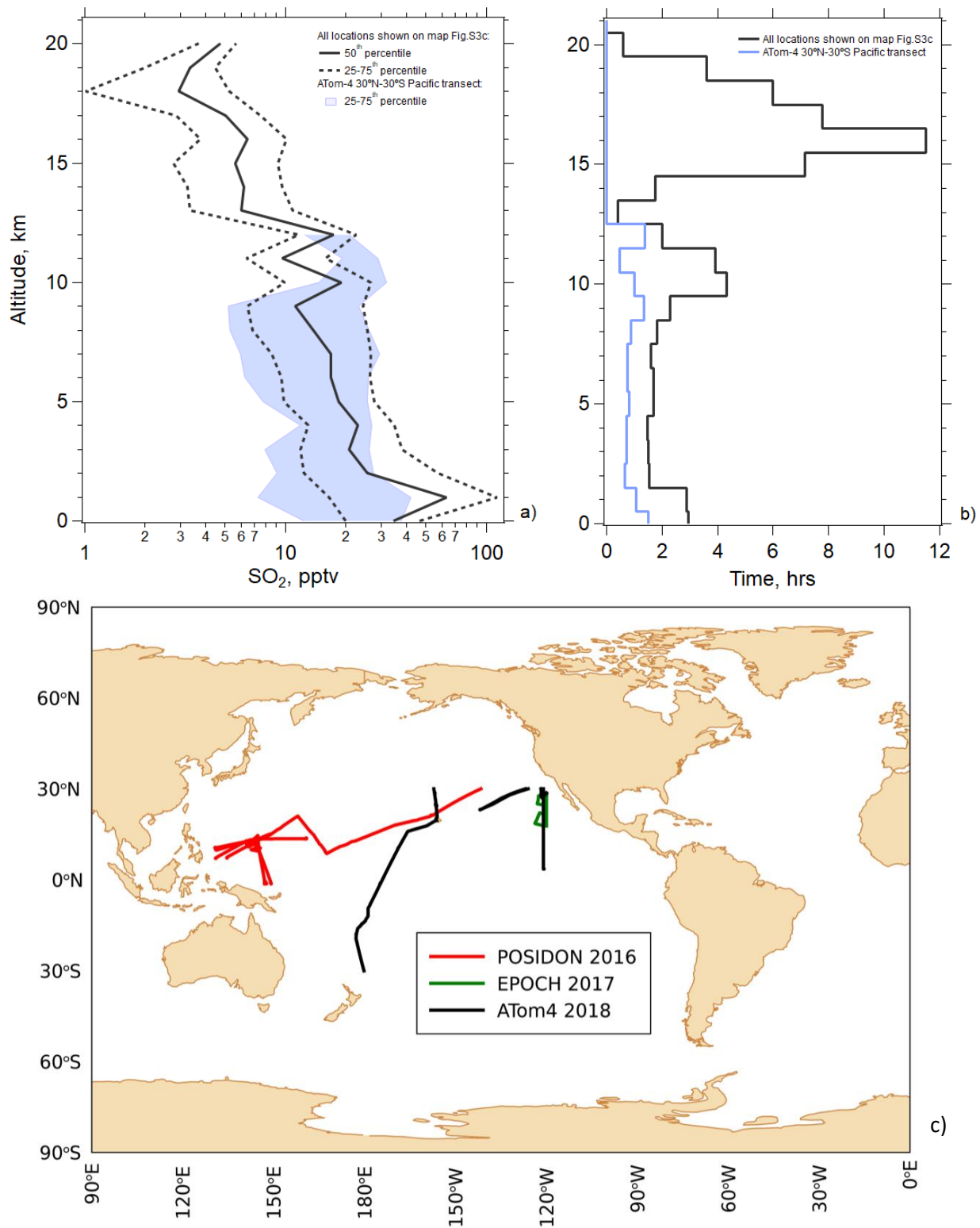


Figure S4: SO₂ measurements used to constrain box model simulations. (a) Median and interquartile range of the SO₂ measurements from 3 missions: POSIDON (October 2016), EPOCH (August 2017), and ATom-4 (May 2018). (b) Histogram showing integrated time of measurements that contributed to (a) as a function of altitude. (c) Corresponding flight tracks.

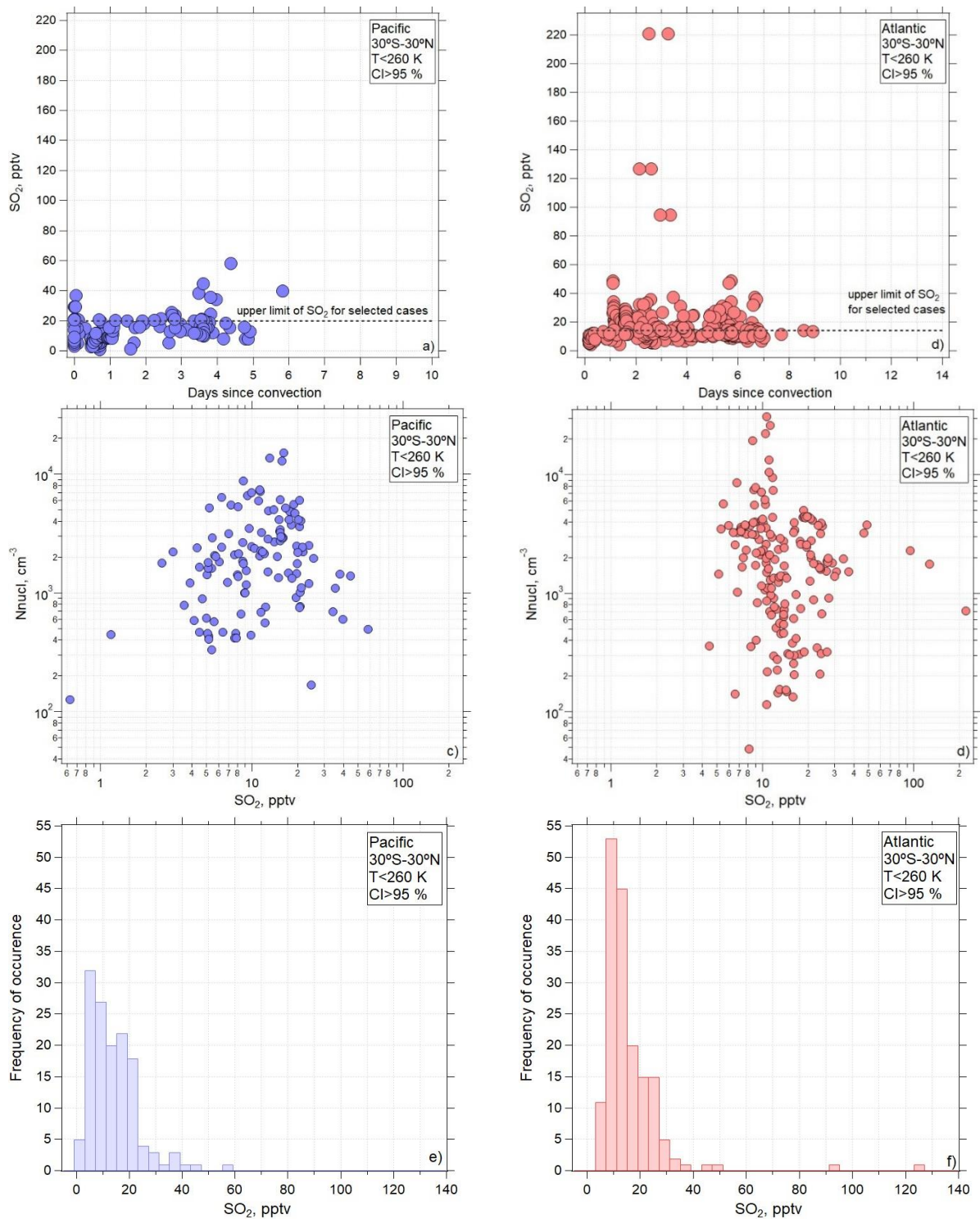


Figure S5: SO₂ mixing ratios for ATom 4 Pacific (a) and Atlantic (b) flights as a function of time since convective influence. Particle number concentration of nucleation-mode particles (Nnucl; 3-12 nm) for ATom 4 Pacific (c) and Atlantic (d) as a function of SO₂ mixing ratio. SO₂ mixing ratio frequency of occurrence for ATom 4 Pacific (e) and Atlantic (f). For Pacific cases selected for simulations (within 1 day since convection), the SO₂ mixing ratio over Pacific does not exceed 20 pptv.

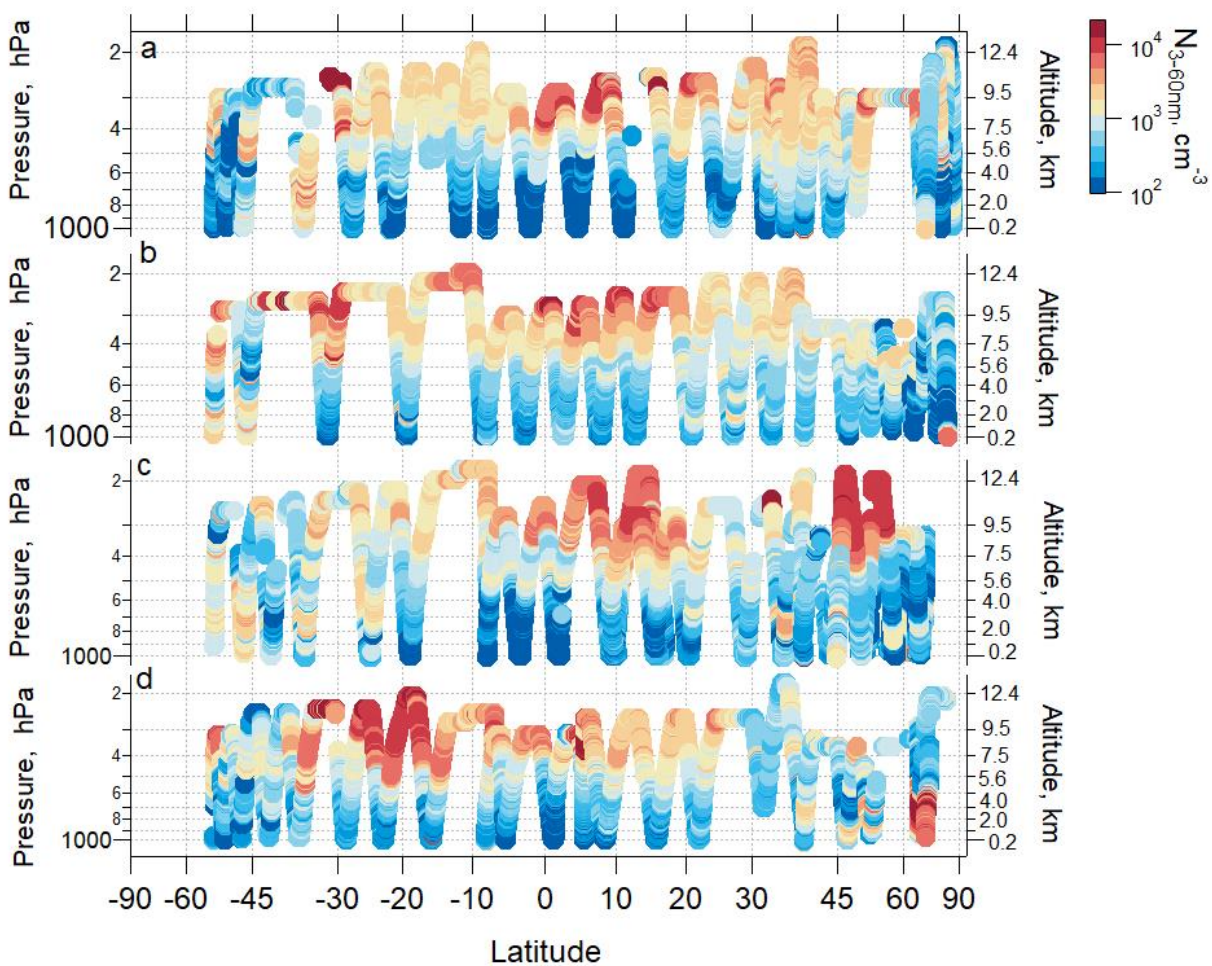


Figure S6: Ambient pressure as a function of sine-weighted latitude colored by the measured number concentration of nucleation and Aitken mode particles (D_p from 3 - 60 nm) over the Atlantic Ocean for a) ATom 1, July-August 2016; b) ATom 2, January-February 2017; c) ATom 3, September-October 2017; and d) ATom 4, April-May 2018). Periods of flight in clouds, over continents and near airports have been removed.

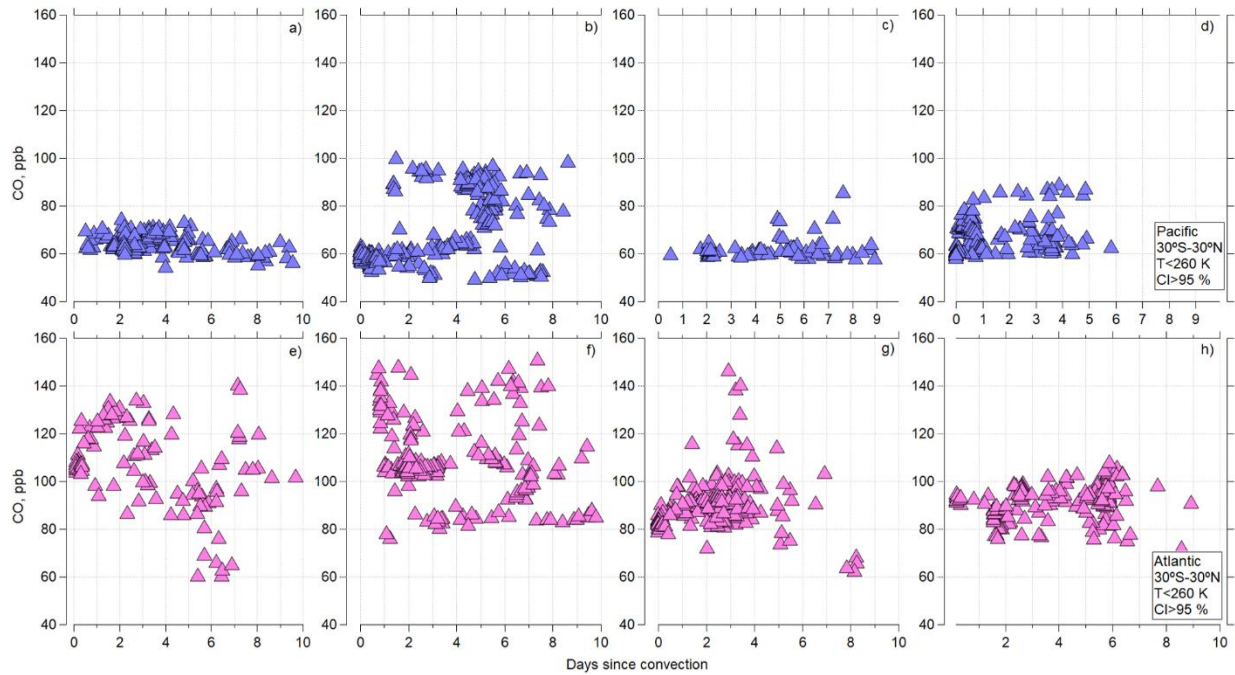


Figure S7: Carbon monoxide (CO) mixing ratio as a function of time since convective influence for ATom 1-4 over the Pacific (a-d) and Atlantic Oceans (e-h) (30° S - 30° N), where temperature <260 K and probability of CI is >95 %. If these conditions are met, and an aerosol number mode with a modal peak diameter <12 nm is present within one day since CI, we consider the case for analysis by box modelling.

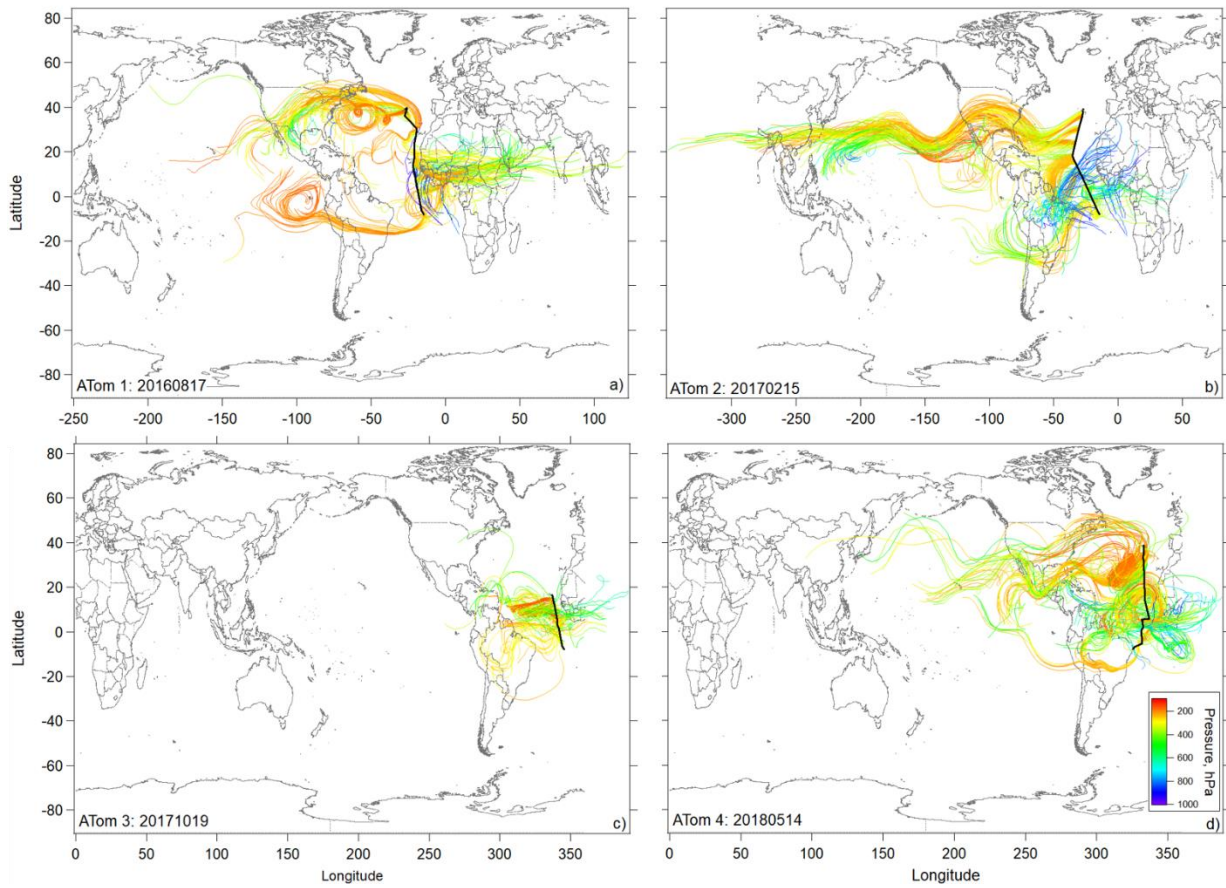


Figure S8: Flight track and selected 10-day back trajectories initiated for times in flight at pressures <400 hPa (<~260 K) sampled along the DC-8 flight track during ATom 1, 2 (a,b), 3 and 4 (c, d) during the most tropical flight in each deployment (Ascension Island-Terceira on ATom 1-2, Ascension Island-Cape Verde on Atom 3, and Recife-Terceira on ATom 4). Trajectories are colored according to the pressure along their pathway.

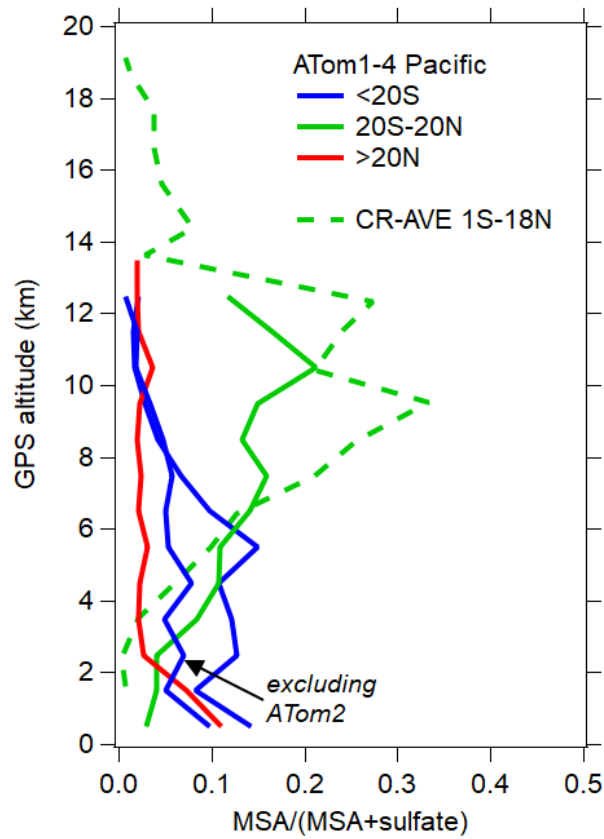


Figure S9: Vertical profiles of the PALMS methanesulfonic acid (MSA) signal fraction for ATom1-4. The raw MSA signal (positive m/z 97) is plotted relative to the sum of MSA and sulfate (positive m/z 99) signals. During ATom the MSA maximum occurred in the tropical upper troposphere, indicating a relatively high influence of marine boundary layer air and that DMS contributed directly to sulfuric acid production. One anomalously high MSA period also occurred in southern latitudes during ATom2, where the signal fraction averaged ~ 0.3 for altitudes < 6 km. High concentrations of 3-60 nm particles were observed during this anomalously high MSA period (Fig 2). The southern MSA signal fraction was < 0.1 for all other ATom campaigns. A similar enhancement of MSA in the Pacific tropical upper troposphere was also observed during the NASA Costa Rica Aura Validation Experiment (CR-AVE) campaign (Froyd et al., 2009). For this study the PALMS size range is restricted to 0.125-1.5 μm .

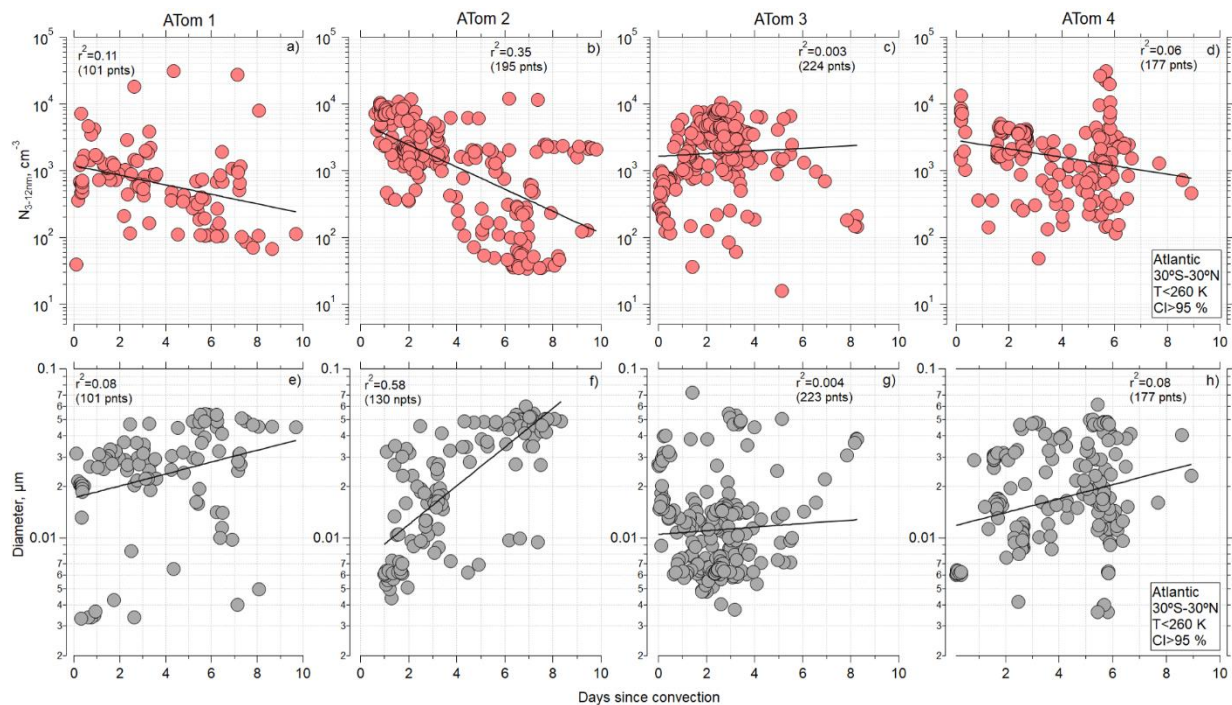


Figure S10: (a-d) Concentration of nucleation mode particles as a function of time since convective influence for ATom 1-4, over the Atlantic Ocean (30° S - 30° N) and temperature <260 K and probability of convective influence $>95\%$, respectively. (e-h) Modal diameter of particles with $D_p < 60$ nm as a function of time since convective influence (30° S - 30° N) for ATom 1-4, respectively. Black line, used to guide the eye, represents the linear regression fitted to log-y values. A corresponding Pearson correlation coefficient r^2 is indicated.

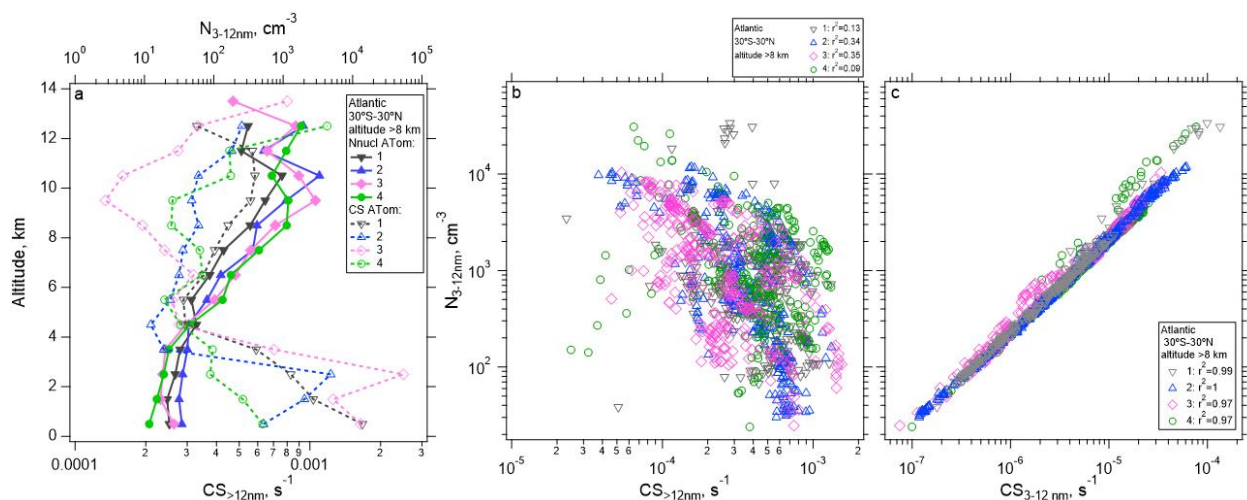


Figure S11: a) Vertical profile of the median number concentration of nucleation mode particles (3-12 nm) and condensation sink ($CS_{>12\text{nm}}$) averaged between 30° S - 30° N as a function of altitude for the four ATom deployments over the Atlantic Ocean. (b-c) One minute average nucleation mode particle concentrations at >8 km in altitude as a function of $CS_{>12\text{nm}}$ (b) and $CS_{3-12\text{nm}}$ (c) and between 30° S - 30° N over the Pacific Ocean. Pearson correlation coefficient values (r^2) are indicated in the legend.

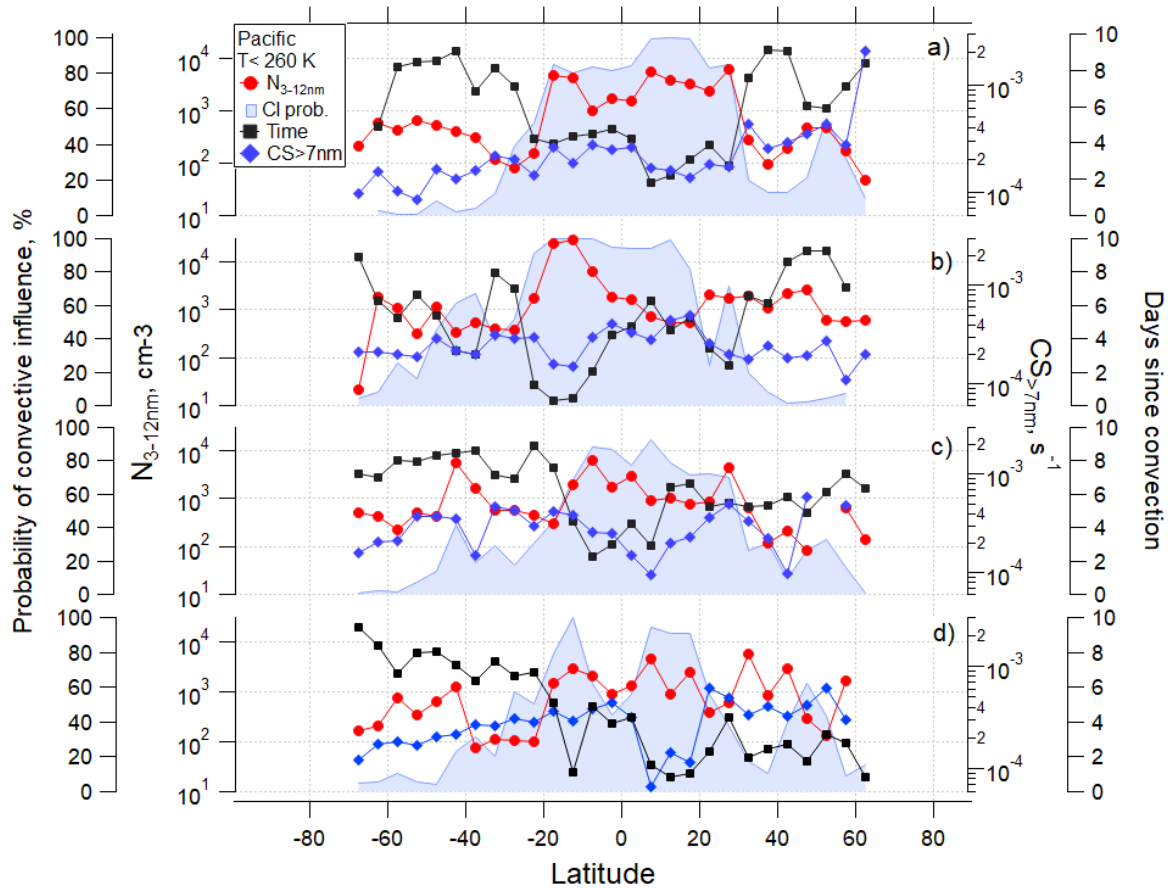


Figure S12: The number of nucleation mode particles (N_{3-12}), probability of convective influence (CI), time since most recent CI, and condensation sink (CS) >7 nm, as a function of latitude binned in 5° increments for temperature <260 K for ATom 1-4 over the Pacific Ocean (a-d). The largest number concentration of nucleation mode (D_p from 3-12 nm) particles was found to spatially coexist with the lowest CS, the shortest time since recent convective activity, and the highest probability of convection. Tropical convection does not produce uniquely low condensation sinks at high altitudes where the most NPF is observed; for example, very low CS was also found in the middle troposphere over the Southern Ocean at $T < 260$ K. Therefore, it is likely that a stronger source of condensable material must be available in the tropical regions than in other cold areas with low CS where NPF was not encountered as frequently (Williamson et al., 2019). This means that the significant occurrence of NPF in this region is likely due to a combination of convective activity bringing precursor gases from lower altitudes and removing pre-existing particles, cold temperatures, and high solar zenith angles in the tropics photo-oxidizing these precursors to produce condensable species (Gao et al., 2014).

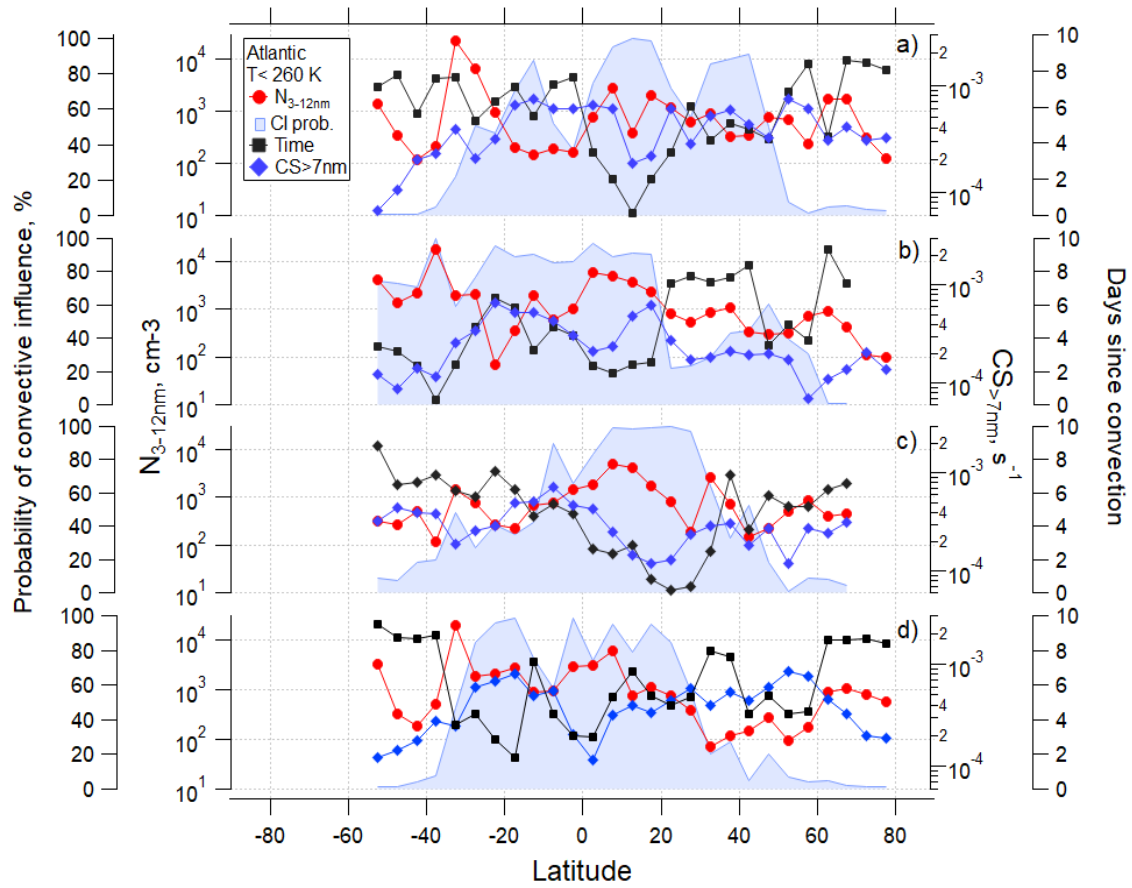
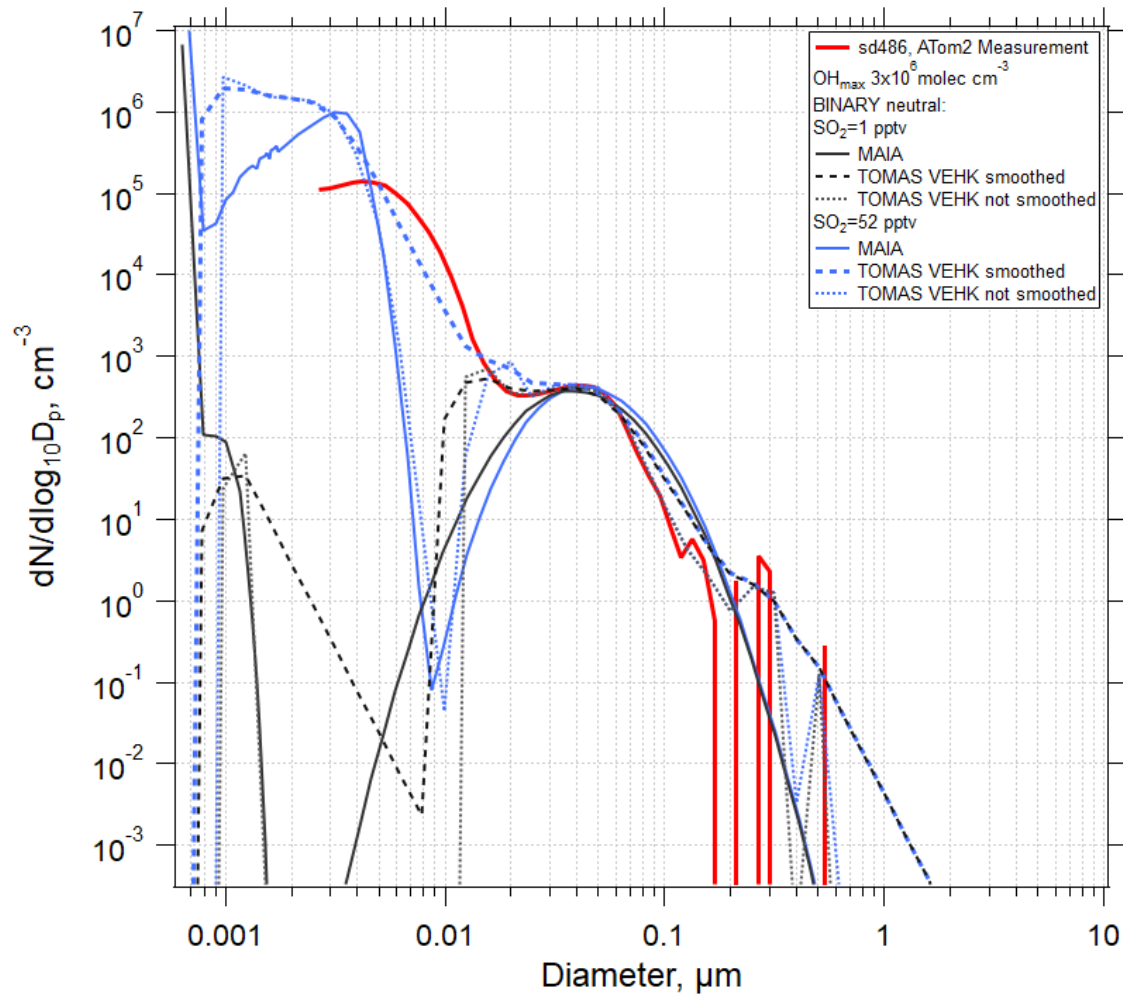


Figure S13: As in Fig. S12, but for flights over the Atlantic Ocean.



SO2 pptv	NME		
	TOMAS		MAIA
	Smoothed	Not smoothed	Not smoothed
1	0.980	0.979	0.999
51.8	0.991	0.870	0.973

Figure S14: An example of the smoothed and not-smoothed TOMAS size distribution for VEHK scheme and comparison to non-smoothed MAIA neutral binary output. Table presents NME values for the corresponding curves presented in the figure.

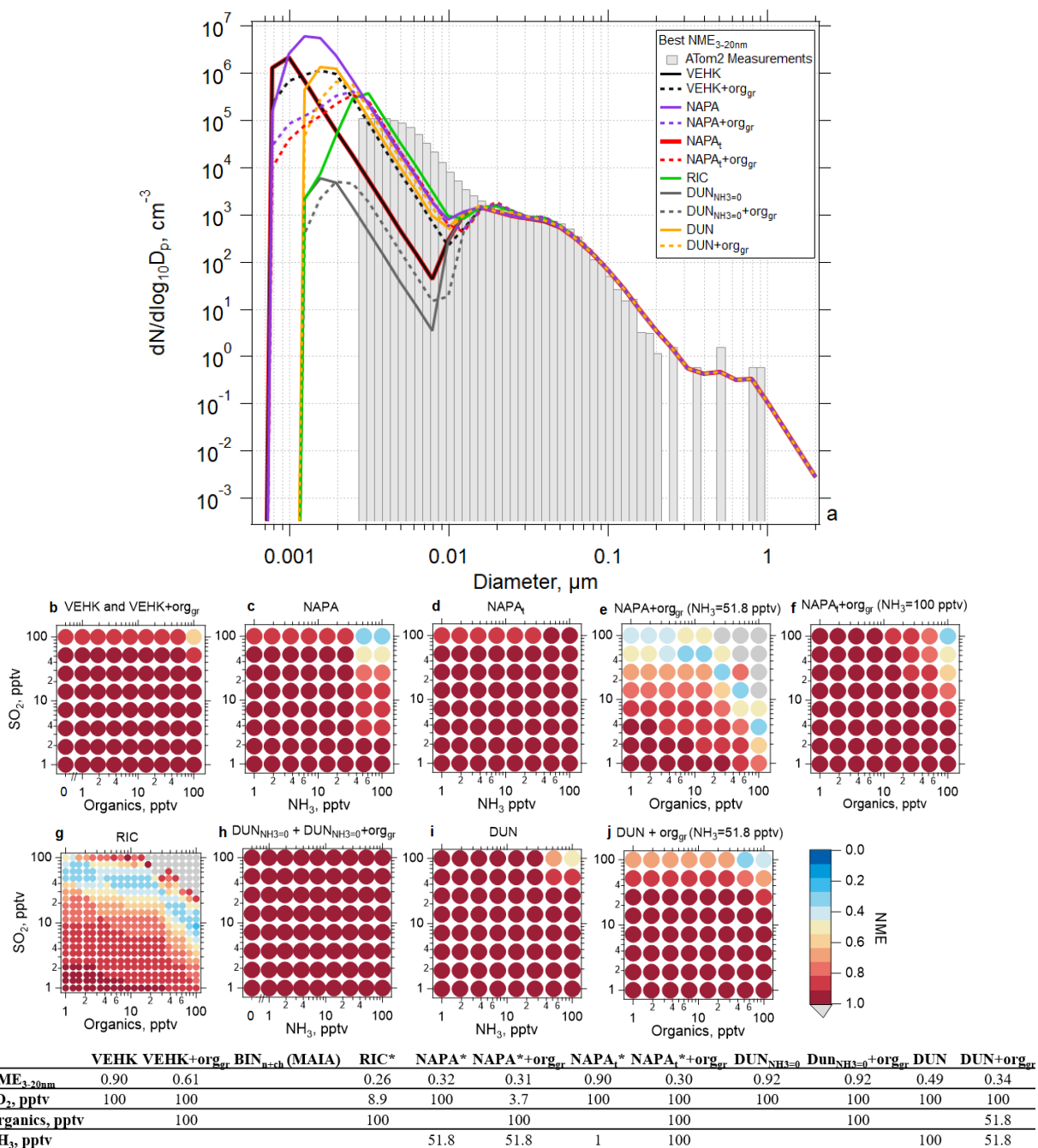


Figure S15: Results of simulations using the TOMAS box model for case sd390 (ATom 2, 2017-02-04, 01:29:31-01:30:30 UTC) where measurements were made 1 hour following convective influence, and temperature along the trajectory varied between 230 and 231 K. (a) Observed (shaded bars) and simulated (lines) aerosol size distributions with best normalized mean error (*NME*) for each of the NPF and growth schemes investigated. (b) *NME* between the modeled and measured size distribution for the VEHK scheme with varying organics mixing ratios for condensational growth. The color of the circle indicates the value of *NME* corresponding to a particular initial mixing ratio of SO₂, NH₃, or organics that varied between 0 and 100 pptv. Blue represents the best agreement, red poorer agreement, and grey the worst ($NME > 1$). There were 64 sensitivity tests. (c) As in (b), but for the NAPA scheme. (d) As in (c), but for the NAPAt scheme. (e) and (f) as in (c) and (d) respectively, but with NH₃ fixed and varying organics for condensational growth. (g) as in (b) but for the RIC scheme, which provides the lowest *NME*. There were 400 sensitivity tests for this scheme. (h) as in (b) but for the DUN scheme with NH₃ set to 0 (DUN_{NH3=0}). (i) as in (c) but for the DUN scheme. (j) as in (i) but with varying organics for condensational growth. The table presents the *NME* results for the corresponding size distributions in panel (a) and associated initial mixing ratios of gas-phase precursors.

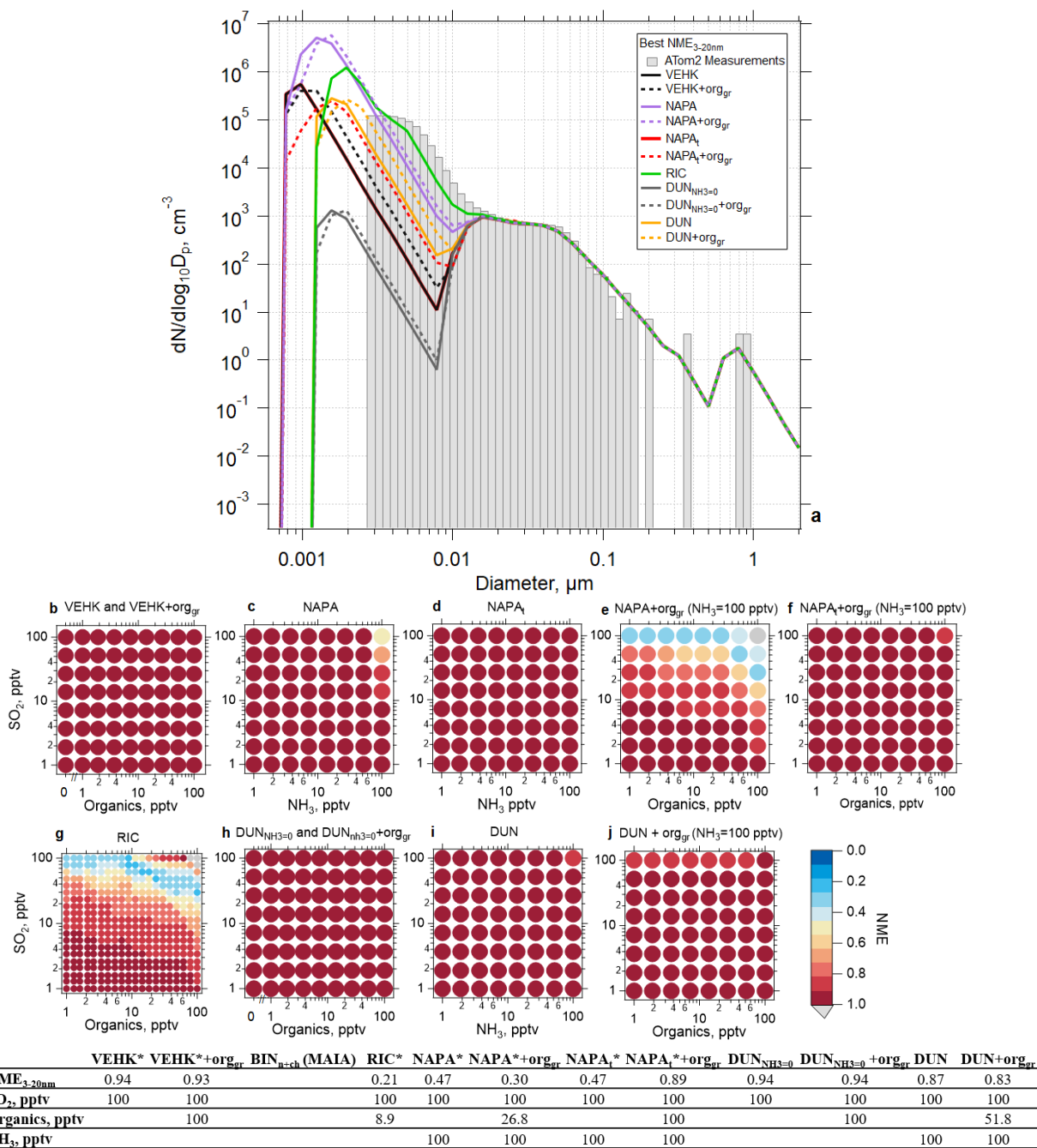


Figure S16: Results of simulations using the TOMAS box model for case sd391 (ATom 2, 2017-02-04, 01:20:31-01:31:30 UTC) where measurements were made 0.66 hours following convective influence, and temperature along the trajectory varied around 228 K. (a) Observed (shaded bars) and simulated (lines) aerosol size distributions with best normalized mean error (*NME*) for each of the NPF and growth schemes investigated. (b) *NME* between the modeled and measured size distribution for the VEHK scheme with varying organics mixing ratios for condensational growth. The color of the circle indicates the value of *NME* corresponding to a particular initial mixing ratio of SO₂, NH₃, or organics that varied between 0 and 100 pptv. Blue represents the best agreement, red poorer agreement, and grey the worst (*NME* > 1). There were 64 sensitivity tests. (c) As in (b), but for the NAPA scheme. (d) As in (c), but for the NAPAt scheme. (e) and (f) as in (c) and (d) respectively, but with NH₃ fixed and varying organics for condensational growth. (g) as in (b) but for the RIC scheme, which provides the lowest *NME*. There were 400 sensitivity tests for this scheme. (h) as in (b) but for the DUN scheme with NH₃ set to 0 (DUN_{NH3=0}). (i) as in (c) but for the DUN scheme. (j) as in (i) but with varying organics for condensational growth. The table presents the *NME* results for the corresponding size distributions in panel (a) and associated initial mixing ratios of gas-phase precursors.

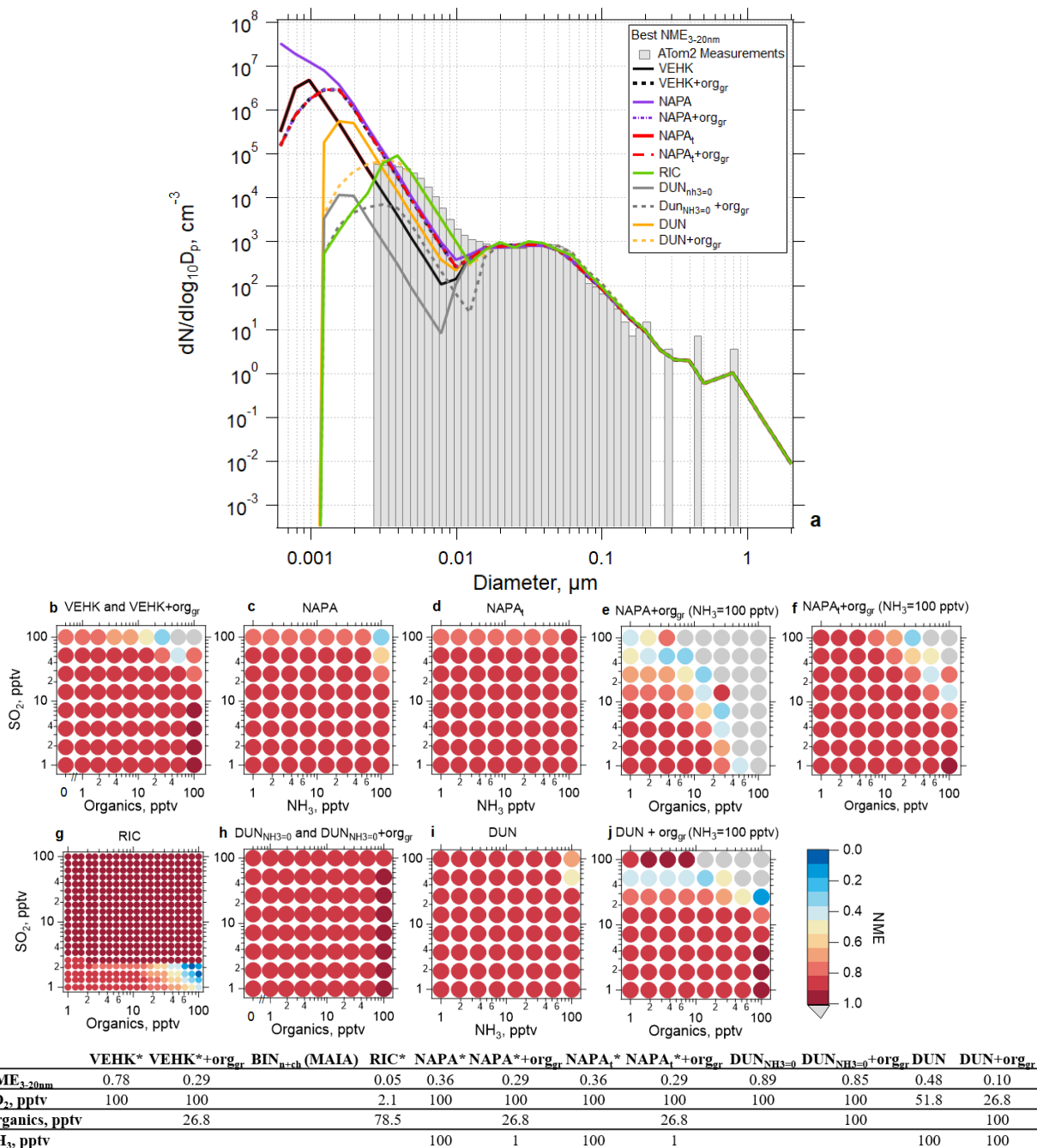
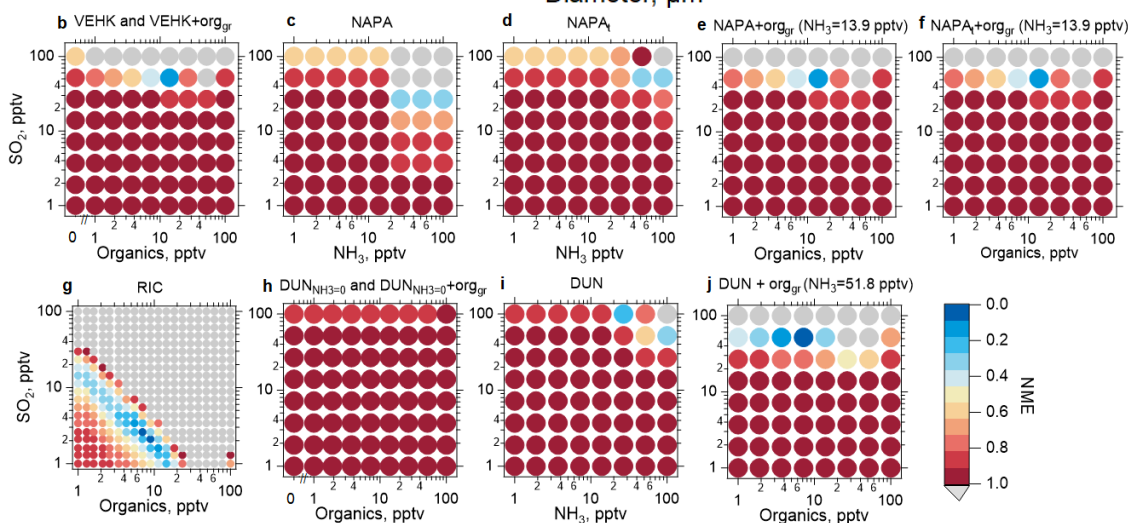
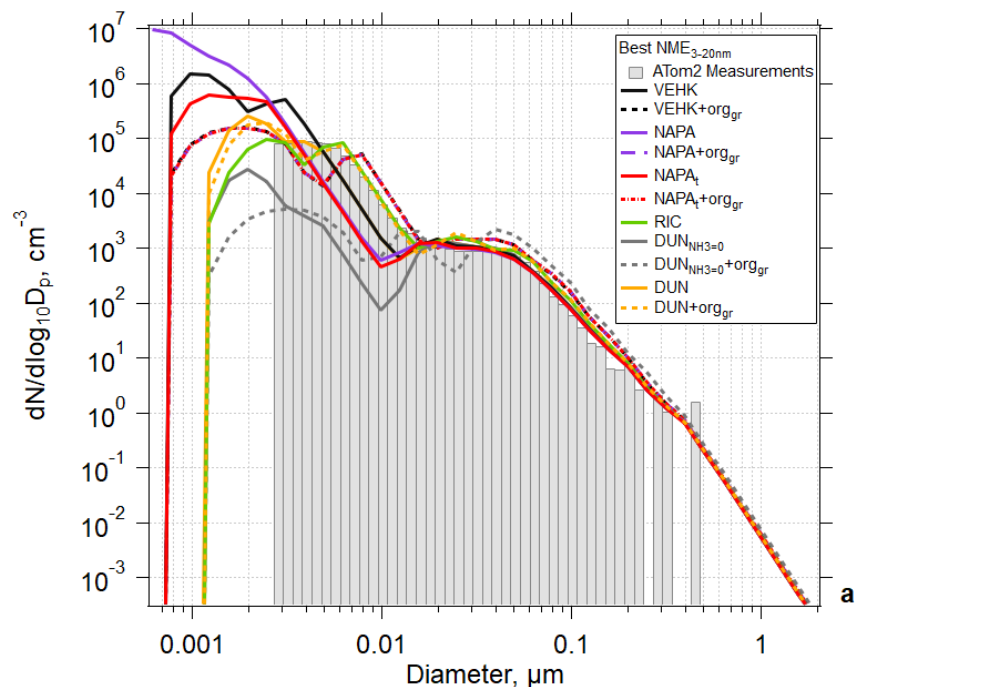


Figure S17: Results of simulations using the TOMAS box model for case sd400 (ATom 2, 2017-02-04, 01:39:31-01:40:30 UTC) where measurements were made 1.17 hours following convective influence, and temperature along the trajectory varied between 224 and 226 K. (a) Observed (shaded bars) and simulated (lines) aerosol size distributions with best normalized mean error (NME) for each of the NPF and growth schemes investigated. (b) NME between the modeled and measured size distribution for the VEHK scheme with varying organics mixing ratios for condensational growth. The color of the circle indicates the value of NME corresponding to a particular initial mixing ratio of SO₂, NH₃, or organics that varied between 0 and 100 pptv. Blue represents the best agreement, red poorer agreement, and grey the worst (NME >1). There were 64 sensitivity tests. (c) As in (b), but for the NAPA scheme. (d) As in (c), but for the NAPAt scheme. (e) and (f) as in (c) and (d) respectively, but with NH₃ fixed and varying organics for condensation growth. (g) as in (b) but for the RIC scheme, which provides the lowest NME. There were 400 sensitivity tests for this scheme. (h) as in (b) but for the DUN scheme with NH₃ set to 0 (DUN_{NH3=0}). (i) as in (c) but for the DUN scheme. (j) as in (i) but with varying organics for condensation growth. The table presents the NME results for the corresponding size distributions in panel (a) and associated initial mixing ratios of gas-phase precursors.



	VEHK	VEHK+org _{gr}	BIN _{NH3} (MAIA)	RIC*	NAPA*	NAPA*+org _{gr}	NAPA _t *	NAPA _t *+org _{gr}	DUN _{NH3=0}	DUN _{NH3=0} +org _{gr}	DUN	DUN+org _{gr}
NME _{3-20nm}	0.63	0.15		0.06	0.33	0.15	0.34	0.15	0.90	0.86	0.27	0.07
SO ₂ , pptv	100	51.8		2.1	26.8	51.8	51.8	51.8	100	100	100	51.8
Organics, pptv		13.9		8.9		13.9		13.9		26.8		7
NH ₃ , pptv					26.8	13.9	100	13.9			26.8	51.8

*Temperature along the trajectory does not lie within the temperature range of the scheme

Figure S18: Results of simulations using the TOMAS box model for case sd404 (ATom 2, 2017-02-04, 01:43:31-01:44:30 UTC) where measurements were made 3.5 hours following convective influence, and temperature along the trajectory varied between 234 and 236 K. (a) Observed (shaded bars) and simulated (lines) aerosol size distributions with best normalized mean error (NME) for each of the NPF and growth schemes investigated. (b) NME between the modeled and measured size distribution for the VEHK scheme with varying organics mixing ratios for condensational growth. The color of the circle indicates the value of NME corresponding to a particular initial mixing ratio of SO₂, NH₃, or organics that varied between 0 and 100 pptv. Blue represents the best agreement, red poorer agreement, and grey the worst (NME >1). There were 64 sensitivity tests. (c) As in (b), but for the NAPA scheme. (d) As in (c), but for the NAPAt scheme. (e) and (f) as in (c) and (d) respectively, but with NH₃ fixed and varying organics for condensation growth. (g) as in (b) but for the RIC scheme, which provides the lowest NME. There were 400 sensitivity tests for this scheme. (h) as in (b) but for the DUN scheme with NH₃ set to 0 (DUN_{NH3=0}). (i) as in (c) but for the DUN scheme. (j) as in (i) but with varying organics for condensation growth. The table presents the NME results for the corresponding size distributions in panel (a) and associated initial mixing ratios of gas-phase precursors.

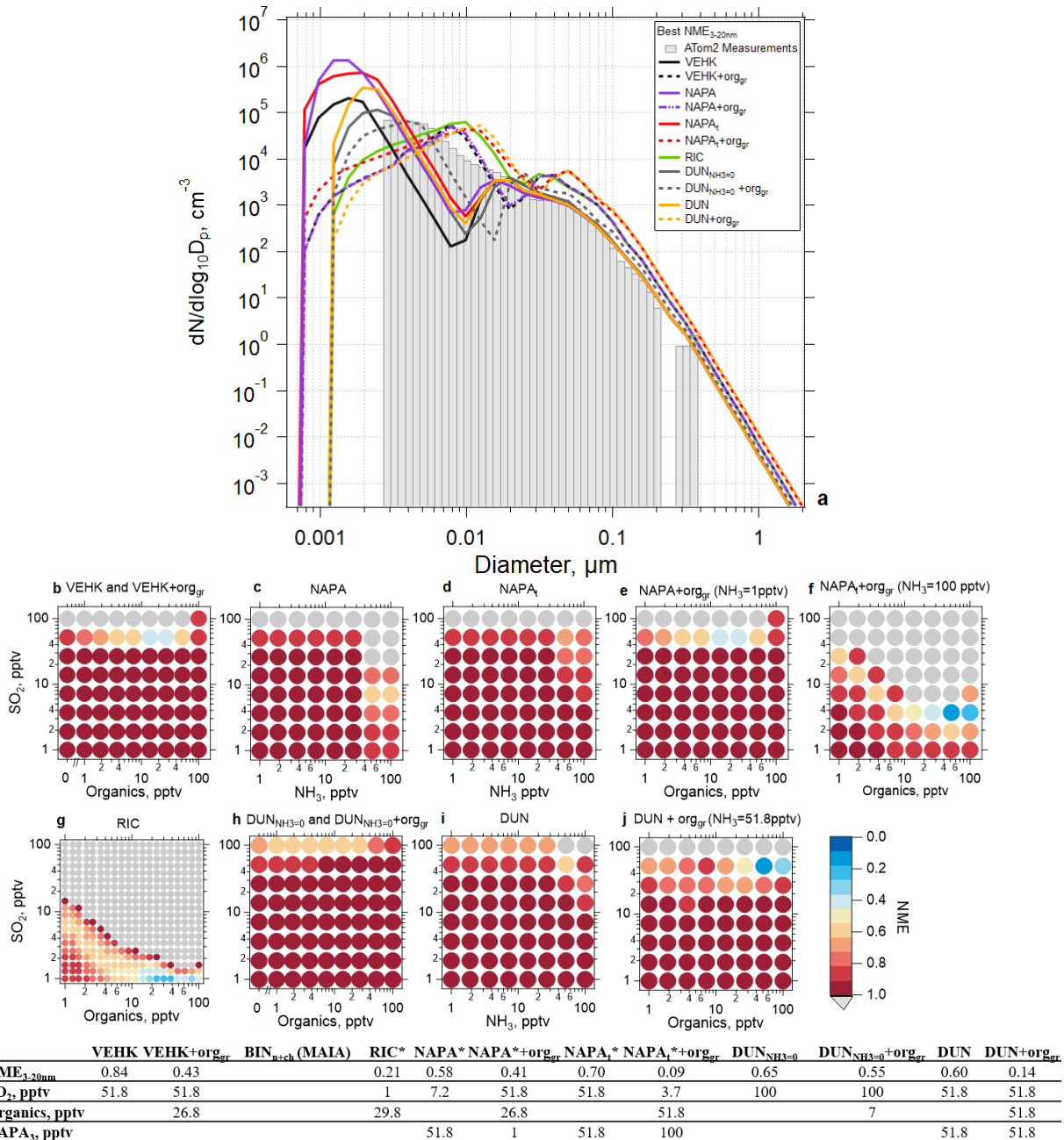
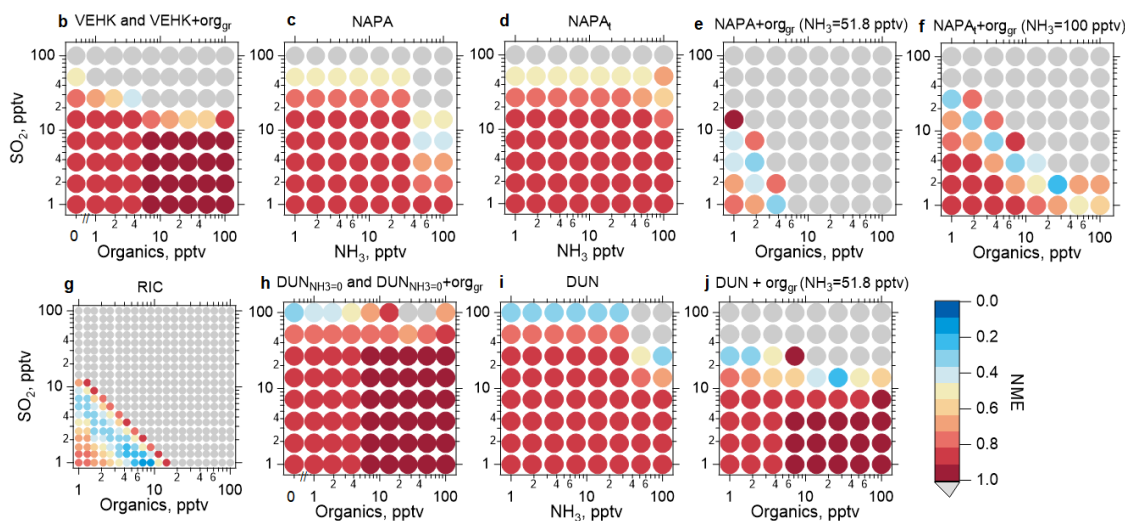
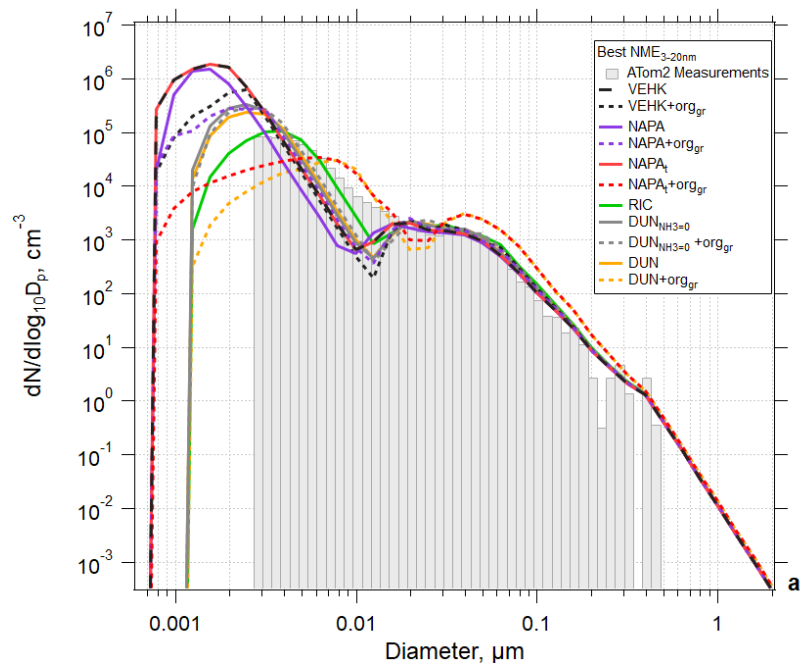
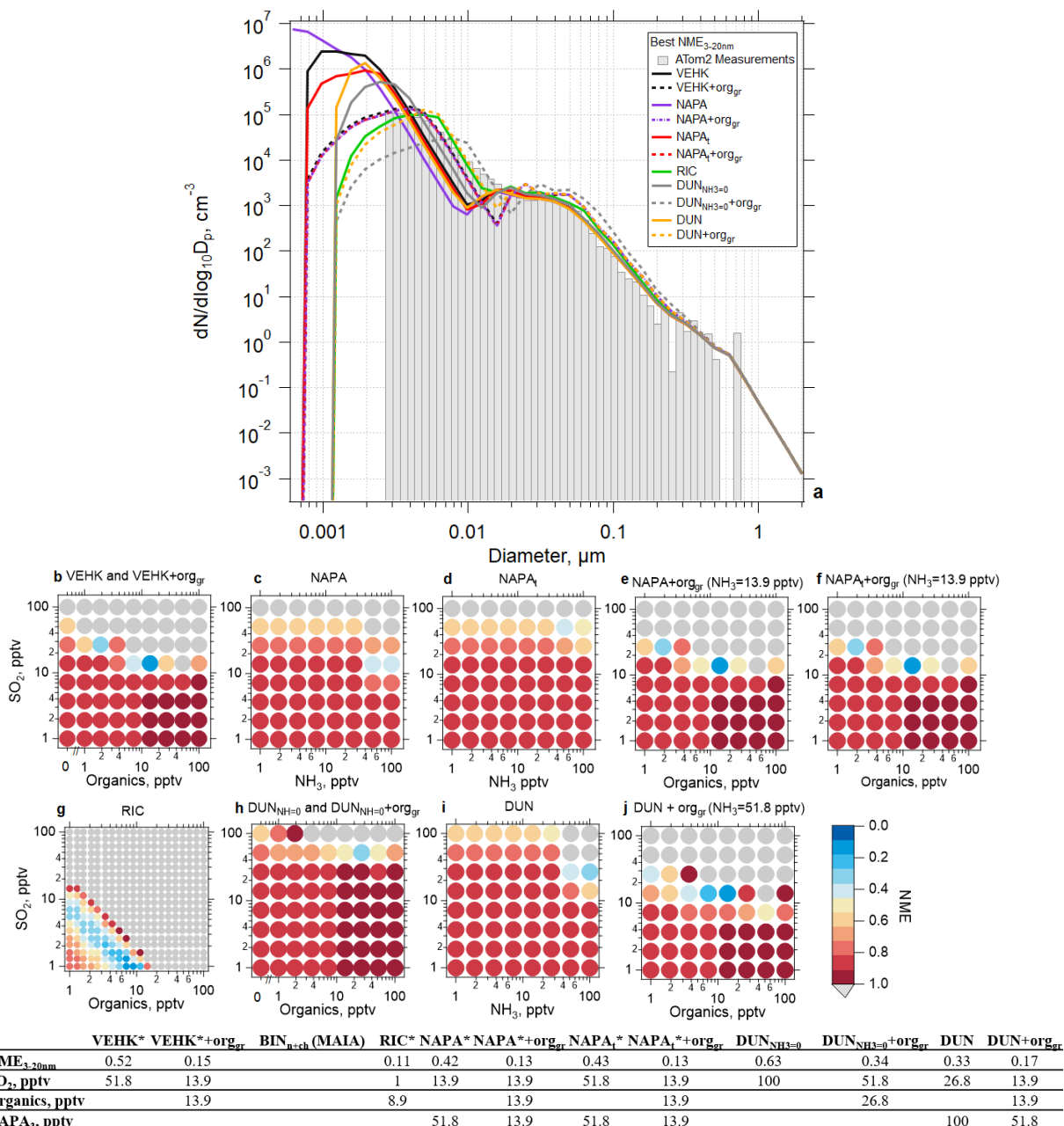


Figure S19: Results of simulations using the TOMAS box model for case sd446 (ATom 2, 2017-02-04, 02:25:31-02:26:30 UTC) where measurements were made 7.85 hours following convective influence, and temperature along the trajectory varied between 238 and 242 K. (a) Observed (shaded bars) and simulated (lines) aerosol size distributions with best normalized mean error (NME) for each of the NPF and growth schemes investigated. (b) NME between the modeled and measured size distribution for the VEHK scheme with varying organics mixing ratios for condensational growth. The color of the circle indicates the value of NME corresponding to a particular initial mixing ratio of SO₂, NH₃, or organics that varied between 0 and 100 pptv. Blue represents the best agreement, red poorer agreement, and grey the worst (NME >1). There were 64 sensitivity tests. (c) As in (b), but for the NAPA scheme. (d) As in (c), but for the NAPAt scheme. (e) and (f) as in (c) and (d) respectively, but with NH₃ fixed and varying organics for condensation growth. (g) as in (b) but for the RIC scheme, which provides the lowest NME. There were 400 sensitivity tests for this scheme. (h) as in (b) but for the DUN scheme with NH₃ set to 0 (DUN_{NH3=0}). (i) as in (c) but for the DUN scheme. (j) as in (i) but with varying organics for condensation growth. The table presents the NME results for the corresponding size distributions in panel (a) and associated initial mixing ratios of gas-phase precursors.



	VEHK	VEHK+org _{gr}	BIN _{rich} (MAIA)	RIC*	NAPA*	NAPA*+org _{gr}	NAPA _t *	NAPA _t *+org _{gr}	DUN _{NH3=0}	DUN _{NH3=0} +org _{gr}	DUN	DUN+org _{gr}
NME _{3-20nm}	0.47	0.40		0.10	0.40	0.30	0.47	0.21	0.34	0.38	0.28	0.27
SO ₂ , pptv	51.8	26.8		1	7.2	1	51.8	1.9	100	100	100	13.9
Organics, pptv		3.7		7		3.7		26.8		1		26.8
NH ₃ , pptv					51.8	51.8	1	100			51.8	51.8

Figure S20: Results of simulations using the TOMAS box model for case sd448 (ATom 2, 2017-02-04, 02:27:31-02:28:30 UTC) where measurements were made 9.08 hours following convective influence, and temperature along the trajectory varied between 230 and 235 K. (a) Observed (shaded bars) and simulated (lines) aerosol size distributions with best normalized mean error (NME) for each of the NPF and growth schemes investigated. (b) NME between the modeled and measured size distribution for the VEHK scheme with varying organics mixing ratios for condensational growth. The color of the circle indicates the value of NME corresponding to a particular initial mixing ratio of SO₂, NH₃, or organics that varied between 0 and 100 pptv. Blue represents the best agreement, red poorer agreement, and grey the worst (NME >1). There were 64 sensitivity tests. (c) As in (b), but for the NAPA scheme. (d) As in (c), but for the NAPAt scheme. (e) and (f) as in (c) and (d) respectively, but with NH₃ fixed and varying organics for condensation growth. (g) as in (b) but for the RIC scheme, which provides the lowest NME. There were 400 sensitivity tests for this scheme. (h) as in (b) but for the DUN scheme with NH₃ set to 0 (DUN_{NH3=0}). (i) as in (c) but for the DUN scheme. (j) as in (i) but with varying organics for condensation growth. The table presents the NME results for the corresponding size distributions in panel (a) and associated initial mixing ratios of gas-phase precursors.



*Temperature along the trajectory does not lie within the temperature range of the scheme

Figure S21: Results of simulations using the TOMAS box model for case sd452 (ATom 2, 2017-02-43, 02:31:31-02:32:30 UTC) where measurements were made 6.5 hours following convective influence, and temperature along the trajectory varied between 224 and 230 K. (a) Observed (shaded bars) and simulated (lines) aerosol size distributions with best normalized mean error (NME) for each of the NPF and growth schemes investigated. (b) NME between the modeled and measured size distribution for the VEHK scheme with varying organics mixing ratios for condensational growth. The color of the circle indicates the value of NME corresponding to a particular initial mixing ratio of SO₂, NH₃, or organics that varied between 0 and 100 pptv. Blue represents the best agreement, red poorer agreement, and grey the worst (NME >1). There were 64 sensitivity tests. (c) As in (b), but for the NAPA scheme. (d) As in (c), but for the NAPAt scheme. (e) and (f) as in (c) and (d) respectively, but with NH₃ fixed and varying organics for condensational growth. (g) as in (b) but for the RIC scheme, which provides the lowest NME. There were 400 sensitivity tests for this scheme. (h) as in (b) but for the DUN scheme with NH₃ set to 0 (DUN_{NH3=0}). (i) as in (c) but for the DUN scheme. (j) as in (i) but with varying organics for condensational growth. The table presents the NME results for the corresponding size distributions in panel (a) and associated initial mixing ratios of gas-phase precursors.

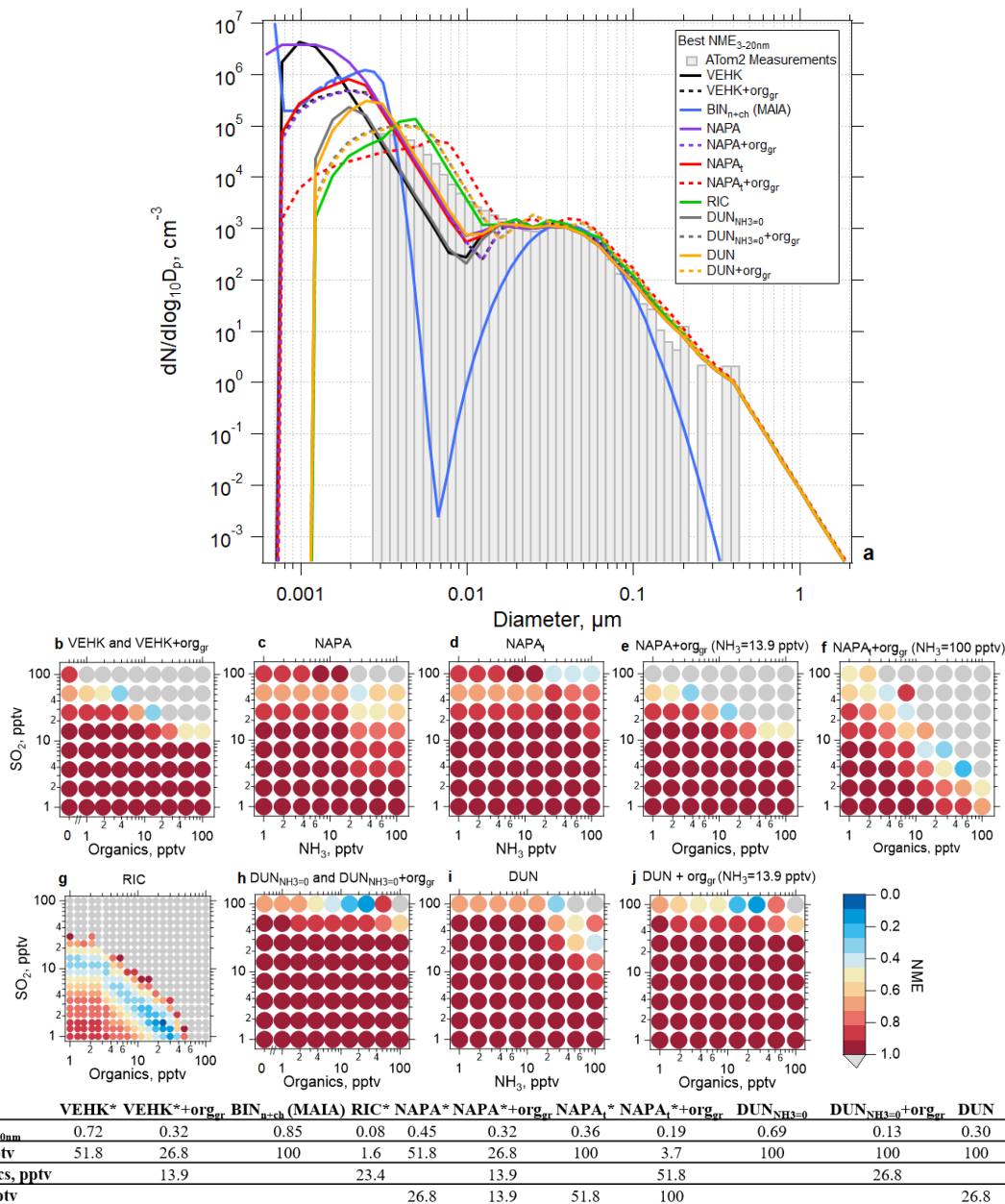


Figure S22: Results of simulations using the TOMAS box model for case sd461 (ATom 2, 2017-02-04, 02:40:31-02:41:30 UTC) where measurements were made 2.83 hours following convective influence, and temperature along the trajectory varied between 223 and 226 K. (a) Observed (shaded bars) and simulated (lines) aerosol size distributions with best normalized mean error (*NME*) for each of the NPF and growth schemes investigated. Best results from the MAIA box model ion-assisted + neutral binary nucleation scheme shown as a blue line. (b) *NME* between the modeled and measured size distribution for the VEHK scheme with varying organics mixing ratios for condensational growth. The color of the circle indicates the value of *NME* corresponding to a particular initial mixing ratio of SO₂, NH₃, or organics that varied between 0 and 100 pptv. Blue represents the best agreement, red poorer agreement, and grey the worst (*NME* >1). There were 64 sensitivity tests. (c) As in (b), but for the NAPA scheme. (d) As in (c), but for the NAPAt scheme. (e) and (f) as in (c) and (d) respectively, but with NH₃ fixed and varying organics for condensational growth. (g) as in (b) but for the RIC scheme, which provides the lowest *NME*. There were 400 sensitivity tests for this scheme. (h) as in (b) but for the DUN scheme with NH₃ set to 0 (DUN_{NH3=0}). (i) as in (c) but for the DUN scheme. (j) as in (i) but with varying organics for condensation growth. The table presents the *NME* results for the corresponding size distributions in panel (a) and associated initial mixing ratios of gas-phase precursors.

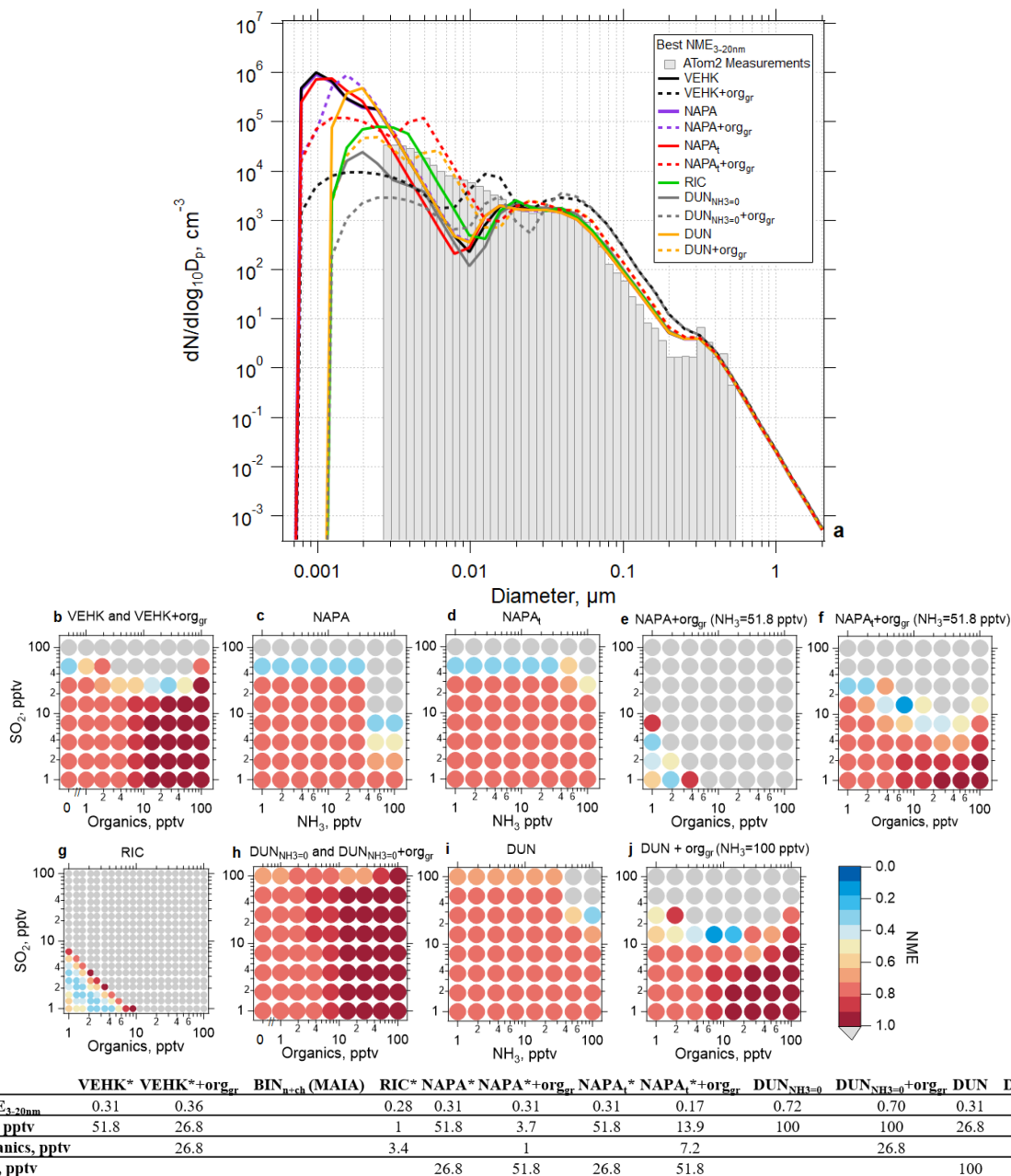


Figure S23: Results of simulations using the TOMAS box model for case sd470 (ATom 2, 2017-02-04, 02:49:31-02:50:30 UTC) where measurements were made 4.5 hours following convective influence, and temperature along the trajectory varied between 223 and 226 K. (a) Observed (shaded bars) and simulated (lines) aerosol size distributions with best normalized mean error (NME) for each of the NPF and growth schemes investigated. (b) NME between the modeled and measured size distribution for the VEHK scheme with varying organics mixing ratios for condensational growth. The color of the circle indicates the value of NME corresponding to a particular initial mixing ratio of SO₂, NH₃, or organics that varied between 0 and 100 pptv. Blue represents the best agreement, red poorer agreement, and grey the worst (NME >1). There were 64 sensitivity tests. (c) As in (b), but for the NAPA scheme. (d) As in (c), but for the NAPAt scheme. (e) and (f) as in (c) and (d) respectively, but with NH₃ fixed and varying organics for condensation growth. (g) as in (b) but for the RIC scheme, which provides the lowest NME. There were 400 sensitivity tests for this scheme. (h) as in (b) but for the DUN scheme with NH₃ set to 0 (DUN_{NH3=0}). (i) as in (c) but for the DUN scheme. (j) as in (i) but with varying organics for condensation growth. The table presents the NME results for the corresponding size distributions in panel (a) and associated initial mixing ratios of gas-phase precursors.

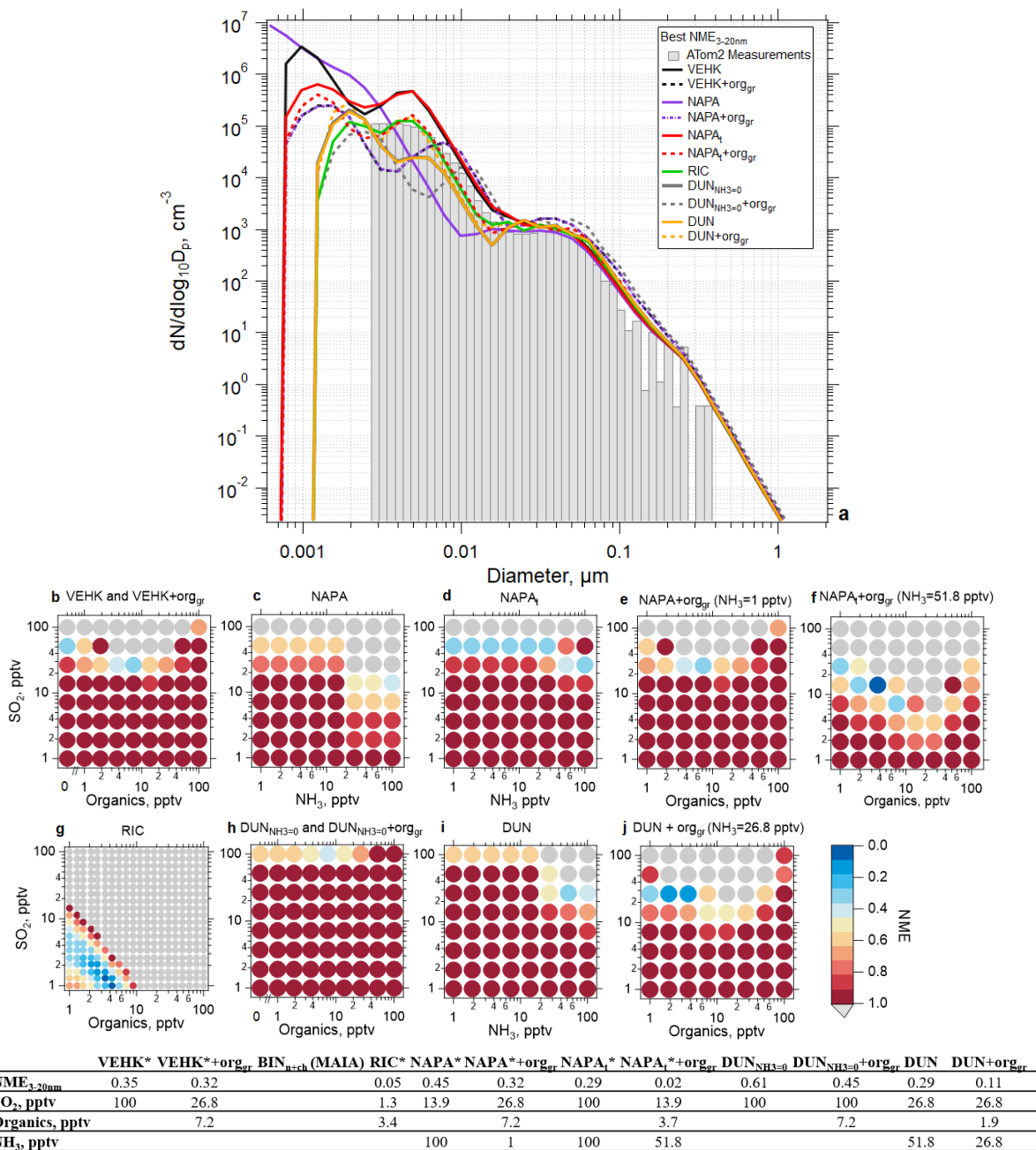


Figure S24: Results of simulations using the TOMAS box model for case sd477 (ATom 2, 2017-02-04, 02:56:31-02:57:30 UTC) where measurements were made 10.5 hours following convective influence, and temperature along the trajectory varied between 220 and 226 K. (a) Observed (shaded bars) and simulated (lines) aerosol size distributions with best normalized mean error (*NME*) for each of the NPF and growth schemes investigated. (b) *NME* between the modeled and measured size distribution for the VEHK scheme with varying organics mixing ratios for condensational growth. The color of the circle indicates the value of *NME* corresponding to a particular initial mixing ratio of SO₂, NH₃, or organics that varied between 0 and 100 pptv. Blue represents the best agreement, red poorer agreement, and grey the worst (*NME* > 1). There were 64 sensitivity tests. (c) As in (b), but for the NAPA scheme. (d) As in (c), but for the NAPAt scheme. (e) and (f) as in (c) and (d) respectively, but with NH₃ fixed and varying organics for condensation growth. (g) as in (b) but for the RIC scheme, which provides the lowest *NME*. There were 400 sensitivity tests for this scheme. (h) as in (b) but for the DUN scheme with NH₃ set to 0 (DUN_{NH3=0}). (i) as in (c) but for the DUN scheme. (j) as in (i) but with varying organics for condensation growth. The table presents the *NME* results for the corresponding size distributions in panel (a) and associated initial mixing ratios of gas-phase precursors.

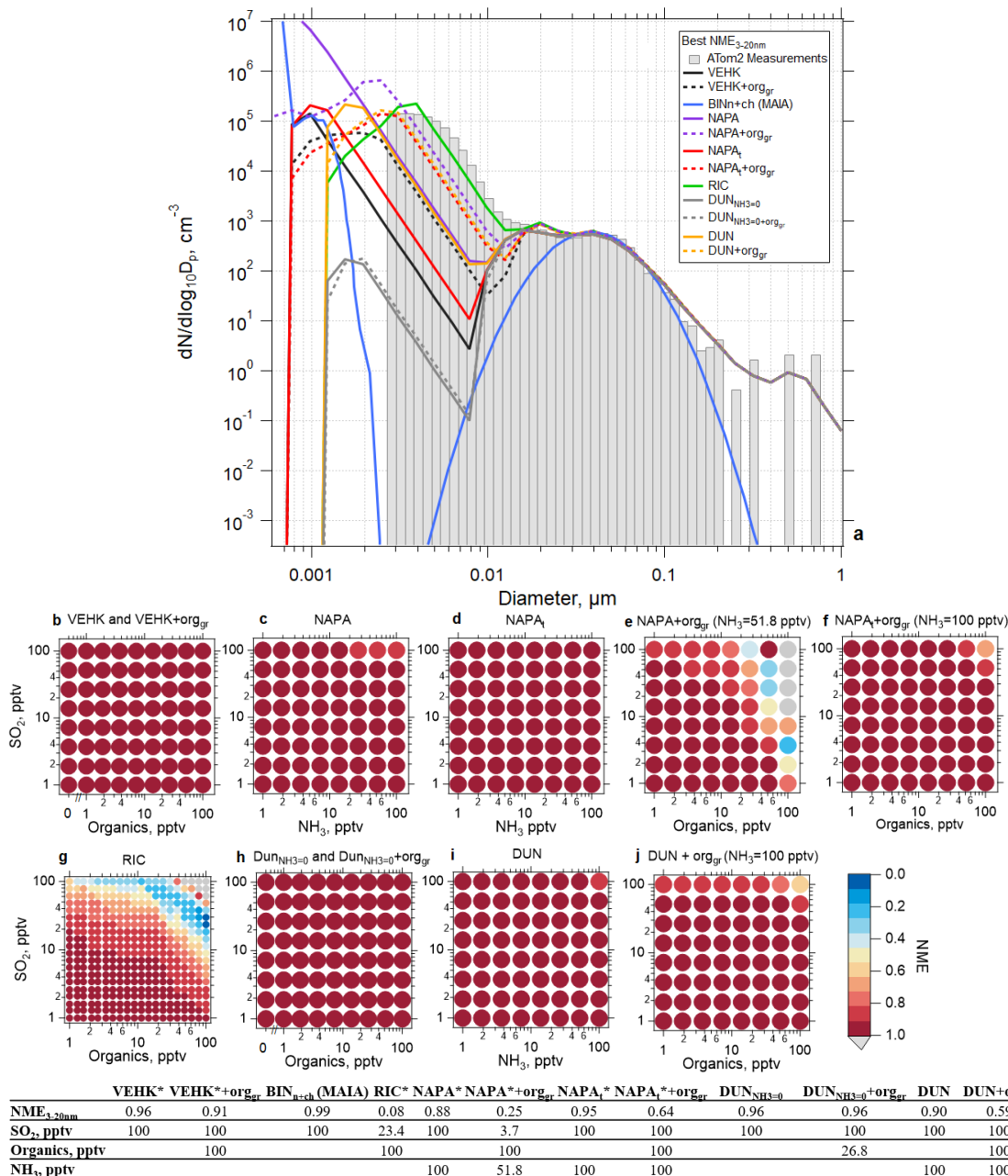


Figure S25: Results of simulations using the TOMAS box model for case sd491 (ATom 2, 2017-02-40, 03:10:31-03:11:30 UTC) where measurements were made 0.4 hour following convective influence, and temperature along the trajectory varied around 226 K. (a) Observed (shaded bars) and simulated (lines) aerosol size distributions with best normalized mean error (*NME*) for each of the NPF and growth schemes investigated. Best results from the MAIA box model ion-assisted + neutral binary nucleation scheme shown as a blue line. (b) *NME* between the modeled and measured size distribution for the VEHK scheme with varying organics mixing ratios for condensational growth. The color of the circle indicates the value of *NME* corresponding to a particular initial mixing ratio of SO₂, NH₃, or organics that varied between 0 and 100 pptv. Blue represents the best agreement, red poorer agreement, and grey the worst (*NME* > 1). There were 64 sensitivity tests. (c) As in (b), but for the NAPA scheme. (d) As in (c), but for the NAPAt scheme. (e) and (f) as in (c) and (d) respectively, but with NH₃ fixed and varying organics for condensation growth. (g) as in (b) but for the RIC scheme, which provides the lowest *NME*. There were 400 sensitivity tests for this scheme. (h) as in (b) but for the DUN scheme with NH₃ set to 0 (DUN_{NH3=0}). (i) as in (c) but for the DUN scheme. (j) as in (i) but with varying organics for condensation growth. The table presents the *NME* results for the corresponding size distributions in panel (a) and associated initial mixing ratios of gas-phase precursors.

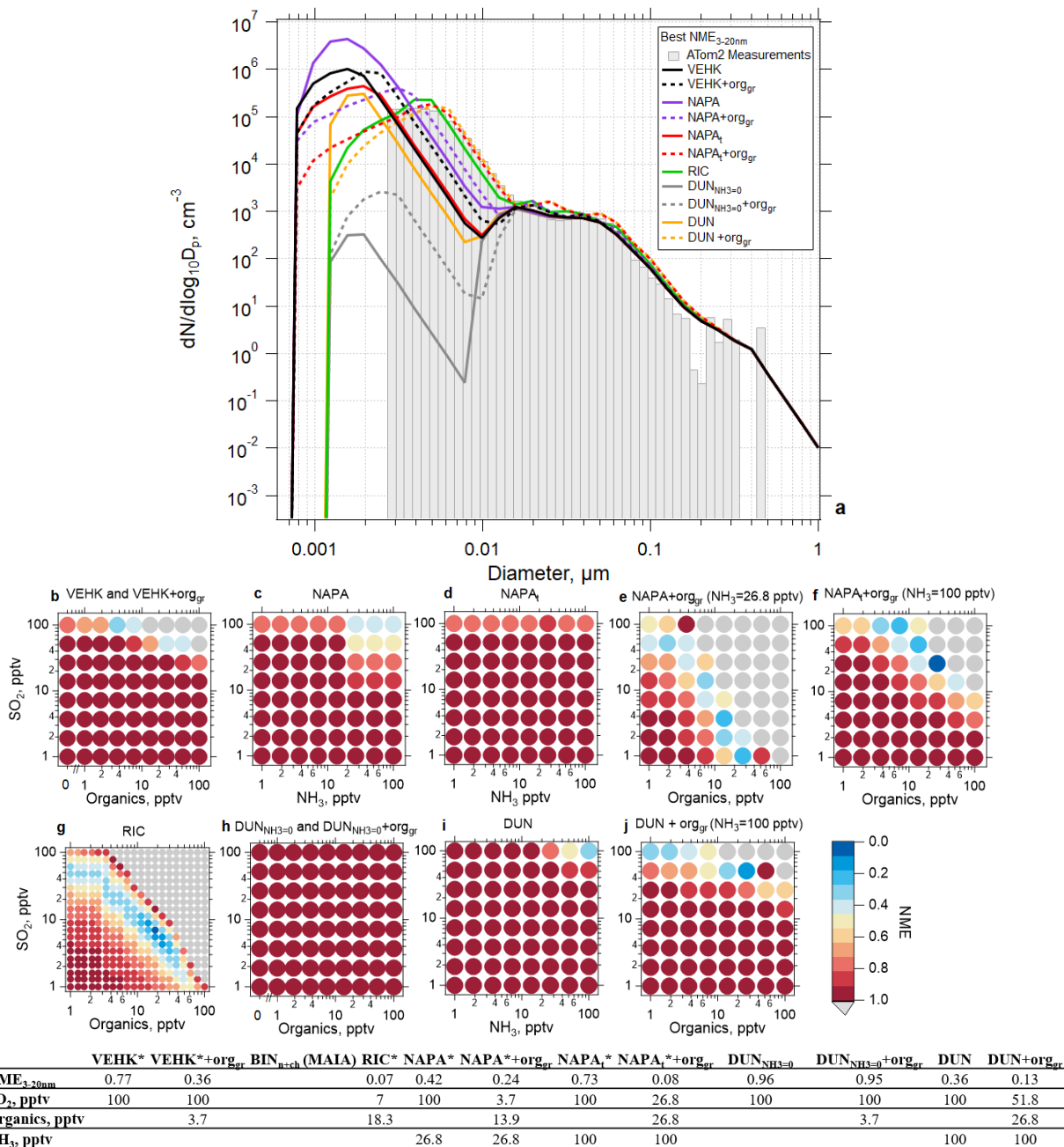


Figure S26: Results of simulations using the TOMAS box model for case sd496 (ATom 2, 2017-02-04, 03:15:31-03:16:30 UTC) where measurements were made 1.48 hours following convective influence, and temperature along the trajectory varied between 226 and 230 K. (a) Observed (shaded bars) and simulated (lines) aerosol size distributions with best normalized mean error (NME) for each of the NPF and growth schemes investigated. (b) NME between the modeled and measured size distribution for the VEHK scheme with varying organics mixing ratios for condensational growth. The color of the circle indicates the value of NME corresponding to a particular initial mixing ratio of SO₂, NH₃, or organics that varied between 0 and 100 pptv. Blue represents the best agreement, red poorer agreement, and grey the worst (NME >1). There were 64 sensitivity tests. (c) As in (b), but for the NAPA scheme. (d) As in (c), but for the NAPA_t scheme. (e) and (f) as in (c) and (d) respectively, but with NH₃ fixed and varying organics for condensation growth. (g) as in (b) but for the RIC scheme, which provides the lowest NME. There were 400 sensitivity tests for this scheme. (h) as in (b) but for the DUN scheme with NH₃ set to 0 (DUN_{NH3=0}). (i) as in (c) but for the DUN scheme. (j) as in (i) but with varying organics for condensation growth. The table presents the NME results for the corresponding size distributions in panel (a) and associated initial mixing ratios of gas-phase precursors.

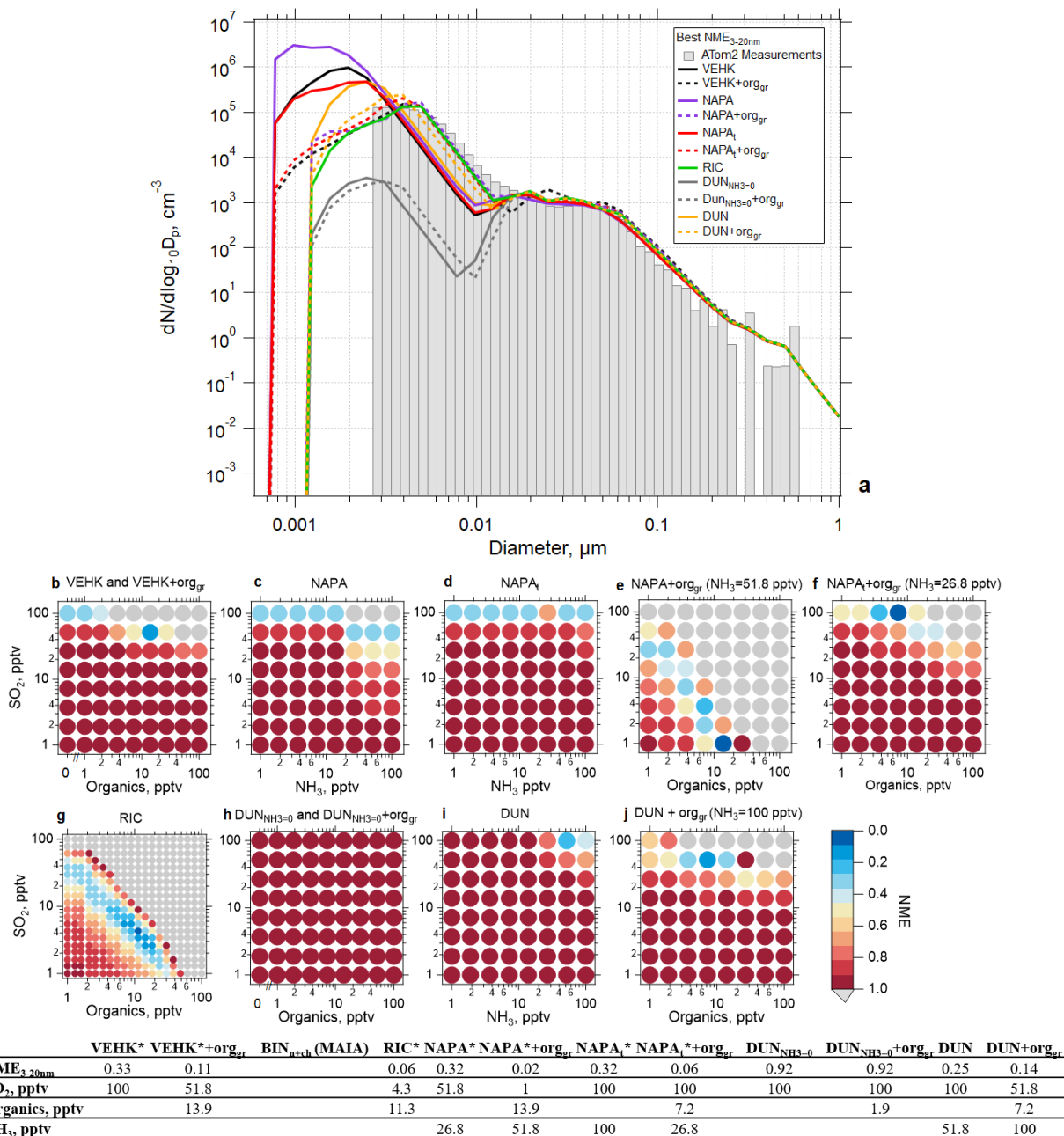


Figure S27: Results of simulations using the TOMAS box model for case sd498 (ATom 2, 2017-02-04, 03:17:31-03:18:30 UTC) where measurements were made 1.95 hours following convective influence, and temperature along the trajectory varied between 226 and 232 K. (a) Observed (shaded bars) and simulated (lines) aerosol size distributions with best normalized mean error (NME) for each of the NPF and growth schemes investigated. (b) NME between the modeled and measured size distribution for the VEHK scheme with varying organics mixing ratios for condensational growth. The color of the circle indicates the value of NME corresponding to a particular initial mixing ratio of SO₂, NH₃, or organics that varied between 0 and 100 pptv. Blue represents the best agreement, red poorer agreement, and grey the worst (NME >1). There were 64 sensitivity tests. (c) As in (b), but for the NAPA scheme. (d) As in (c), but for the NAPAt scheme. (e) and (f) as in (c) and (d) respectively, but with NH₃ fixed and varying organics for condensation growth. (g) as in (b) but for the RIC scheme, which provides the lowest NME. There were 400 sensitivity tests for this scheme. (h) as in (b) but for the DUN scheme with NH₃ set to 0 (DUN_{NH3=0}). (i) as in (c) but for the DUN scheme. (j) as in (i) but with varying organics for condensation growth. The table presents the NME results for the corresponding size distributions in panel (a) and associated initial mixing ratios of gas-phase precursors.

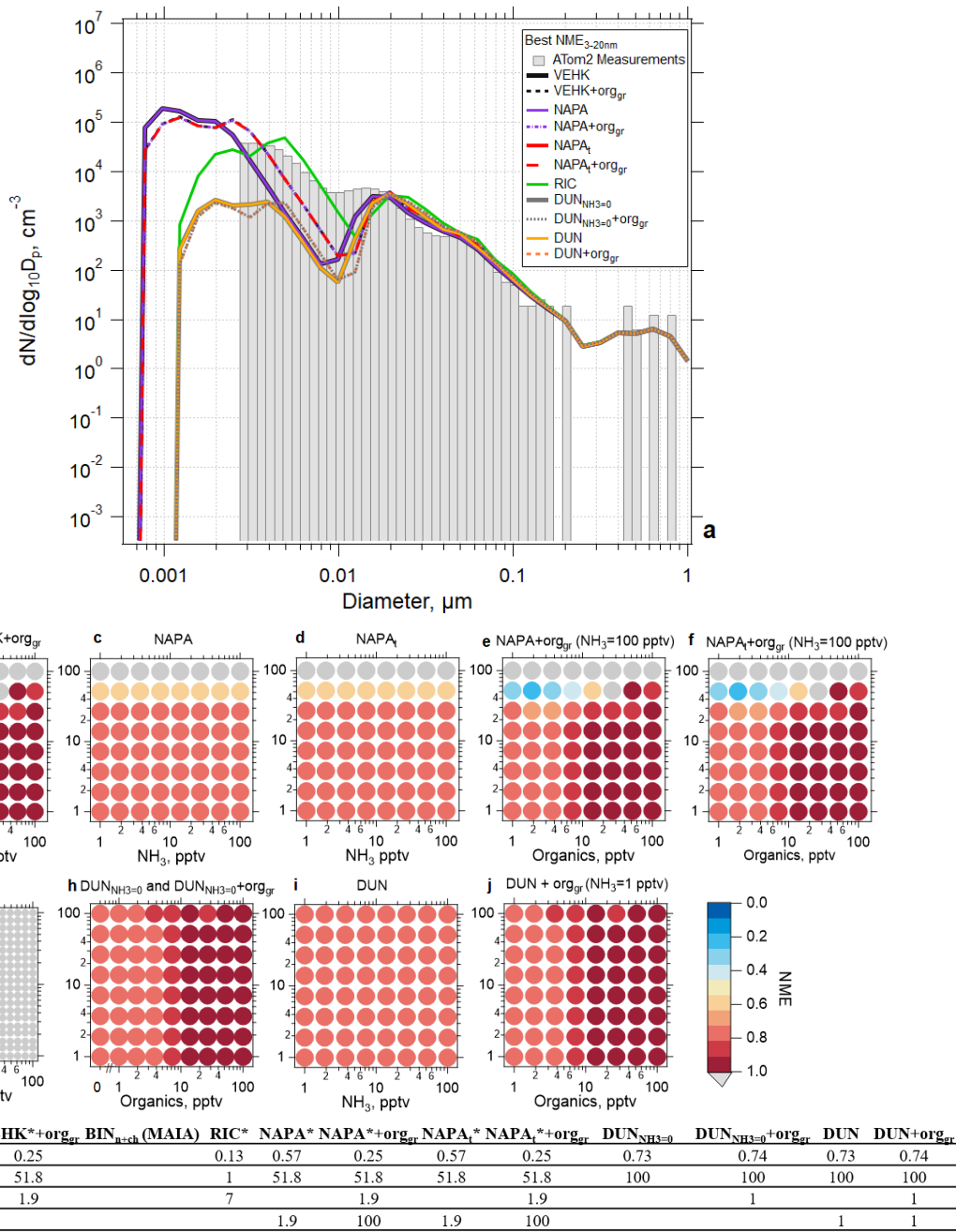


Figure S28: Results of simulations using the TOMAS box model for case sd530 (ATom 2, 2017-02-04, 03:49:31-03:50:30 UTC) where measurements were made 3.72 hours following convective influence, and temperature along the trajectory varied between 228 and 236 K. (a) Observed (shaded bars) and simulated (lines) aerosol size distributions with best normalized mean error (*NME*) for each of the NPF and growth schemes investigated. (b) *NME* between the modeled and measured size distribution for the VEHK scheme with varying organics mixing ratios for condensational growth. The color of the circle indicates the value of *NME* corresponding to a particular initial mixing ratio of SO₂, NH₃, or organics that varied between 0 and 100 pptv. Blue represents the best agreement, red poorer agreement, and grey the worst (*NME* >1). There were 64 sensitivity tests. (c) As in (b), but for the NAPA scheme. (d) As in (c), but for the NAPAt scheme. (e) and (f) as in (c) and (d) respectively, but with NH₃ fixed and varying organics for condensation growth. (g) as in (b) but for the RIC scheme, which provides the lowest *NME*. There were 400 sensitivity tests for this scheme. (h) as in (b) but for the DUN scheme with NH₃ set to 0 (DUN_{NH3=0}). (i) as in (c) but for the DUN scheme. (j) as in (i) but with varying organics for condensation growth. The table presents the *NME* results for the corresponding size distributions in panel (a) and associated initial mixing ratios of gas-phase precursors.

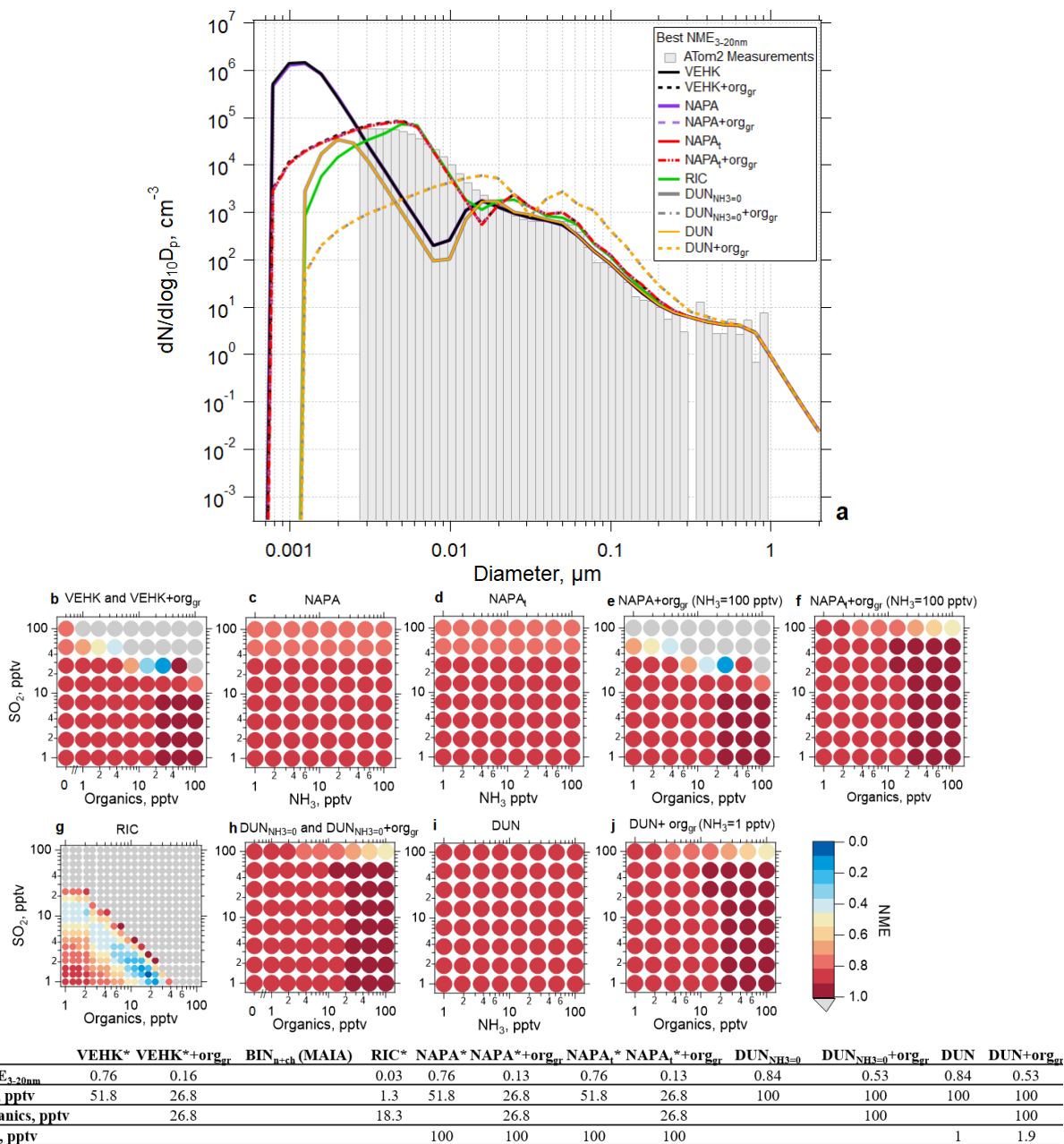


Figure S29: Results of simulations using the TOMAS box model for case sd533 (ATom 2, 2017-02-04, 03:52:31-03:53:30 UTC) where measurements were made 2.9 hours following convective influence, and temperature along the trajectory varied between 228 and 230 K. (a) Observed (shaded bars) and simulated (lines) aerosol size distributions with best normalized mean error (NME) for each of the NPF and growth schemes investigated. (b) NME between the modeled and measured size distribution for the VEHK scheme with varying organics mixing ratios for condensational growth. The color of the circle indicates the value of NME corresponding to a particular initial mixing ratio of SO₂, NH₃, or organics that varied between 0 and 100 pptv. Blue represents the best agreement, red poorer agreement, and grey the worst (NME >1). There were 64 sensitivity tests. (c) As in (b), but for the NAPA scheme. (d) As in (c), but for the NAPAt scheme. (e) and (f) as in (c) and (d) respectively, but with NH₃ fixed and varying organics for condensation growth. (g) as in (b) but for the RIC scheme, which provides the lowest NME. There were 400 sensitivity tests for this scheme. (h) as in (b) but for the DUN scheme with NH₃ set to 0 (DUN_{NH3=0}). (i) as in (c) but for the DUN scheme. (j) as in (i) but with varying organics for condensation growth. The table presents the NME results for the corresponding size distributions in panel (a) and associated initial mixing ratios of gas-phase precursors.

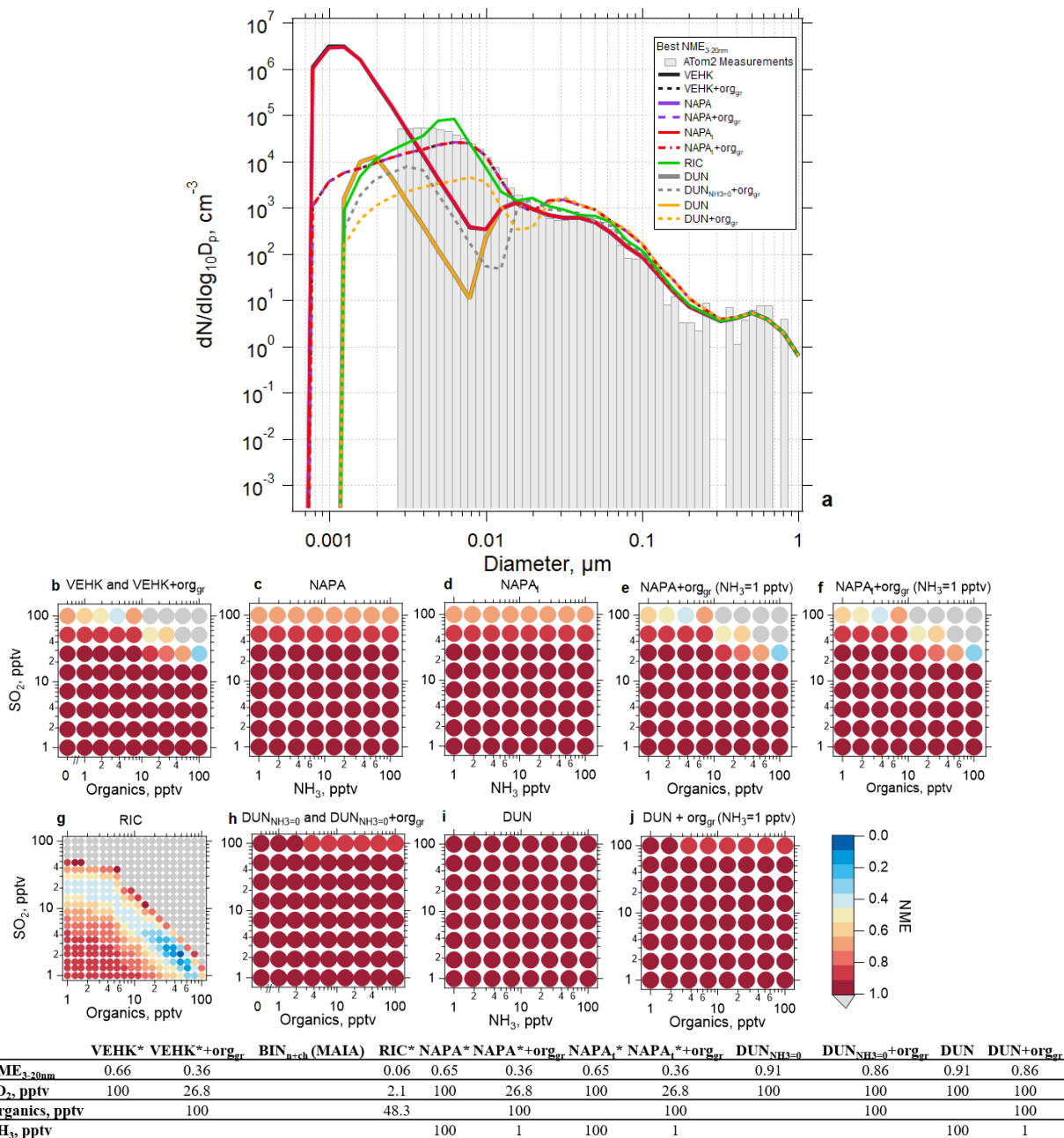


Figure S30: Results of simulations using the TOMAS box model for case sd535 (ATom 2, 2017-02-04, 03:54:31-03:55:30 UTC) where measurements were made 1.88 hours following convective influence, and temperature along the trajectory varied around 228 K. (a) Observed (shaded bars) and simulated (lines) aerosol size distributions with best normalized mean error (NME) for each of the NPF and growth schemes investigated. (b) NME between the modeled and measured size distribution for the VEHK scheme with varying organics mixing ratios for condensational growth. The color of the circle indicates the value of NME corresponding to a particular initial mixing ratio of SO_2 , NH_3 , or organics that varied between 0 and 100 pptv. Blue represents the best agreement, red poorer agreement, and grey the worst ($NME > 1$). There were 64 sensitivity tests. (c) As in (b), but for the NAPA scheme. (d) As in (c), but for the NAPA_t scheme. (e) and (f) as in (c) and (d) respectively, but with NH_3 fixed and varying organics for condensation growth. (g) as in (b) but for the RIC scheme, which provides the lowest NME . There were 400 sensitivity tests for this scheme. (h) as in (b) but for the DUN scheme with NH_3 set to 0 (DUN_{NH3=0}). (i) as in (c) but for the DUN scheme. (j) as in (i) but with varying organics for condensation growth. The table presents the NME results for the corresponding size distributions in panel (a) and associated initial mixing ratios of gas-phase precursors.

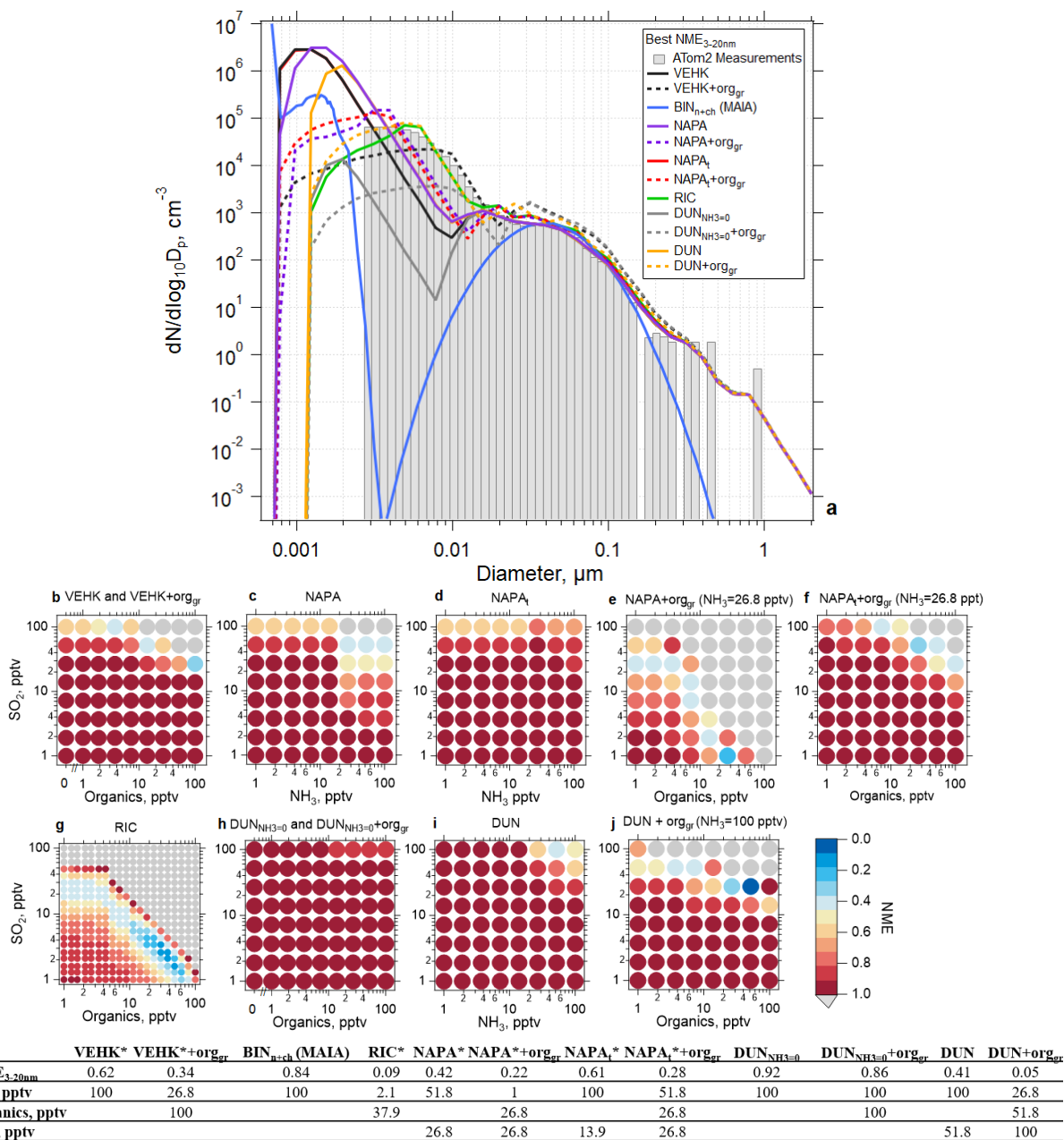


Figure S31: Results of simulations using the TOMAS box model for case sd537 (ATom 2, 2017-02-04, 03:56:31-03:57:30 UTC) where measurements were made 1.7 hours following convective influence, and temperature along the trajectory varied around 228 K. (a) Observed (shaded bars) and simulated (lines) aerosol size distributions with best normalized mean error (*NME*) for each of the NPF and growth schemes investigated. Best results from the MAIA box model ion-assisted + neutral binary nucleation scheme shown as a blue line. (b) *NME* between the modeled and measured size distribution for the VEHK scheme with varying organics mixing ratios for condensational growth. The color of the circle indicates the value of *NME* corresponding to a particular initial mixing ratio of SO₂, NH₃, or organics that varied between 0 and 100 pptv. Blue represents the best agreement, red poorer agreement, and grey the worst (*NME* > 1). There were 64 sensitivity tests. (c) As in (b), but for the NAPA scheme. (d) As in (c), but for the NAPAt scheme. (e) and (f) as in (c) and (d) respectively, but with NH₃ fixed and varying organics for condensation growth. (g) as in (b) but for the RIC scheme, which provides the lowest *NME*. There were 400 sensitivity tests for this scheme. (h) as in (b) but for the DUN scheme with NH₃ set to 0 (DUN_{NH3=0}). (i) as in (c) but for the DUN scheme. (j) as in (i) but with varying organics for condensation growth. The table presents the *NME* results for the corresponding size distributions in panel (a) and associated initial mixing ratios of gas-phase precursors.

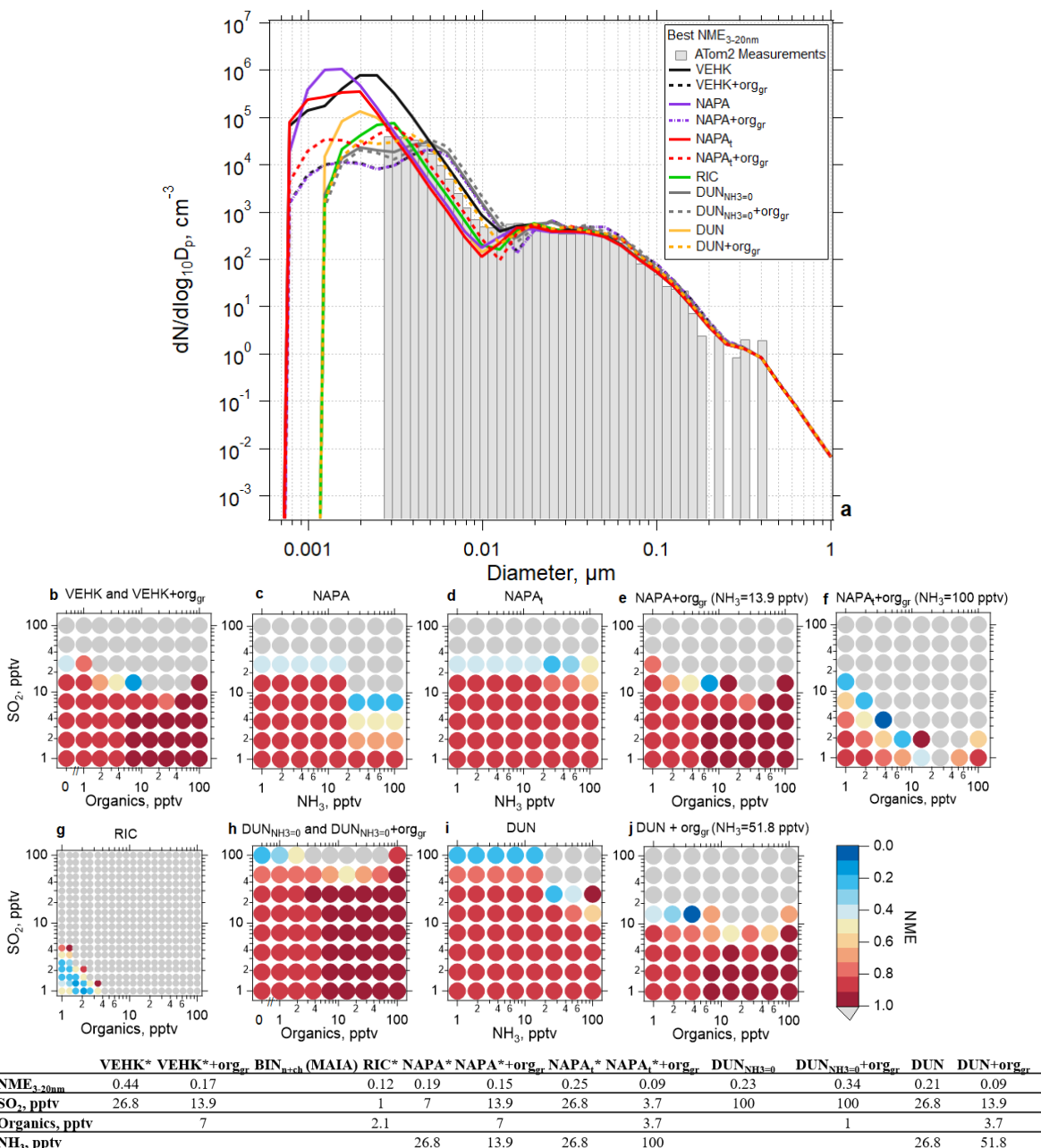
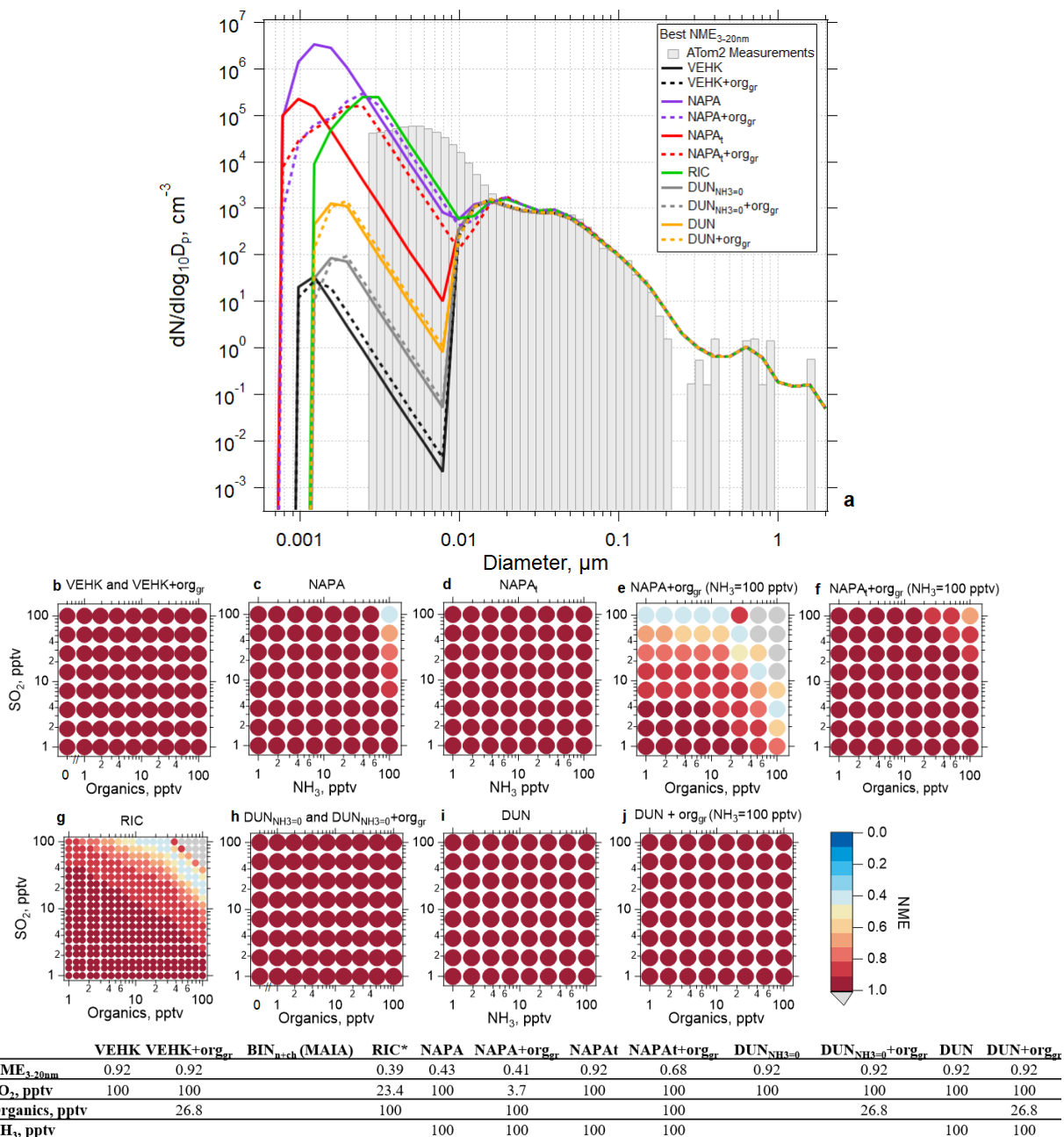


Figure S32: Results of simulations using the TOMAS box model for case sd540 (ATom 2, 2017-02-04, 03:59:31-04:00:30 UTC) where measurements were made 3.4 hours following convective influence, and temperature along the trajectory varied between 228 and 231 K. (a) Observed (shaded bars) and simulated (lines) aerosol size distributions with best normalized mean error (*NME*) for each of the NPF and growth schemes investigated. Best results from the MAIA box model ion-assisted + neutral binary nucleation scheme shown as a blue line. (b) *NME* between the modeled and measured size distribution for the VEHK scheme with varying organics mixing ratios for condensational growth. The color of the circle indicates the value of *NME* corresponding to a particular initial mixing ratio of SO₂, NH₃, or organics that varied between 0 and 100 pptv. Blue represents the best agreement, red poorer agreement, and grey the worst (*NME* >1). There were 64 sensitivity tests. (c) As in (b), but for the NAPA scheme. (d) As in (c), but for the NAPAt scheme. (e) and (f) as in (c) and (d) respectively, but with NH₃ fixed and varying organics for condensational growth. (g) as in (b) but for the RIC scheme, which provides the lowest *NME*. There were 400 sensitivity tests for this scheme. (h) as in (b) but for the DUN scheme with NH₃ set to 0 (DUN_{NH3=0}). (i) as in (c) but for the DUN scheme. (j) as in (i) but with varying organics for condensation growth. The table presents the *NME* results for the corresponding size distributions in panel (a) and associated initial mixing ratios of gas-phase precursors.



*Temperature along the trajectory does not lie within the temperature range of the scheme

Figure S33: Results of simulations using the TOMAS box model for case sd543 (ATom 2, 2017-02-04, 03:02:31-03:03:30 UTC) where measurements were made 0.81 hour following convective influence, and temperature along the trajectory varied between 247 and 248 K. (a) Observed (shaded bars) and simulated (lines) aerosol size distributions with best normalized mean error (NME) for each of the NPF and growth schemes investigated. (b) NME between the modeled and measured size distribution for the VEHK scheme with varying organics mixing ratios for condensational growth. The color of the circle indicates the value of NME corresponding to a particular initial mixing ratio of SO₂, NH₃, or organics that varied between 0 and 100 pptv. Blue represents the best agreement, red poorer agreement, and grey the worst (NME >1). There were 64 sensitivity tests. (c) As in (b), but for the NAPA scheme. (d) As in (c), but for the NAPAt scheme. (e) and (f) as in (c) and (d) respectively, but with NH₃ fixed and varying organics for condensational growth. (g) as in (b) but for the RIC scheme, which provides the lowest NME. There were 400 sensitivity tests for this scheme. (h) as in (b) but for the DUN scheme with NH₃ set to 0 (DUN_{NH3=0}). (i) as in (c) but for the DUN scheme. (j) as in (i) but with varying organics for condensational growth. The table presents the NME results for the corresponding size distributions in panel (a) and associated initial mixing ratios of gas-phase precursors.

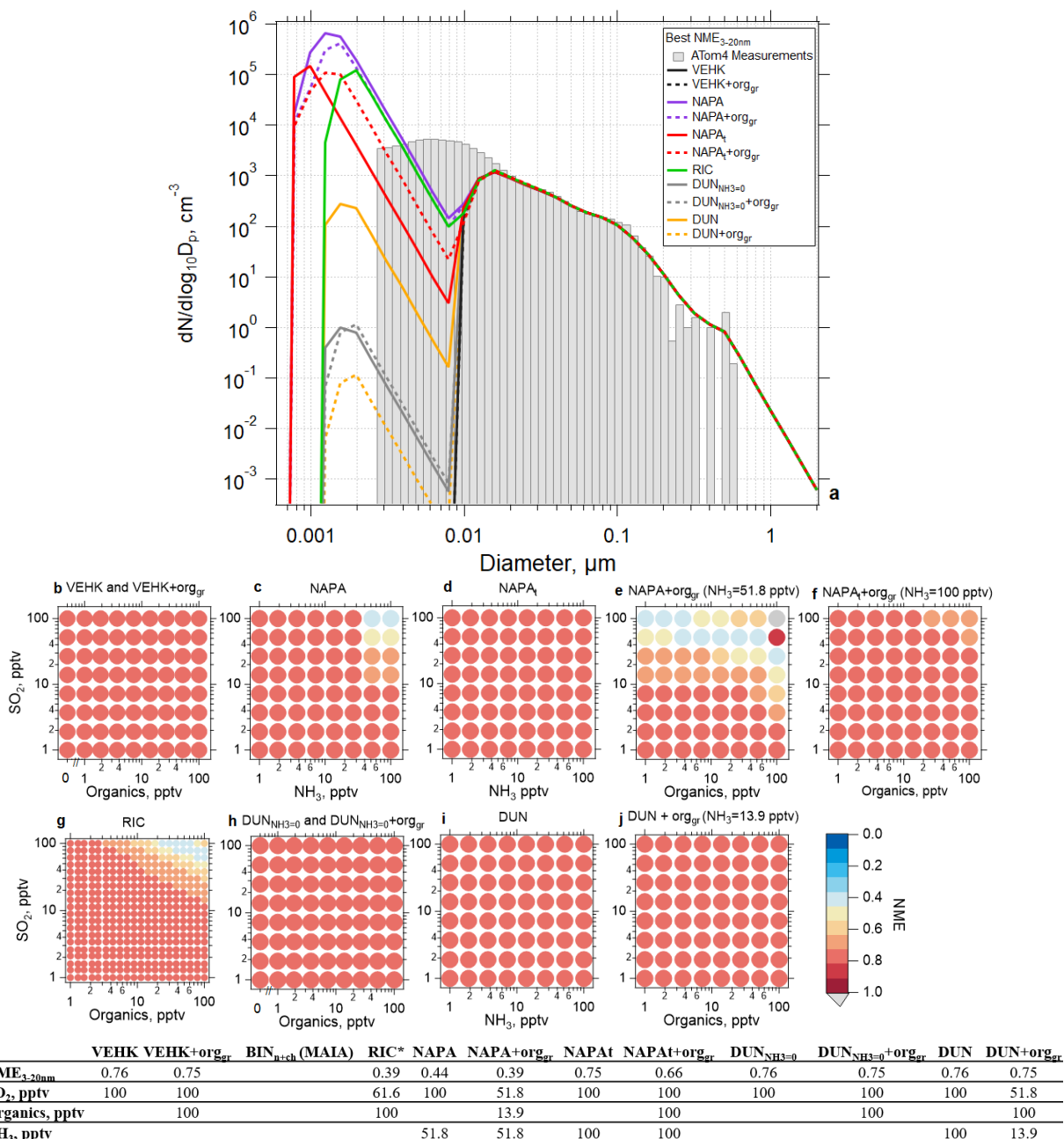


Figure S34: Results of simulations using the TOMAS box model for case sd22 (ATom 4, 2018-05-01, 19:17:31-19:18:30 UTC) where measurements were made 2.84 hours following convective influence, and temperature along the trajectory varied between 245 and 246 K. (a) Observed (shaded bars) and simulated (lines) aerosol size distributions with best normalized mean error (*NME*) for each of the NPF and growth schemes investigated. (b) *NME* between the modeled and measured size distribution for the VEHK scheme with varying organics mixing ratios for condensational growth. The color of the circle indicates the value of *NME* corresponding to a particular initial mixing ratio of SO₂, NH₃, or organics that varied between 0 and 100 pptv. Blue represents the best agreement, red poorer agreement, and grey the worst (*NME* >1). There were 64 sensitivity tests. (c) As in (b), but for the NAPA scheme. (d) As in (c), but for the NAPAt scheme. (e) and (f) as in (c) and (d) respectively, but with NH₃ fixed and varying organics for condensational growth. (g) as in (b) but for the RIC scheme, which provides the lowest *NME*. There were 400 sensitivity tests for this scheme. (h) as in (b) but for the DUN scheme with NH₃ set to 0 (DUN_{NH3=0}). (i) as in (c) but for the DUN scheme. (j) as in (i) but with varying organics for condensational growth. The table presents the *NME* results for the corresponding size distributions in panel (a) and associated initial mixing ratios of gas-phase precursors.

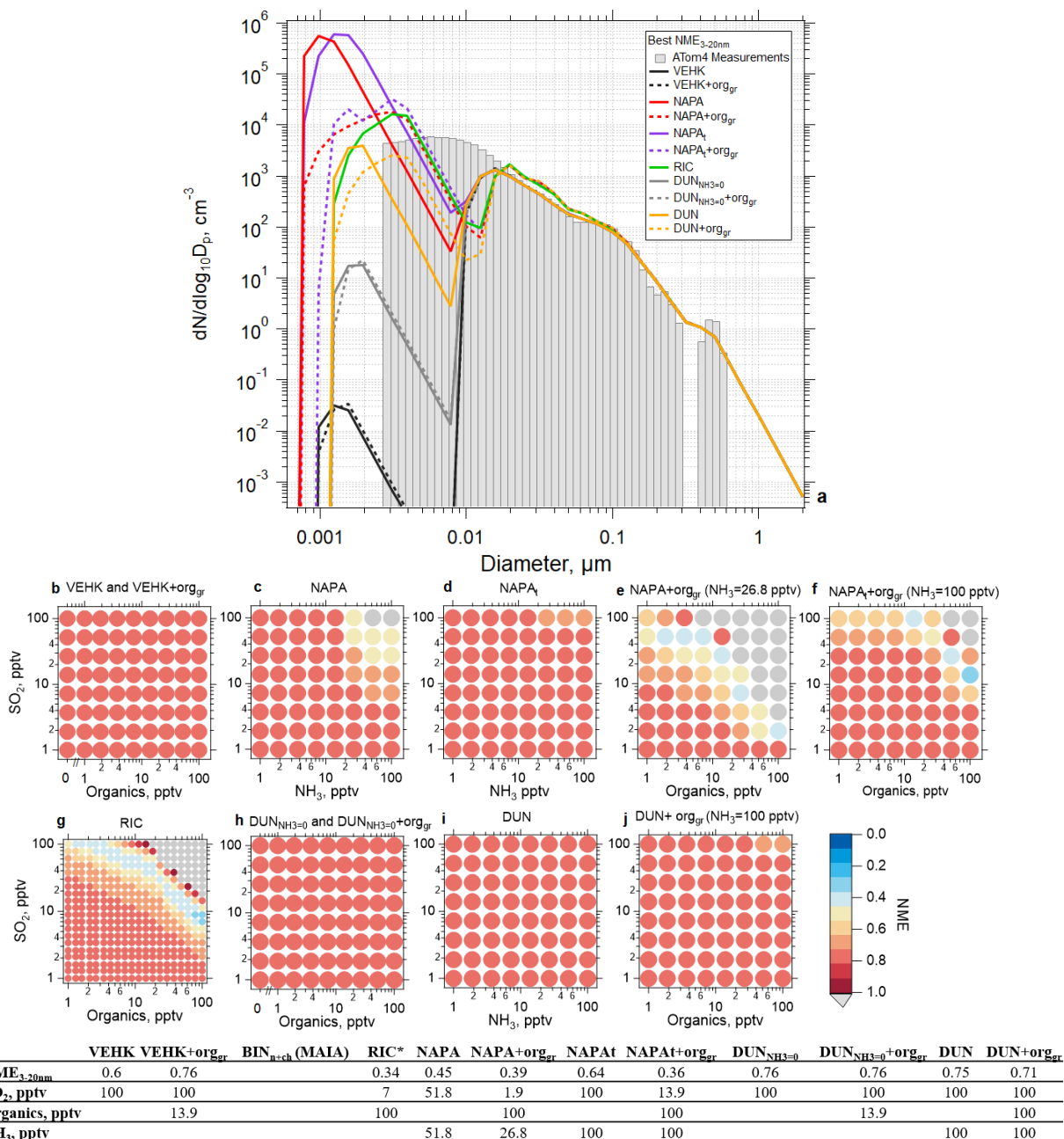


Figure S35: Results of simulations using the TOMAS box model for case sd32 (ATom 4, 2018-05-01, 19:27:31-19:28:30 UTC) where measurements were made 6.55 hours following convective influence, and temperature along the trajectory varied between 245 and 247 K. (a) Observed (shaded bars) and simulated (lines) aerosol size distributions with best normalized mean error (*NME*) for each of the NPF and growth schemes investigated. (b) *NME* between the modeled and measured size distribution for the VEHK scheme with varying organics mixing ratios for condensational growth. The color of the circle indicates the value of *NME* corresponding to a particular initial mixing ratio of SO₂, NH₃, or organics that varied between 0 and 100 pptv. Blue represents the best agreement, red poorer agreement, and grey the worst (*NME* >1). There were 64 sensitivity tests. (c) As in (b), but for the NAPA scheme. (d) As in (c), but for the NAPAt scheme. (e) and (f) as in (c) and (d) respectively, but with NH₃ fixed and varying organics for condensational growth. (g) as in (b) but for the RIC scheme, which provides the lowest *NME*. There were 400 sensitivity tests for this scheme. (h) as in (b) but for the DUN scheme with NH₃ set to 0 (DUN_{NH3=0}). (i) as in (c) but for the DUN scheme. (j) as in (i) but with varying organics for condensational growth. The table presents the *NME* results for the corresponding size distributions in panel (a) and associated initial mixing ratios of gas-phase precursors.

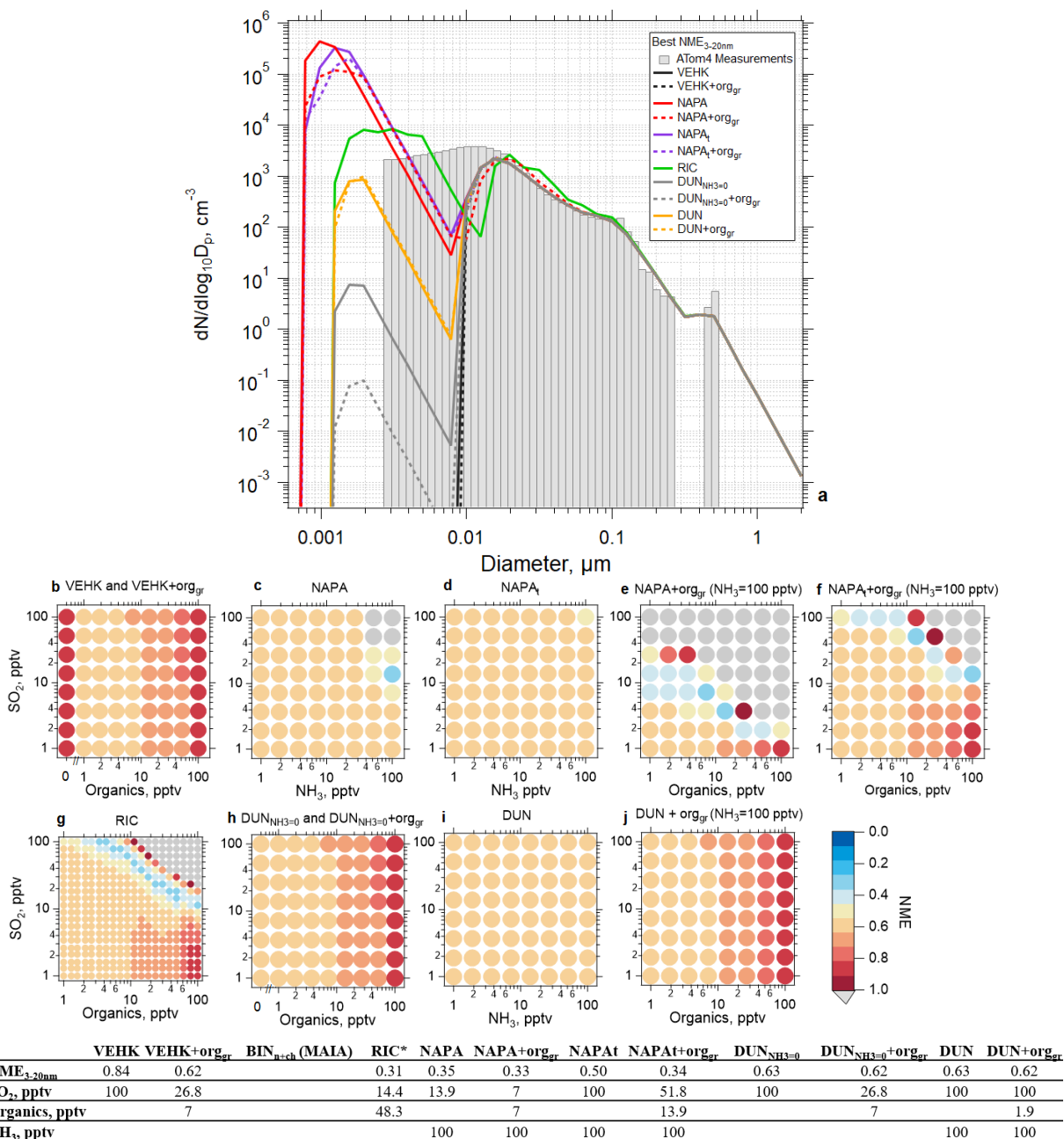
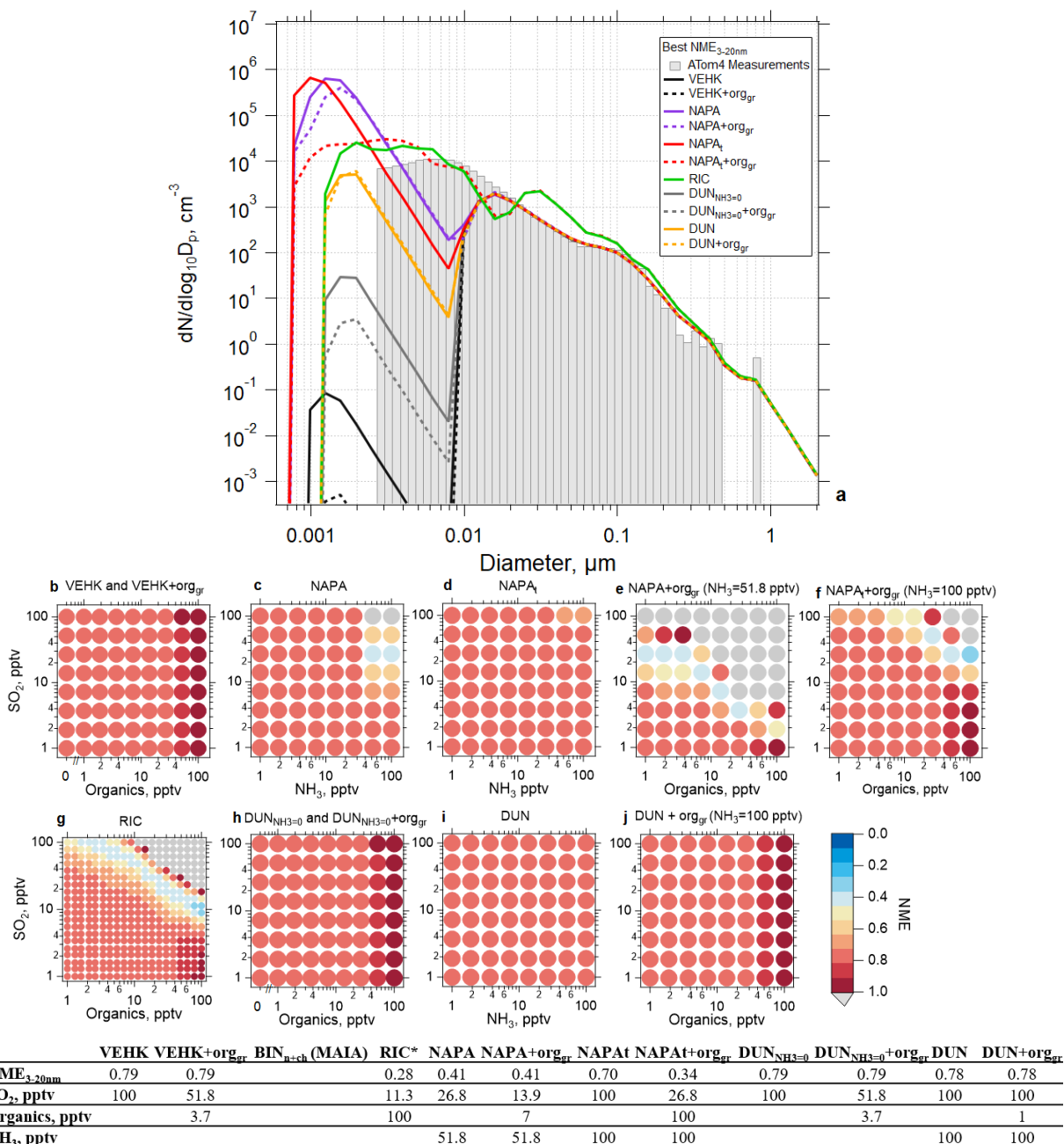
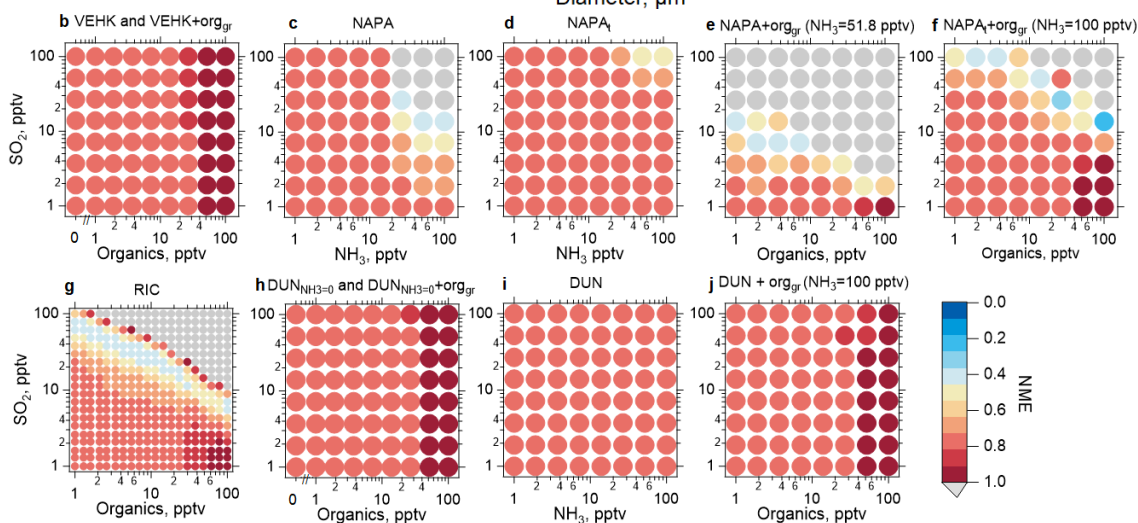
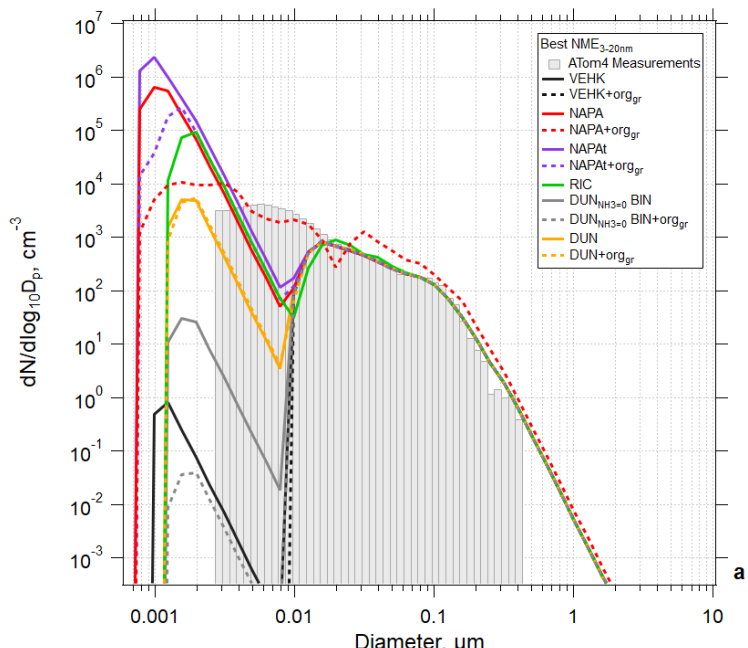


Figure S36: Results of simulations using the TOMAS box model for case sd72 (ATom 4, 2018-05-01, 20:07:31-20:18:30 UTC) where measurements were made 11.04 hours following convective influence, and temperature along the trajectory varied between 249 and 252 K. (a) Observed (shaded bars) and simulated (lines) aerosol size distributions with best normalized mean error (*NME*) for each of the NPF and growth schemes investigated. (b) *NME* between the modeled and measured size distribution for the VEHK scheme with varying organics mixing ratios for condensational growth. The color of the circle indicates the value of *NME* corresponding to a particular initial mixing ratio of SO₂, NH₃, or organics that varied between 0 and 100 pptv. Blue represents the best agreement, red poorer agreement, and grey the worst (*NME* >1). There were 64 sensitivity tests. (c) As in (b), but for the NAPA scheme. (d) As in (c), but for the NAPAt scheme. (e) and (f) as in (c) and (d) respectively, but with NH₃ fixed and varying organics for condensational growth. (g) as in (b) but for the RIC scheme, which provides the lowest *NME*. There were 400 sensitivity tests for this scheme. (h) as in (b) but for the DUN scheme with NH₃ set to 0 (DUN_{NH3=0}). (i) as in (c) but for the DUN scheme. (j) as in (i) but with varying organics for condensational growth. The table presents the *NME* results for the corresponding size distributions in panel (a) and associated initial mixing ratios of gas-phase precursors.



*Temperature along the trajectory does not lie within the temperature range of the scheme

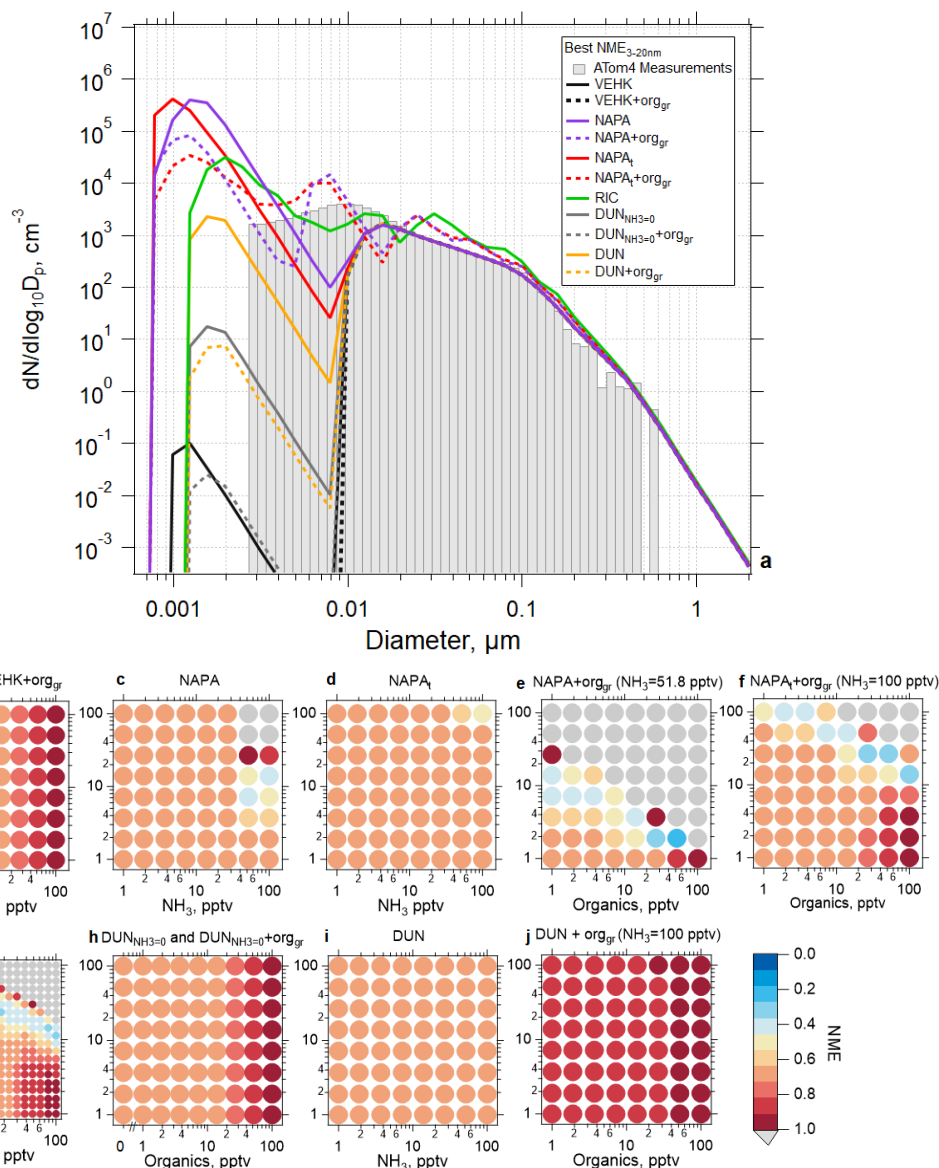
Figure S37: Results of simulations using the TOMAS box model for case sd75 (ATom 4, 2018-05-01, 20:10:31-20:10:30 UTC) where measurements were made 11.99 hours following convective influence, and temperature along the trajectory varied between 243 and 247 K. (a) Observed (shaded bars) and simulated (lines) aerosol size distributions with best normalized mean error (NME) for each of the NPF and growth schemes investigated. (b) NME between the modeled and measured size distribution for the VEHK scheme with varying organics mixing ratios for condensational growth. The color of the circle indicates the value of NME corresponding to a particular initial mixing ratio of SO₂, NH₃, or organics that varied between 0 and 100 pptv. Blue represents the best agreement, red poorer agreement, and grey the worst (NME >1). There were 64 sensitivity tests. (c) As in (b), but for the NAPA scheme. (d) As in (c), but for the NAPAt scheme. (e) and (f) as in (c) and (d) respectively, but with NH₃ fixed and varying organics for condensational growth. (g) as in (b) but for the RIC scheme, which provides the lowest NME. There were 400 sensitivity tests for this scheme. (h) as in (b) but for the DUN scheme with NH₃ set to 0 (DUN_{NH3=0}). (i) as in (c) but for the DUN scheme. (j) as in (i) but with varying organics for condensational growth. The table presents the NME results for the corresponding size distributions in panel (a) and associated initial mixing ratios of gas-phase precursors.



	VEHK	VEHK+org _{gr}	BIN _{n=ch} (MAIA)	RIC*	NAPA	NAPA+org _{gr}	NAPAt	NAPAt+org _{gr}	DUN _{NH3=0}	DUN _{NH3=0} +org _{gr}	DUN	DUN+org
Best NME _{3-20nm}	0.76	0.76		0.38	0.43	0.37	0.47	0.20	0.76	0.76	0.74	0.74
SO ₂ , pptv	100	7		23.4	26.8	7	100	13.9	100	13.9	100	100
Organics, pptv		3.7		8.9		3.7		100		3.7		1
NH ₃ , pptv					26.8	51.8	100	100			100	100

*Temperature along the trajectory does not lie within the temperature range of the scheme

Figure S38: Results of simulations using the TOMAS box model for case sd78 (ATom 4, 2018-05-01, 20:13:31-20:14:30 UTC) where measurements were made 13.76 hours following convective influence, and temperature along the trajectory varied between 244 and 250 K. (a) Observed (shaded bars) and simulated (lines) aerosol size distributions with best normalized mean error (NME) for each of the NPF and growth schemes investigated. (b) NME between the modeled and measured size distribution for the VEHK scheme with varying organics mixing ratios for condensational growth. The color of the circle indicates the value of NME corresponding to a particular initial mixing ratio of SO₂, NH₃, or organics that varied between 0 and 100 pptv. Blue represents the best agreement, red poorer agreement, and grey the worst (NME >1). There were 64 sensitivity tests. (c) As in (b), but for the NAPA scheme. (d) As in (c), but for the NAPAt scheme. (e) and (f) as in (c) and (d) respectively, but with NH₃ fixed and varying organics for condensation growth. (g) as in (b) but for the RIC scheme, which provides the lowest NME. There were 400 sensitivity tests for this scheme. (h) as in (b) but for the DUN scheme with NH₃ set to 0 (DUN_{NH3=0}). (i) as in (c) but for the DUN scheme. (j) as in (i) but with varying organics for condensation growth. The table presents the NME results for the corresponding size distributions in panel (a) and associated initial mixing ratios of gas-phase precursors.



	VEHK	VEHK+org _{gr}	BIN _{n=ch} (MAIA)	RIC*	NAPA	NAPA+org _{gr}	NAPAt	NAPAt+org _{gr}	DUN _{NH3=0}	DUN _{NH3=0} +org _{gr}	DUN	DUN+org _{gr}
NME_{3-20nm}	0.67	0.67		0.27	0.44	0.21	0.54	0.32	0.67	0.67	0.67	0.85
SO₂, pptv	100	13.9		11.3	13.9	1.9	100	26.8	100	13.9	100	13.9
Organics, pptv		3.7		100		51.8		51.8		3.7		3.7
NH₃, pptv					100	51.8	100	100				100

Figure S39: Results of simulations using the TOMAS box model for case sd82 (ATom 4, 2018-05-01, 20:17:31-20:18:30 UTC) where measurements were made 14.57 hours following convective influence, and temperature along the trajectory varied between 245 and 245 K. (a) Observed (shaded bars) and simulated (lines) aerosol size distributions with best normalized mean error (NME) for each of the NPF and growth schemes investigated. (b) NME between the modeled and measured size distribution for the VEHK scheme with varying organics mixing ratios for condensational growth. The color of the circle indicates the value of NME corresponding to a particular initial mixing ratio of SO₂, NH₃, or organics that varied between 0 and 100 pptv. Blue represents the best agreement, red poorer agreement, and grey the worst (NME >1). There were 64 sensitivity tests. (c) As in (b), but for the NAPA scheme. (d) As in (c), but for the NAPAt scheme. (e) and (f) as in (c) and (d) respectively, but with NH₃ fixed and varying organics for condensation growth. (g) as in (b) but for the RIC scheme, which provides the lowest NME. There were 400 sensitivity tests for this scheme. (h) as in (b) but for the DUN scheme with NH₃ set to 0 (DUN_{NH3=0}). (i) as in (c) but for the DUN scheme. (j) as in (i) but with varying organics for condensation growth. The table presents the NME results for the corresponding size distributions in panel (a) and associated initial mixing ratios of gas-phase precursors.

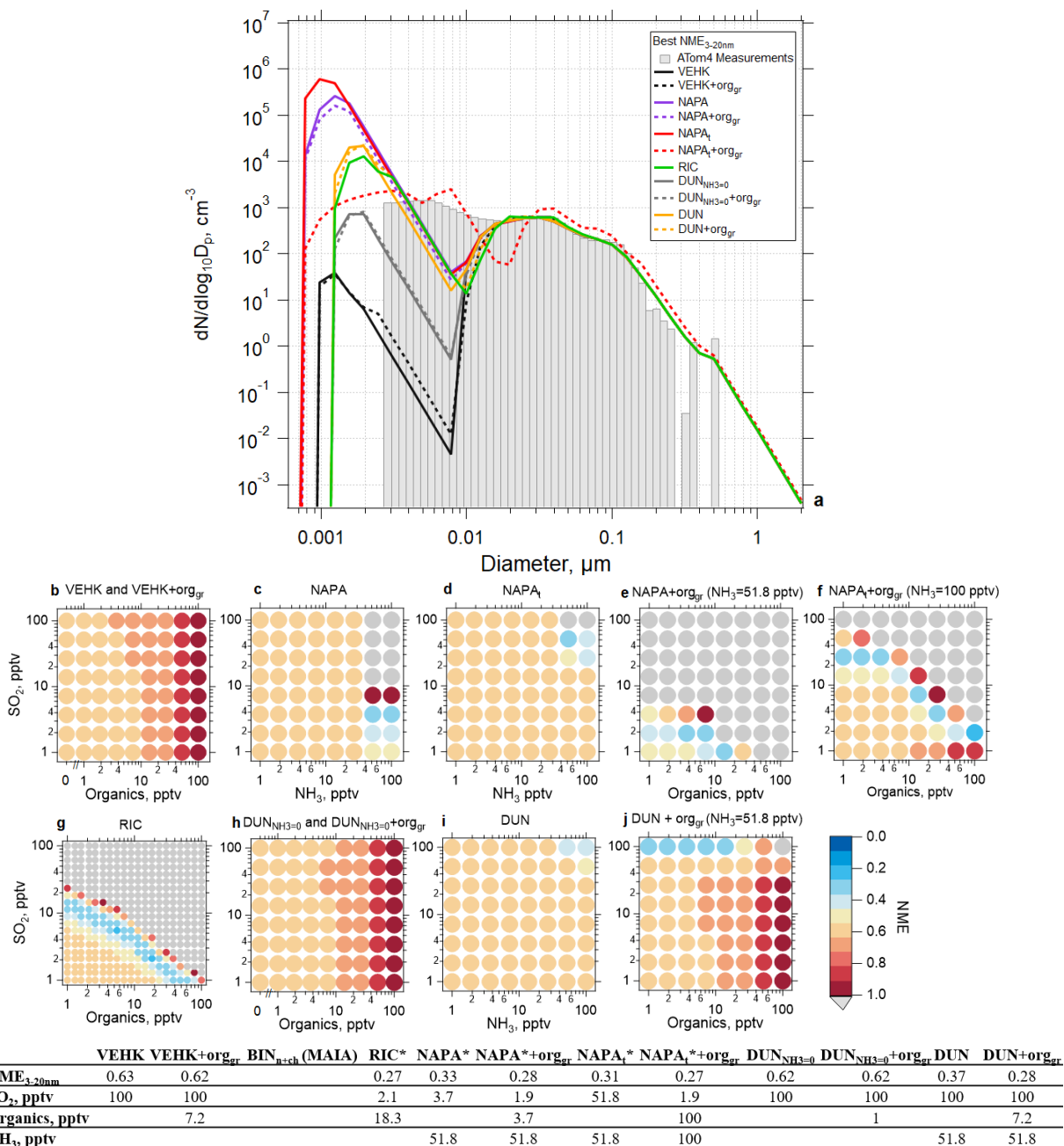
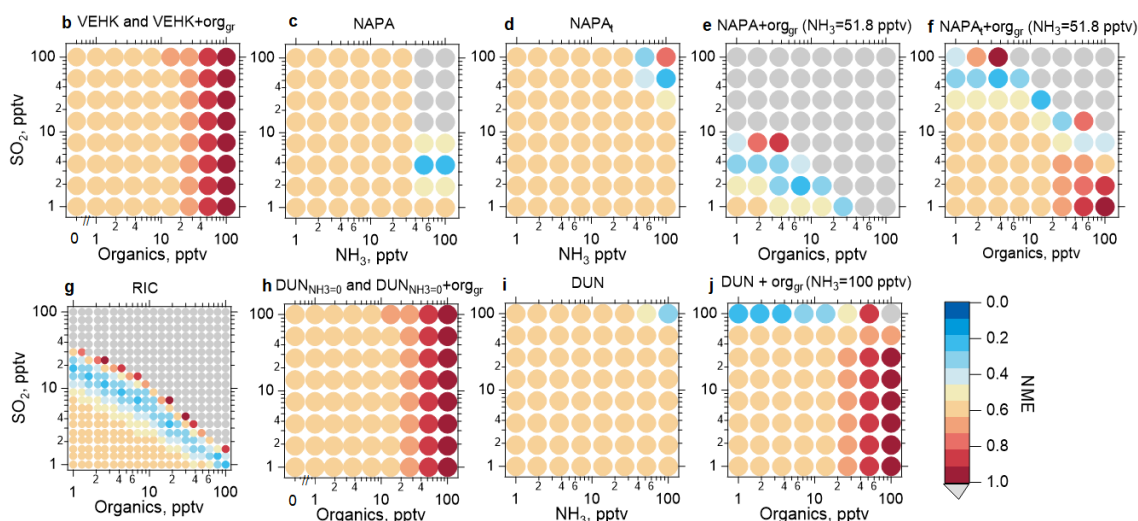
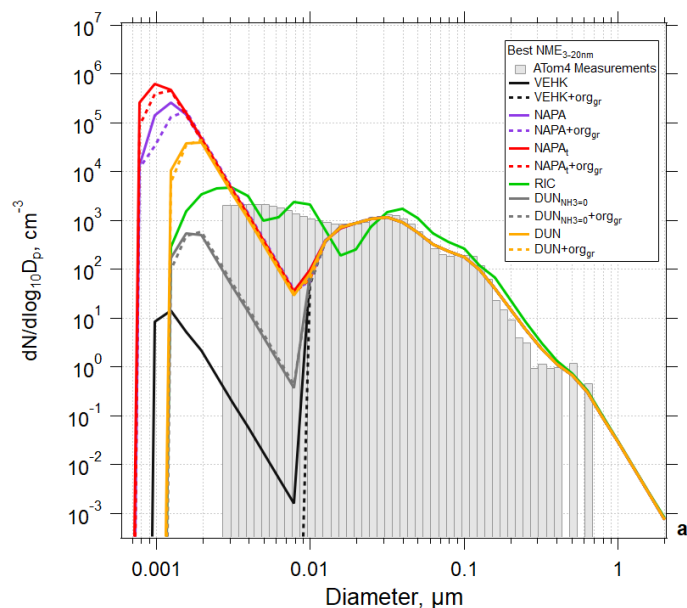


Figure S40: Results of simulations using the TOMAS box model for case sd132 (ATom 4, 2018-05-01, 21:08:31-21:09:30 UTC) where measurements were made 12.99 hours following convective influence, and temperature along the trajectory varied between 235 and 248 K. (a) Observed (shaded bars) and simulated (lines) aerosol size distributions with best normalized mean error (NME) for each of the NPF and growth schemes investigated. (b) NME between the modeled and measured size distribution for the VEHK scheme with varying organics mixing ratios for condensational growth. The color of the circle indicates the value of NME corresponding to a particular initial mixing ratio of SO₂, NH₃, or organics that varied between 0 and 100 pptv. Blue represents the best agreement, red poorer agreement, and grey the worst (NME >1). There were 64 sensitivity tests. (c) As in (b), but for the NAPA scheme. (d) As in (c), but for the NAPAt scheme. (e) and (f) as in (c) and (d) respectively, but with NH₃ fixed and varying organics for condensation growth. (g) as in (b) but for the RIC scheme, which provides the lowest NME. There were 400 sensitivity tests for this scheme. (h) as in (b) but for the DUN scheme with NH₃ set to 0 (DUN_{NH3=0}). (i) as in (c) but for the DUN scheme. (j) as in (i) but with varying organics for condensation growth. The table presents the NME results for the corresponding size distributions in panel (a) and associated initial mixing ratios of gas-phase precursors.



	VEHK	VEHK+org _{gr}	BIN _{n+ch} (MAIA)	RIC*	NAPA*	NAPA*+org _{gr}	NAPA _A *	NAPA*+org _{gr}	DUN _{NH3=0}	DUN _{NH3=0} +org _{gr}	DUN	DUN+org _{gr}
NME _{3-20nm}	0.61	0.60		0.22	0.26	0.26	0.26	0.27	0.60	0.60	0.31	0.27
SO ₂ , pptv	100	7		1	3.7	1.9	51.8	51.8	100	100	100	100
Organics, pptv		7		100		7		3.7		1.9		1
NH ₃ , pptv					51.8	51.8	100	51.8		100	100	100

*Temperature along the trajectory does not lie within the temperature range of the scheme

Figure S41: Results of simulations using the TOMAS box model for case sd134 (ATom 4, 2018-05-01, 21:09:31-21:10:30 UTC) where measurements were made 13.55 hours following convective influence, and temperature along the trajectory varied between 235 and 248 K. (a) Observed (shaded bars) and simulated (lines) aerosol size distributions with best normalized mean error (*NME*) for each of the NPF and growth schemes investigated. (b) *NME* between the modeled and measured size distribution for the VEHK scheme with varying organics mixing ratios for condensational growth. The color of the circle indicates the value of *NME* corresponding to a particular initial mixing ratio of SO₂, NH₃, or organics that varied between 0 and 100 pptv. Blue represents the best agreement, red poorer agreement, and grey the worst (*NME* >1). There were 64 sensitivity tests. (c) As in (b), but for the NAPA scheme. (d) As in (c), but for the NAPAT scheme. (e) and (f) as in (c) and (d) respectively, but with NH₃ fixed and varying organics for condensational growth. (g) as in (b) but for the RIC scheme, which provides the lowest *NME*. There were 400 sensitivity tests for this scheme. (h) as in (b) but for the DUN scheme with NH₃ set to 0 (DUN_{NH3=0}). (i) as in (c) but for the DUN scheme. (j) as in (i) but with varying organics for condensational growth. The table presents the *NME* results for the corresponding size distributions in panel (a) and associated initial mixing ratios of gas-phase precursors.

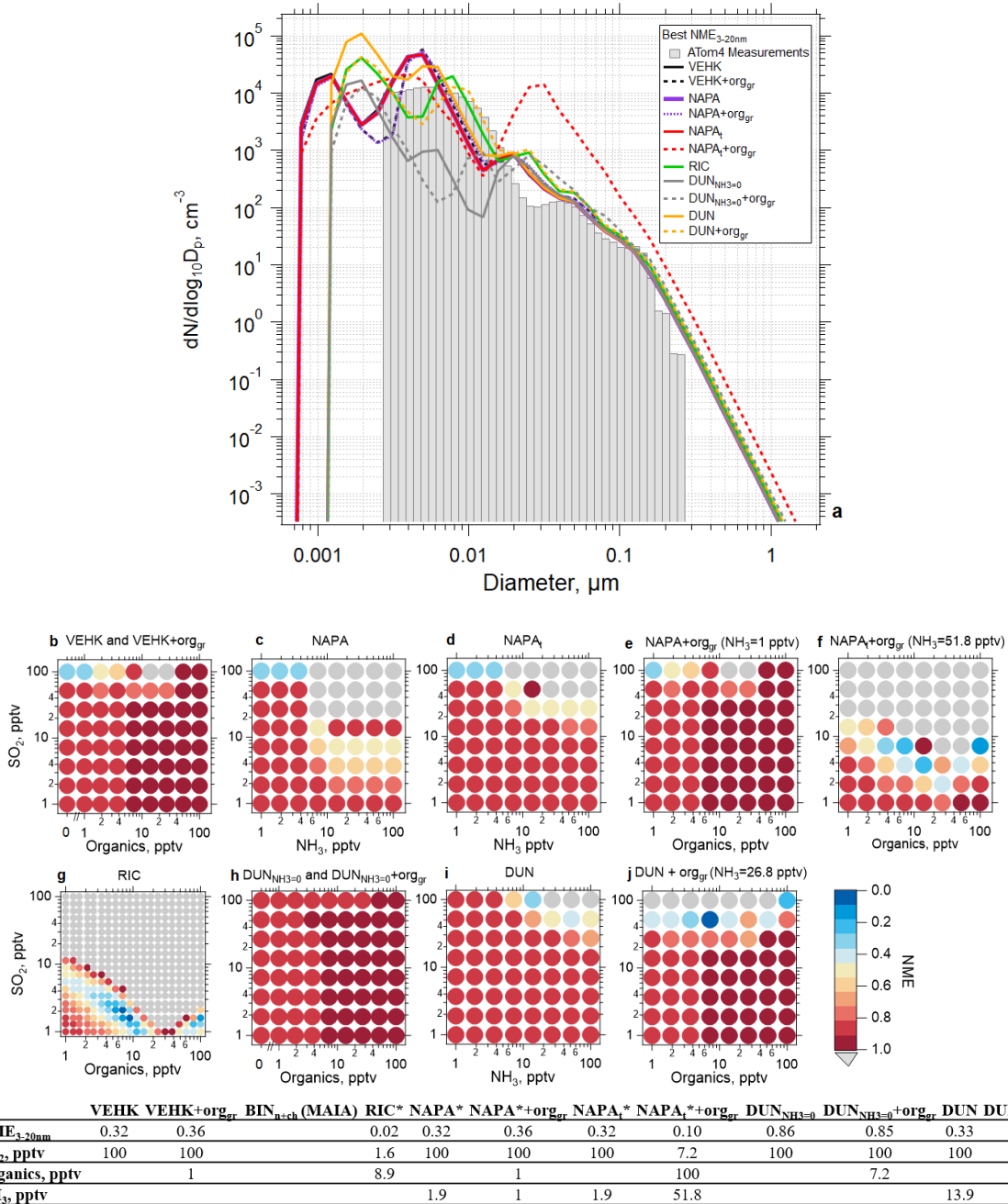


Figure S42: Results of simulations using the TOMAS box model for case sd179 (ATom 4, 2018-05-01, 21:54:31-21:55:30 UTC) where measurements were made 17.23 hours following convective influence, and temperature along the trajectory varied between 234 and 245 K. (a) Observed (shaded bars) and simulated (lines) aerosol size distributions with best normalized mean error (*NME*) for each of the NPF and growth schemes investigated. (b) *NME* between the modeled and measured size distribution for the VEHK scheme with varying organics mixing ratios for condensational growth. The color of the circle indicates the value of *NME* corresponding to a particular initial mixing ratio of SO₂, NH₃, or organics that varied between 0 and 100 pptv. Blue represents the best agreement, red poorer agreement, and grey the worst (*NME* >1). There were 64 sensitivity tests. (c) As in (b), but for the NAPA scheme. (d) As in (c), but for the NAPAt scheme. (e) and (f) as in (c) and (d) respectively, but with NH₃ fixed and varying organics for condensation growth. (g) as in (b) but for the RIC scheme, which provides the lowest *NME*. There were 400 sensitivity tests for this scheme. (h) as in (b) but for the DUN scheme with NH₃ set to 0 (DUN_{NH3=0}). (i) as in (c) but for the DUN scheme. (j) as in (i) but with varying organics for condensation growth. The table presents the *NME* results for the corresponding size distributions in panel (a) and associated initial mixing ratios of gas-phase precursors.

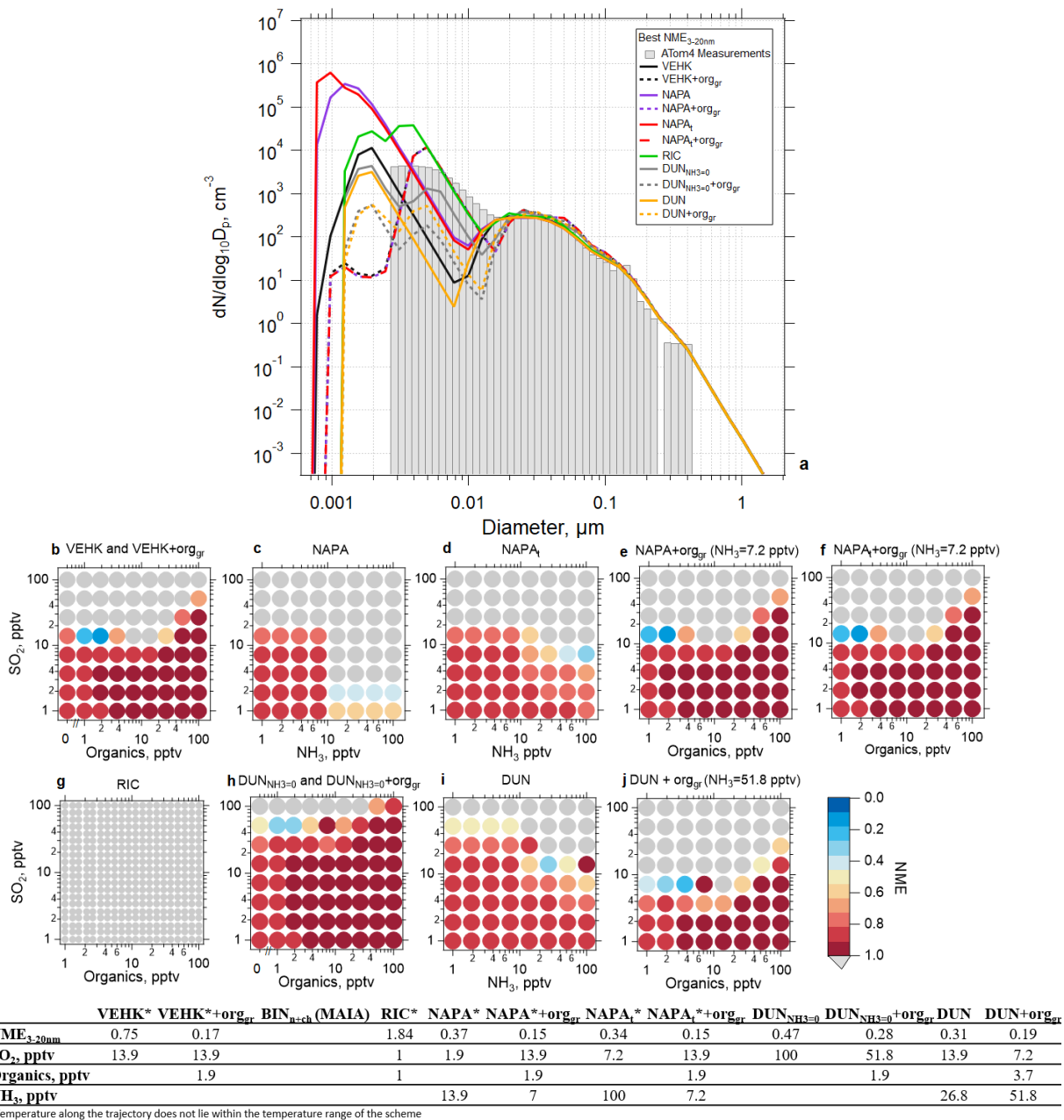


Figure S43: Results of simulations using the TOMAS box model for case sd183 (ATom 4, 2018-05-01, 21:58:31-21:59:30 UTC) where measurements were made 19.39 hours following convective influence, and temperature along the trajectory varied between 226 and 239 K. (a) Observed (shaded bars) and simulated (lines) aerosol size distributions with best normalized mean error (*NME*) for each of the NPF and growth schemes investigated. (b) *NME* between the modeled and measured size distribution for the VEHK scheme with varying organics mixing ratios for condensational growth. The color of the circle indicates the value of *NME* corresponding to a particular initial mixing ratio of SO₂, NH₃, or organics that varied between 0 and 100 pptv. Blue represents the best agreement, red poorer agreement, and grey the worst (*NME* >1). There were 64 sensitivity tests. (c) As in (b), but for the NAPA scheme. (d) As in (c), but for the NAPAt scheme. (e) and (f) as in (c) and (d) respectively, but with NH₃ fixed and varying organics for condensation growth. (g) as in (b) but for the RIC scheme, which provides the lowest *NME*. There were 400 sensitivity tests for this scheme. (h) as in (b) but for the DUN scheme with NH₃ set to 0 (DUN_{NH3=0}). (i) as in (c) but for the DUN scheme. (j) as in (i) but with varying organics for condensation growth. The table presents the *NME* results for the corresponding size distributions in panel (a) and associated initial mixing ratios of gas-phase precursors.

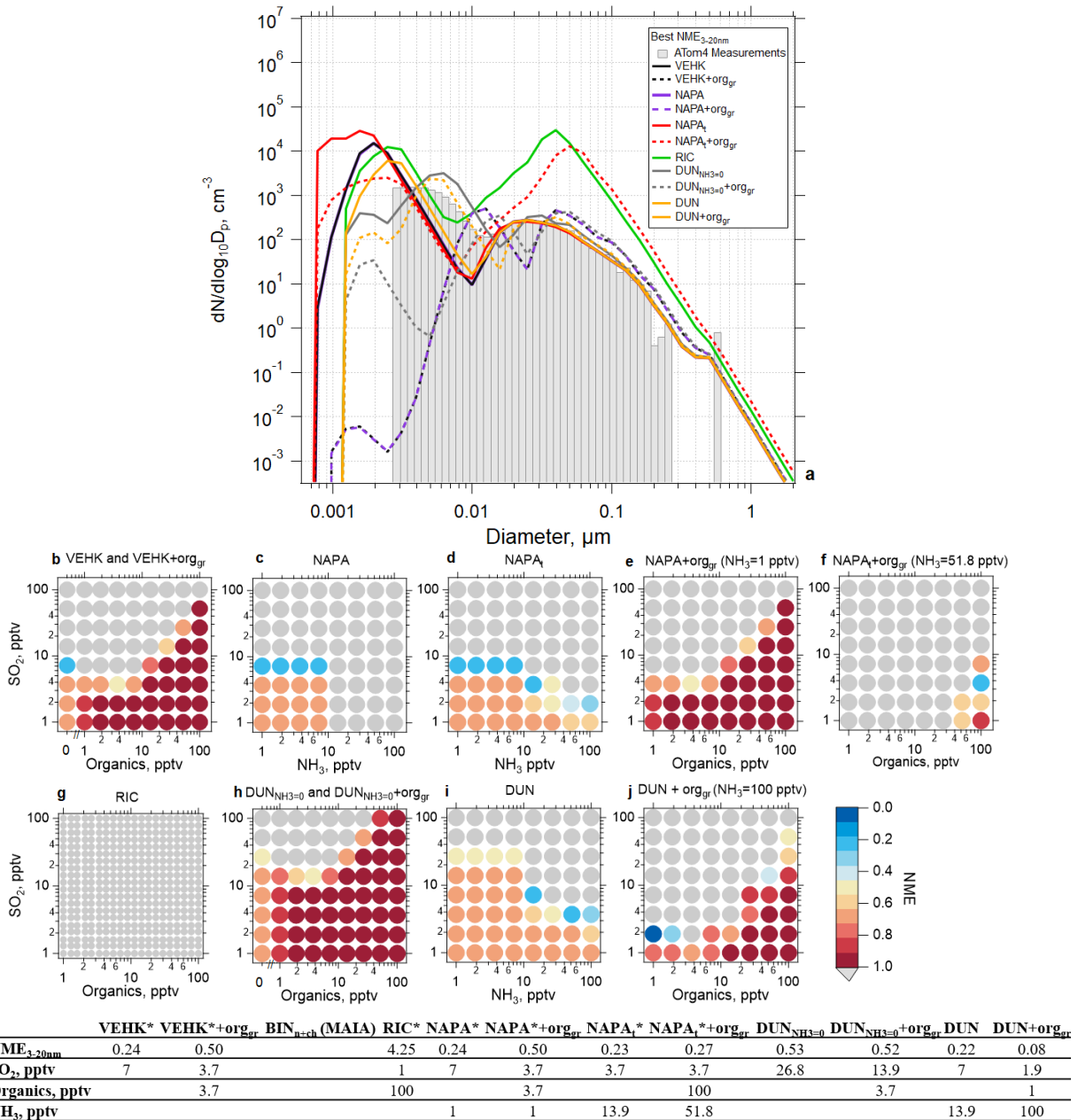


Figure S44: Results of simulations using the TOMAS box model for case sd186 (ATom 4, 2018-05-01, 22:01:31-22:02:30 UTC) where measurements were made 22.36 hours following convective influence, and temperature along the trajectory varied between 226 and 244 K. (a) Observed (shaded bars) and simulated (lines) aerosol size distributions with best normalized mean error (*NME*) for each of the NPF and growth schemes investigated. (b) *NME* between the modeled and measured size distribution for the VEHK scheme with varying organics mixing ratios for condensational growth. The color of the circle indicates the value of *NME* corresponding to a particular initial mixing ratio of SO₂, NH₃, or organics that varied between 0 and 100 pptv. Blue represents the best agreement, red poorer agreement, and grey the worst (*NME* >1). There were 64 sensitivity tests. (c) As in (b), but for the NAPA scheme. (d) As in (c), but for the NAPAt scheme. (e) and (f) as in (c) and (d) respectively, but with NH₃ fixed and varying organics for condensation growth. (g) as in (b) but for the RIC scheme, which provides the lowest *NME*. There were 400 sensitivity tests for this scheme. (h) as in (b) but for the DUN scheme with NH₃ set to 0 (DUN_{NH3=0}). (i) as in (c) but for the DUN scheme. (j) as in (i) but with varying organics for condensation growth. The table presents the *NME* results for the corresponding size distributions in panel (a) and associated initial mixing ratios of gas-phase precursors.

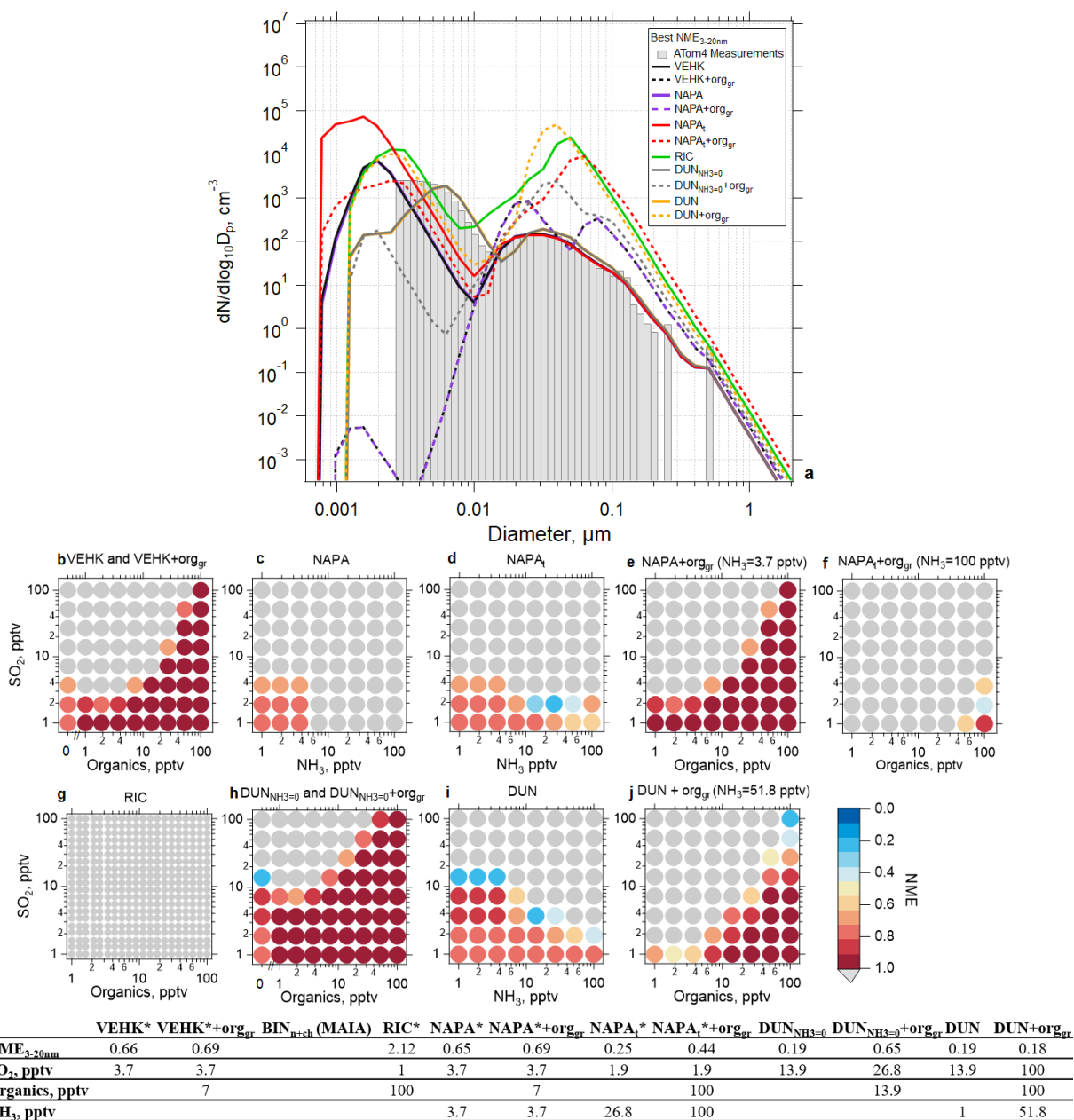
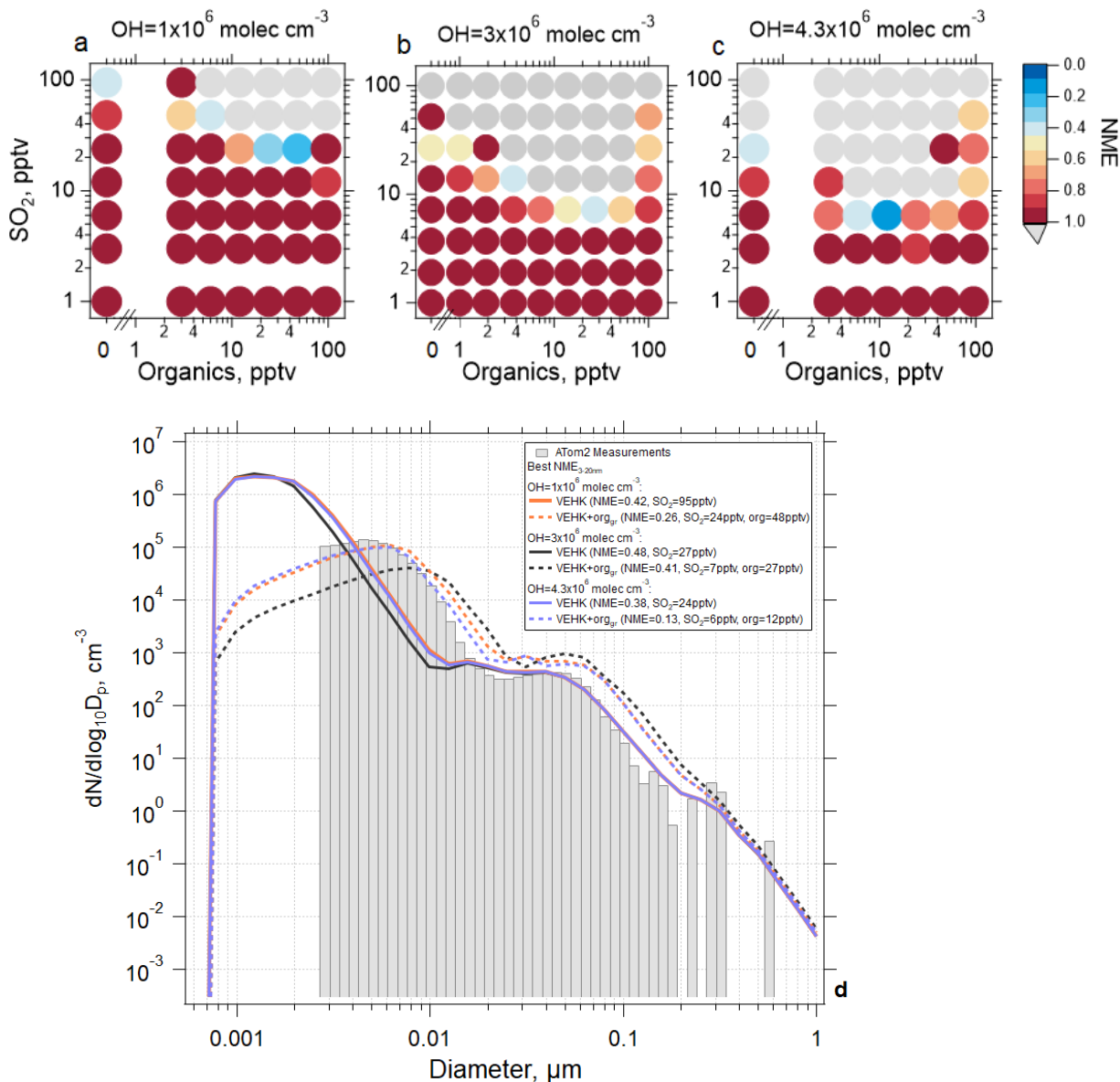


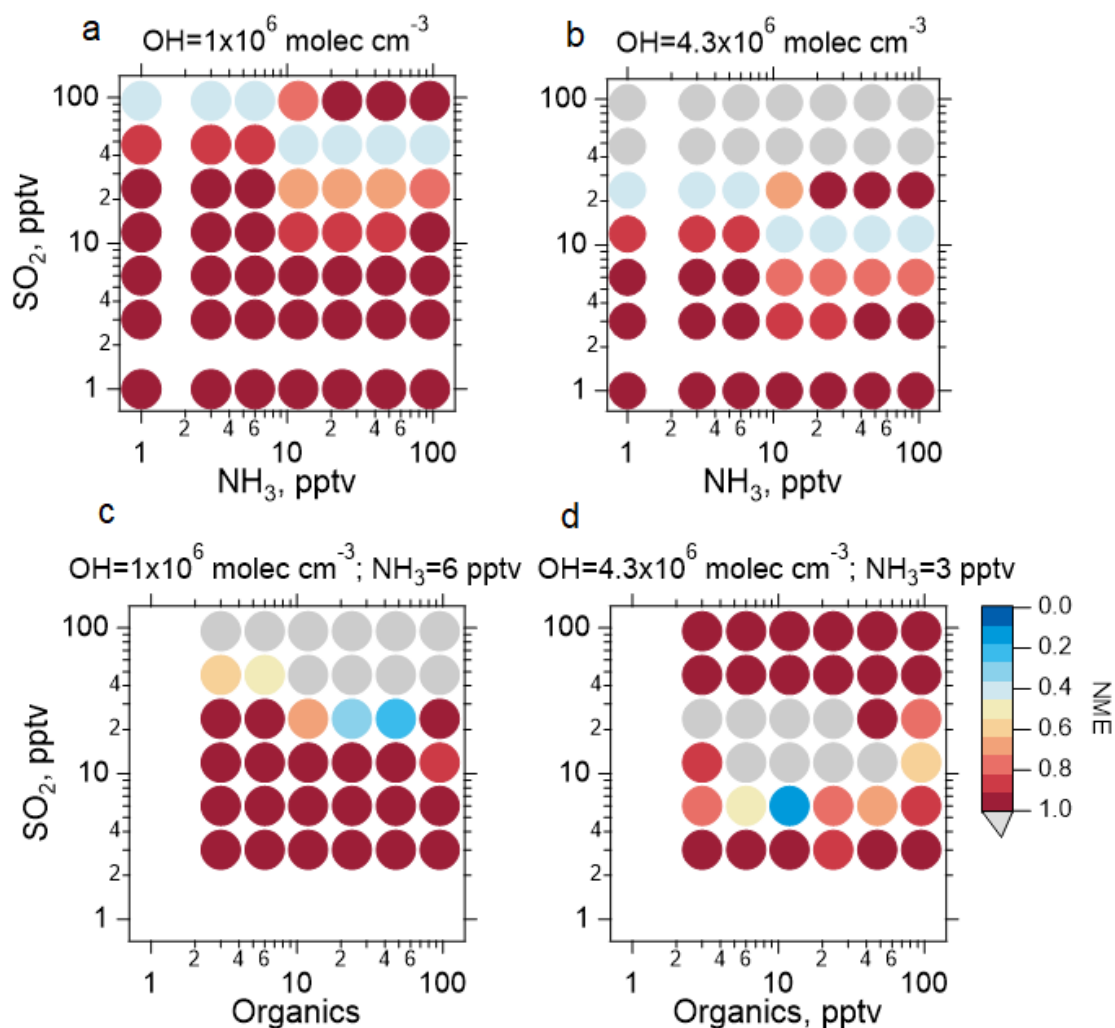
Figure S45: Results of simulations using the TOMAS box model for case sd188 (ATom 4, 2018-05-01, 22:03:31-22:04:30 UTC) where measurements were made 23.27 hours following convective influence, and temperature along the trajectory varied between 227 and 248 K. (a) Observed (shaded bars) and simulated (lines) aerosol size distributions with best normalized mean error (NME) for each of the NPF and growth schemes investigated. (b) NME between the modeled and measured size distribution for the VEHK scheme with varying organics mixing ratios for condensational growth. The color of the circle indicates the value of NME corresponding to a particular initial mixing ratio of SO₂, NH₃, or organics that varied between 0 and 100 pptv. Blue represents the best agreement, red poorer agreement, and grey the worst (NME >1). There were 64 sensitivity tests. (c) As in (b), but for the NAPA scheme. (d) As in (c), but for the NAPAt scheme. (e) and (f) as in (c) and (d) respectively, but with NH₃ fixed and varying organics for condensation growth. (g) as in (b) but for the RIC scheme, which provides the lowest NME. There were 400 sensitivity tests for this scheme. (h) as in (b) but for the DUN scheme with NH₃ set to 0 (DUN_{NH3=0}). (i) as in (c) but for the DUN scheme. (j) as in (i) but with varying organics for condensation growth. The table presents the NME results for the corresponding size distributions in panel (a) and associated initial mixing ratios of gas-phase precursors.

S3. The impact of OH, F_{orgnuc} in RIC, and initial SD on case study sd486



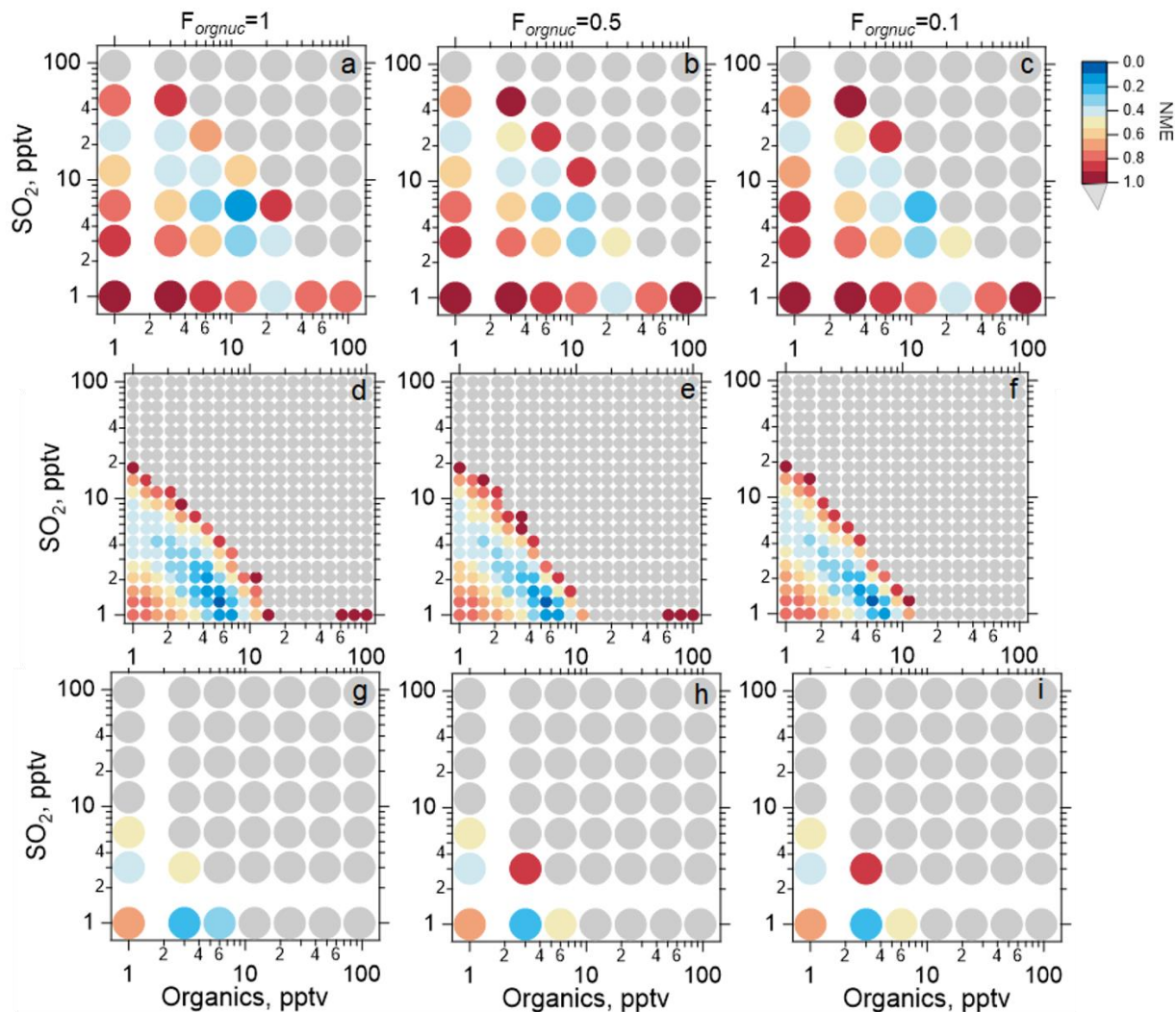
OH, molec cm ⁻³	VEHK		VEHK+org _{gr}		
	Best NME	SO ₂ , pptv	Best NME	SO ₂	Organics, pptv
1x10 ⁶	0.42	95	0.26	24	48
3x10 ⁶	0.48	26.8	0.41	7.2	26.8
4.3x10 ⁶	0.38	24	0.13	6	12

Figure S46: Results of simulations using the TOMAS box model and VEHK nucleation scheme with and without organics added for initial particle growth for case sd486 (ATom2, 2017-02-03, 03:05:31-03:06:30 UTC). OH at solar zenith angle of 0° was varied between 1 and 4.3x10⁶ molec cm⁻³ (a-c). d) Size distribution for the corresponding best NME of each OH setting as in (a-c). Best NME results are summarized in the table. For OH settings of 1 and 4.3x10⁶ molec cm⁻³ simulations were undertaken at slightly different resolution (no mixing ratios of organics equal to 1 pptv was studied).



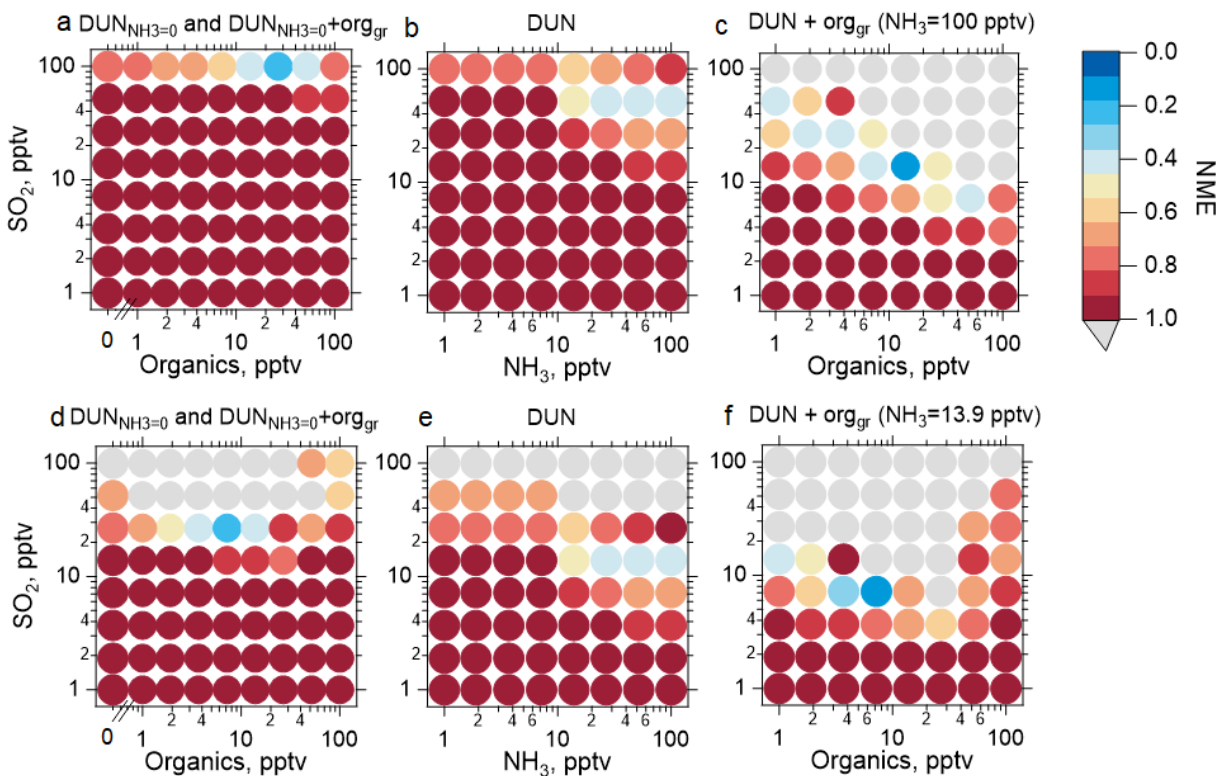
OH, molec cm ⁻³	NAPA			NAPA+org _{gr}			
	Best NME	SO ₂ , pptv	NH ₃ , pptv	Best NME	SO ₂	NH ₃ , pptv	Organics, pptv
1x10 ⁶	0.38	47.5	23.8	0.25	23.8	6	47.5
3x10 ⁶	0.42	13.9	13.9	0.37	7.2	100	1
4.3x10 ⁶	0.39	23.8	1	0.14	6	3	11.9

Fig. S47: Results of simulations using the TOMAS box model and NAPA nucleation scheme with and without organics added for initial particle growth for case sd486 (ATom2, 2017-02-03, 03:05:31-03:06:30 UTC). OH at solar zenith angle of 0° was set to 1 (a,c) and 4.3x10⁶ molec cm⁻³ (b,d). Results for OH=3x10⁶ molec cm⁻³ are presented in Fig. 6 in the manuscript. Best NME results are summarized in the table. OH setting of 1 and 4x10⁶ molec cm⁻³ was simulated at lower resolution than in Figure 6. No simulations were done for SO₂ and organics mixing ratios below 3 pptv in c) and d).



OH , molec cm ⁻³	$F_{organuc}$	RIC		
		Best NME	SO ₂ , pptv	Organics, pptv
1x10 ⁶	1	0.17	6	12
	0.5	0.28	6	12
	0.1	0.26	6	12
3x10 ⁶	1	0.021	1.3	5.5
	0.5	0.015	1.3	5.5
	0.1	0.13	1.3	5.5
4.3x10 ⁶	1	0.191	1	3
	0.5	0.193	1	3
	0.1	0.198	1	3

Figure S48: Example of the impact of the scaling factor ($F_{organuc}$) of organics and OH setting in RIC scheme and case study sd486 (ATom2 measurements, 2017-02-03, 03:05:31-03:06:30 UTC). OH at solar zenith angle of 0° was set to 1 (a-c), 3 (d-f) and 4.3×10^6 (g-i) molec cm⁻³, time since convective influence 7.3 hrs and best normalized mean error (NME) between the modeled and measured size distribution: (a,d,g) at $F_{organuc}=1$, (b,e,h) at $F_{organuc}=0.5$, (c,f,i) at $F_{organuc}=0.1$. $F_{organuc}$ represents the fraction of the condensable organic, labeled *BioOxOrg*, that may participate in nucleation by stabilizing the cluster. The color of the circles indicates the value of NME; grey circles indicate NME >1. Varying $F_{organuc}$ does not change results significantly.



OH, molec cm ⁻³	DUN _{NH₃=0}			DUN _{NH₃=0} +org _{gr}			
	Best NME	SO ₂ , pptv	NH ₃ , pptv	Best NME	SO ₂ , pptv	NH ₃ , pptv	Organics, pptv
1x10 ⁶	0.78	100	0	0.27	100	0	26.8
3x10 ⁶	0.37	51.8	0	0.3	51.8	0	1
4.3x10 ⁶	0.72	51.8	0	0.21	26.8	0	7.2
OH, molec cm ⁻³	DUN			DUN+org _{gr}			
	Best NME	SO ₂ , pptv	NH ₃ , pptv	Best NME	SO ₂ , pptv	NH ₃ , pptv	Organics, pptv
1x10 ⁶	0.38	100	51.8	0.13	13.9	100	13.9
3x10 ⁶	0.34	51.8	7	0.04	7.2	26.8	7.2
4.3x10 ⁶	0.37	13.9	100	0.12	7.2	13.9	7.2

Figure S49: Results of simulations using the TOMAS box model and DUN nucleation scheme, with and without NH₃, and with and without organics added for initial particle growth for case sd486 (ATom2, 2017-02-03, 03:05:31-03:06:30 UTC) where OH has been set to 1 (a,b,c) and 4.3x10⁶ molec cm⁻³ (d,e,f). (a,c) DUN scheme with NH₃ set to 0 and with organics added for initial particle growth; (b,e) DUN nucleation scheme and (c,f) DUN with organics added for initial particle growth. Results for OH=3x10⁶ molec cm⁻³ are presented in Fig. 6 in the manuscript. Best NME results are summarized in the table. OH setting of 1 and 4x10⁶ molec cm⁻³ was simulated at lower resolution than in Figure 6.

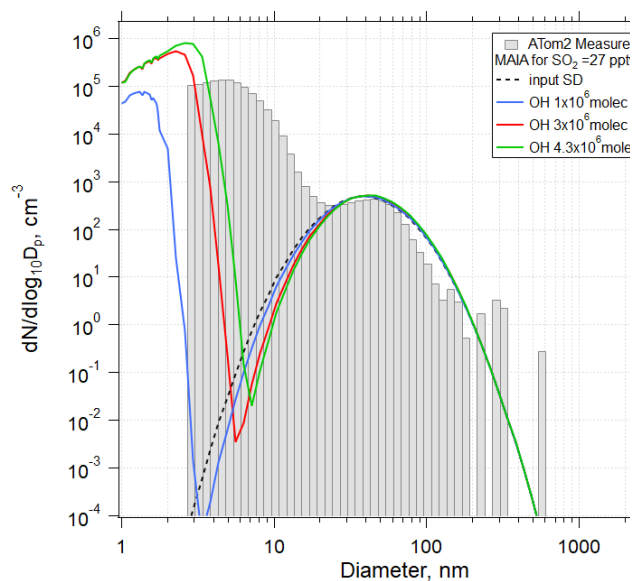
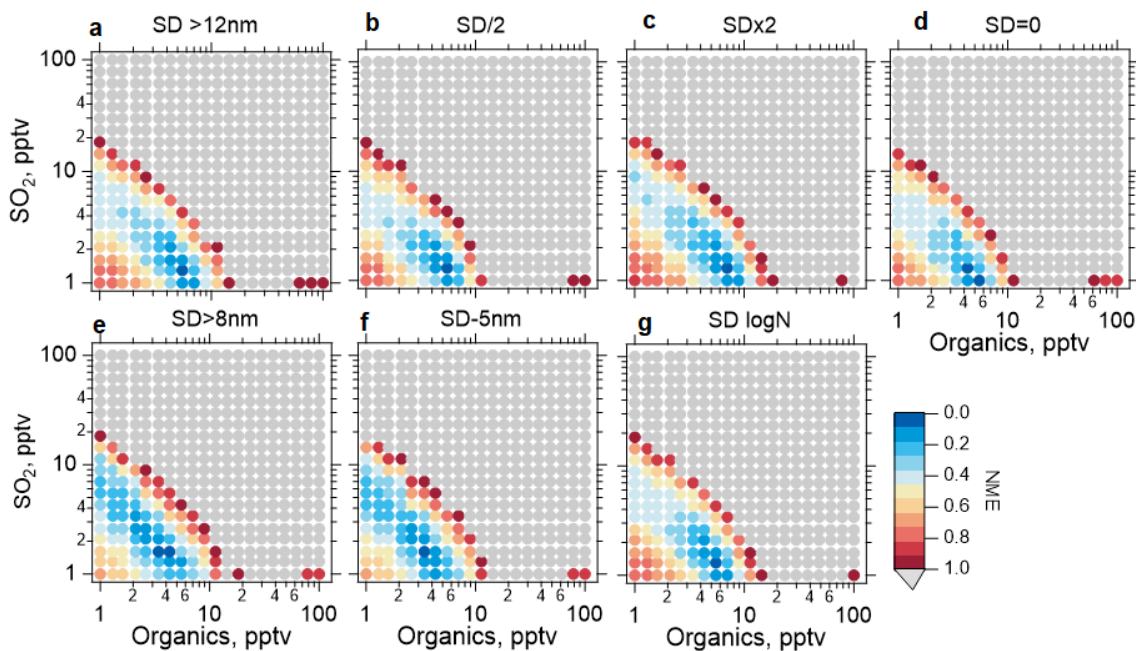
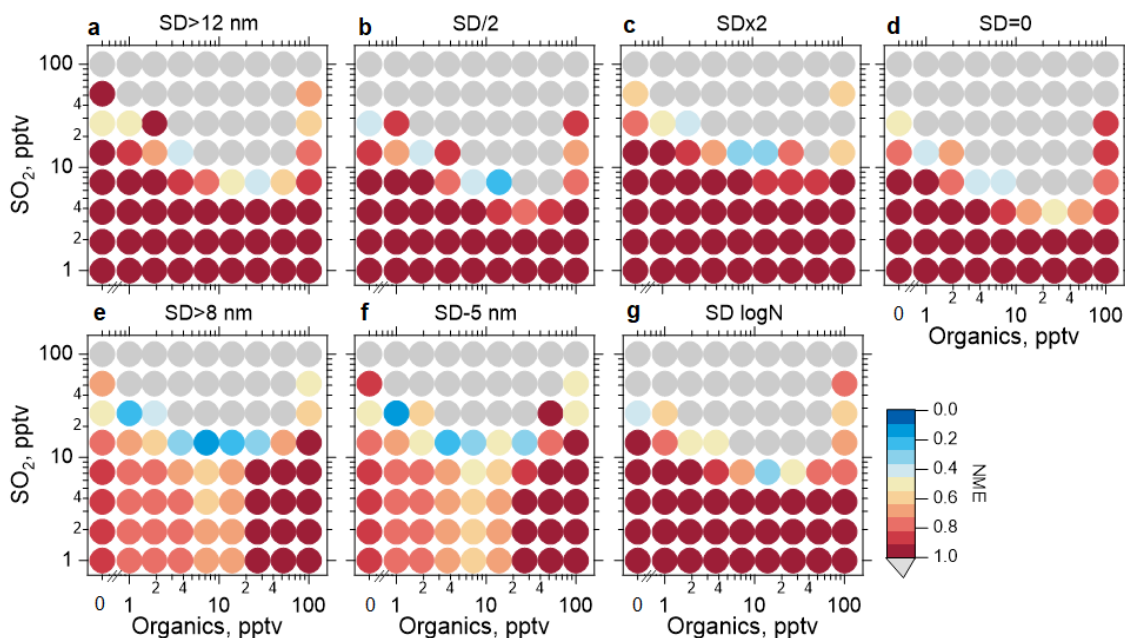


Figure S50: Example of the measured size distribution (2017-02-03, 03:05:31-03:06:30 UTC, sd486) and the simulated case for three different OH at solar zenith angle of 0° was set between 1×10^6 and 4.3×10^6 molecules cm^{-3} . MAIA simulations undertaken using binary neutral and charged (sum of both) nucleation scheme for a range of noon OH concentrations and SO_2 of 27 pptv.



Size distribution as $\text{dn}/\text{dlog}_{10}D_p$	RIC		
	Best NME	SO_2 , pptv	Organics, pptv
SD measured (>12 nm)	0.02	1.3	5.5
SD=0	0.04	1.3	4.3
SDx2	0.04	1.3	7.2
SD/2	0.06	1.3	5.5
SD - 5 nm	0.08	1.6	3.4
SD > 8 nm	0.09	1.6	4.3
SD logN	0.03	1.3	5.5

Figure S51: The effect of the initial background aerosol on the NME in TOMAS for case sd486 (ATom2, 2017-02-03, 03:05:31-03:06:30 UTC) and RIC nucleation scheme. OH at solar zenith angle of 0° was set to 3×10^6 molec cm^{-3} . SD refers to the number size distribution $\text{dN}/\text{dlog}_{10}D_p$. Table 1 in the main manuscript describes the abbreviations used here.



Size distribution as $dN/d\log_{10}D_p$	VEHK		VEHK+org _{gr}		
	Best NME	SO ₂ , pptv	Best NME	SO ₂	Organics, pptv
SD > 12 nm	0.48	26.8	0.41	7.2	26.8
SD = 0	0.53	26.8	0.39	7.2	3.7
SDx2	0.58	51.8	0.3	13.9	7.2
SD/2	0.4	26.8	0.19	7.2	13.9
SD - 5 nm	0.5	26.8	0.17	26.8	1
SD > 8 nm	0.54	26.8	0.14	13.9	7.2
SD logN	0.44	26.8	0.34	7.2	13.9

Figure S52: The effect varying the initial background aerosol on the NME in TOMAS for case sd486 (ATom2, 2017-02-03, 03:05:31-03:06:30 UTC) and VEHK nucleation scheme and VEHK with organics added for initial growth. OH at solar zenith angle of 0° was set to 3×10^6 molec cm^{-3} . SD refers to the number size distribution $dN/d\log_{10}D_p$. Table 1 in the main manuscript describes the abbreviations used here.

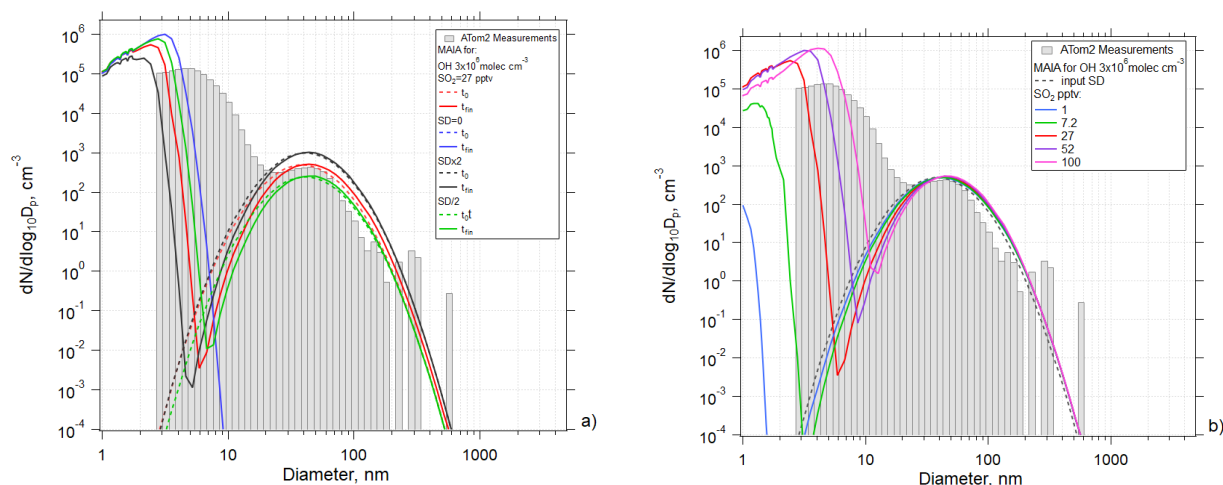
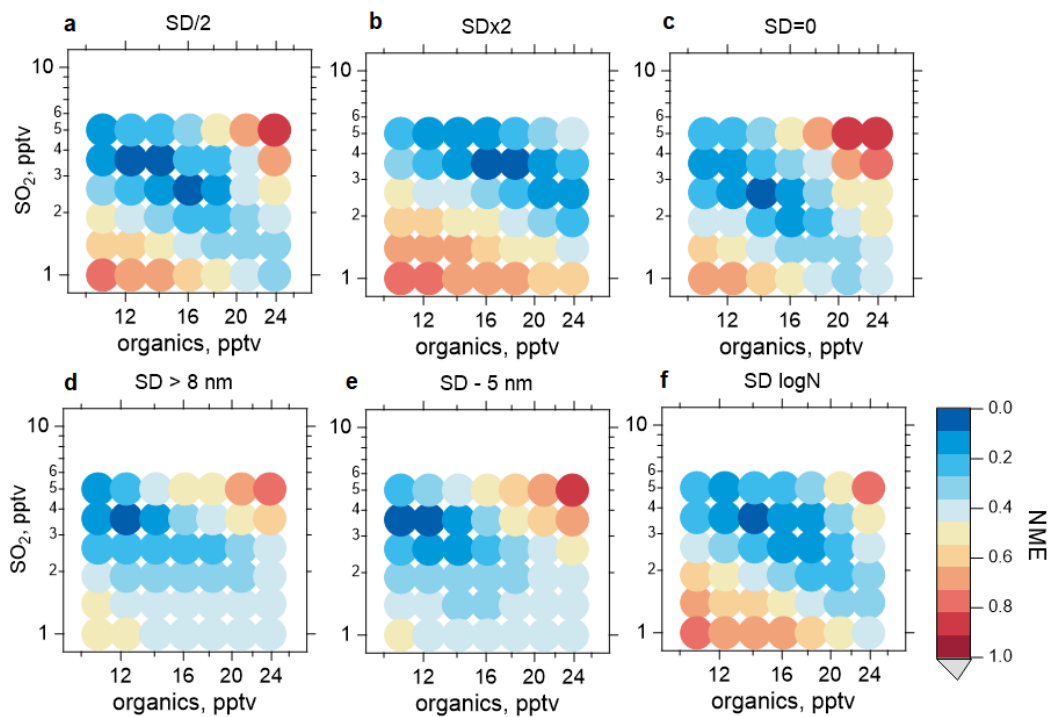


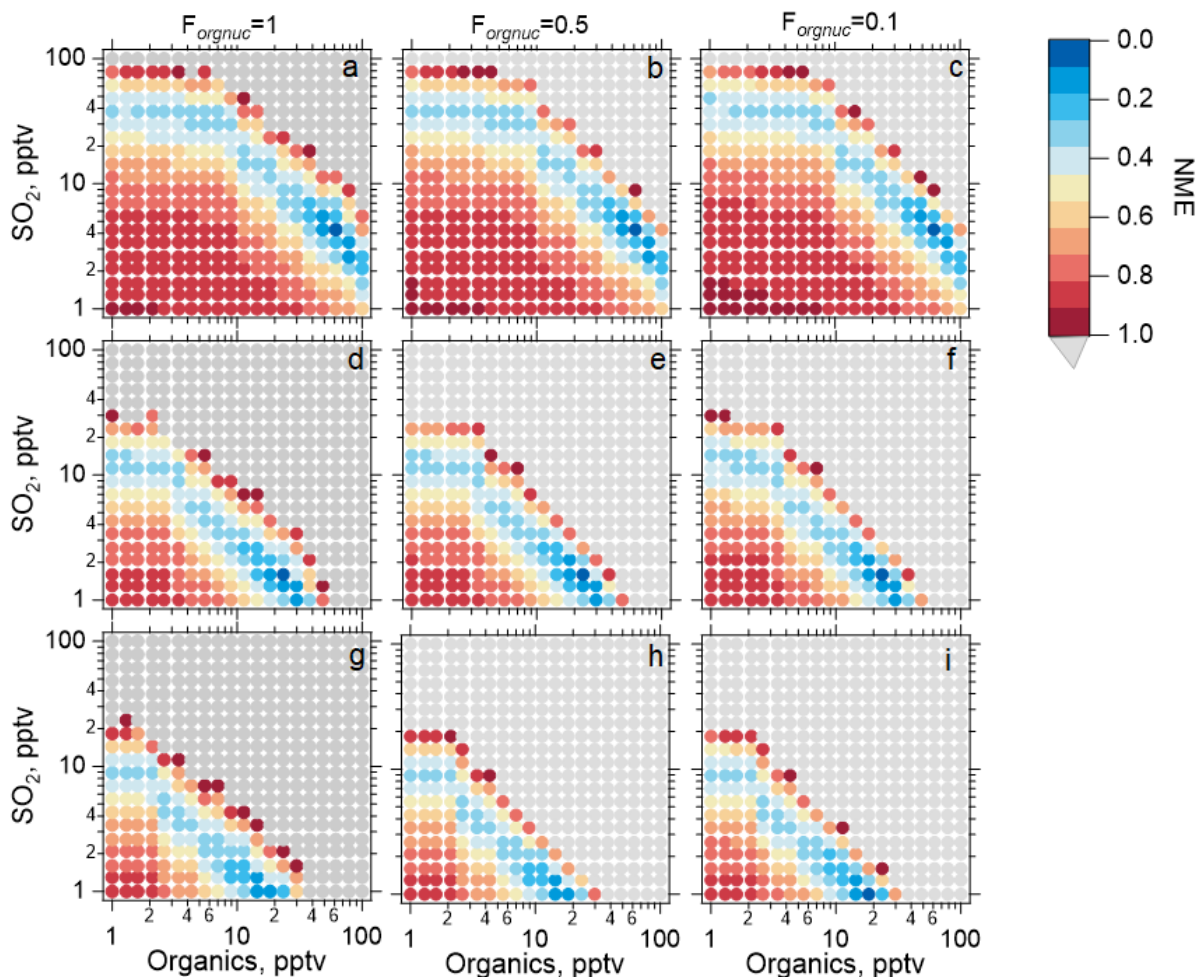
Figure S53: Example of the effect of (a) initial background aerosol and (b) SO₂ mixing ratio on the simulated size distribution (SD as $dN/d\log_{10}D_p$) in MAIA for binary neutral and charged nucleation scheme. Simulations were done for ATom2 measurements (2017-02-03, 03:05:31-03:06:30 UTC, sd486) with time since CI 7.3 hrs. SD refers to the number size distribution $dN/d\log_{10}D_p$. Table 1 in the main manuscript describes the abbreviations used here.



Initial size distribution	RIC		
	Best NME	SO ₂ , pptv	Organics, pptv
SD measured (>12 nm)	0.043	3.6	14.1
SD/2	0.078	3.6	12.3
SDx2	0.069	3.6	18.3
SD=0	0.071	2.6	14.1
SD>8nm	0.079	5	9.5
SD - 5 nm	0.082	3.6	12.3
SD logN	0.047	3.6	14.1

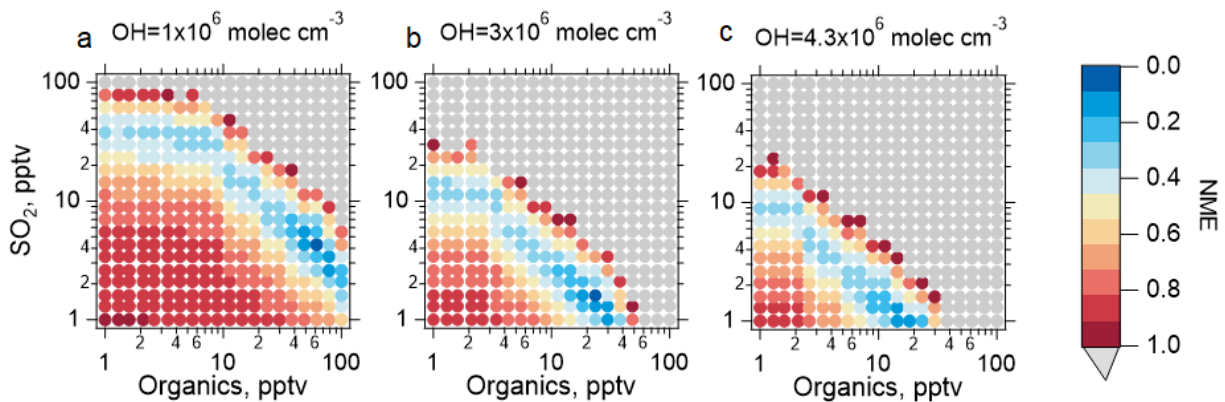
Figure S54: The effect of the initial background aerosol on the NME in TOMAS for case sd486 (ATom2, 2017-02-03, 03:05:31-03:06:30 UTC) and RIC nucleation scheme. OH at solar zenith angle of 0° was set to 1×10^6 molec cm^{-3} . SD refers to the number size distribution $dN/d\log_{10}D_p$. Table 1 in the main manuscript describes the abbreviations used here.

S4. The impact of OH, F_{orgnuc} in RIC, and initial SD on other cases



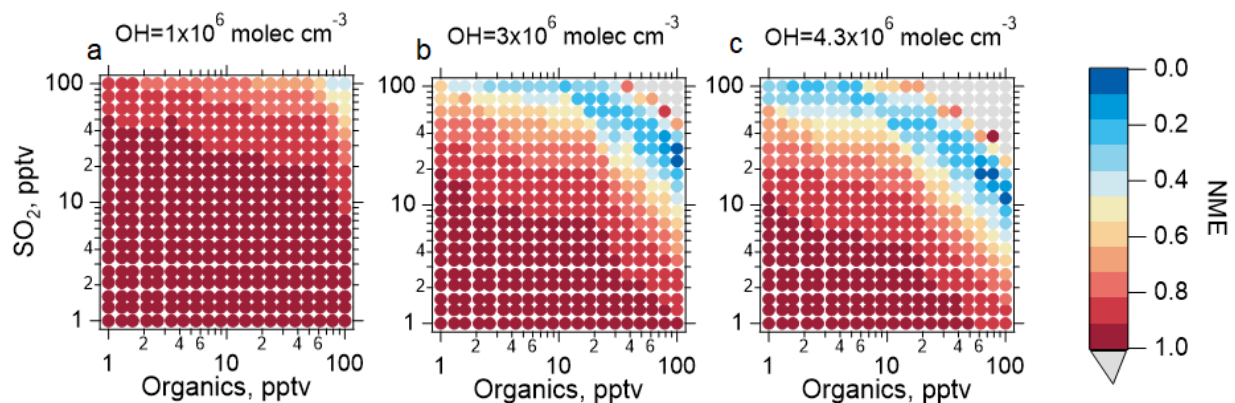
OH, molec cm^{-3}	RIC								
	$F_{orgnuc}=1$			$F_{orgnuc}=0.5$			$F_{orgnuc}=0.1$		
	Best NME	SO ₂ , pptv	Organics, pptv	Best NME	SO ₂ , pptv	Organics, pptv	Best NME	SO ₂ , pptv	Organics, pptv
1×10^6	0.0565	4.3	61.6	0.0560	4.3	61.6	0.0538	4.3	61.6
3×10^6	0.0834	1.6	23.4	0.791	1.6	23.4	0.0616	1.6	23.4
4.3×10^6	0.1085	1	14.4	0.1085	1	18.3	0.0760	1	18.3

Figure S55: Example of the impact of the scaling factor (F_{orgnuc}) of organics and OH in RIC scheme and case study sd461 (ATom 2, 2017-02-04, 02:40:31-02:41:30 UTC). OH at solar zenith angle of 0° was set to 1 (a,b,c), 3 (d,e,f) and $4.3 \times 10^6 \text{ cm}^{-3}$ (g,h,i) time since convective influence 2.83 hrs and best normalized mean error (NME) between the modeled and measured size distribution: (a,d,g) at $F_{orgnuc}=1$, (b,e,h) at $F_{orgnuc}=0.5$, (c,f,i) at $F_{orgnuc}=0.1$. F_{orgnuc} represents the fraction of the condensable organic, labeled *BioOxOrg*, that may participate in nucleation by stabilizing the cluster. The color of the circles indicates the value of NME; grey circles indicate NME > 1. Varying F_{orgnuc} does not change results significantly. The NME best stays best for same initial mixing ratios of SO₂ and organics.



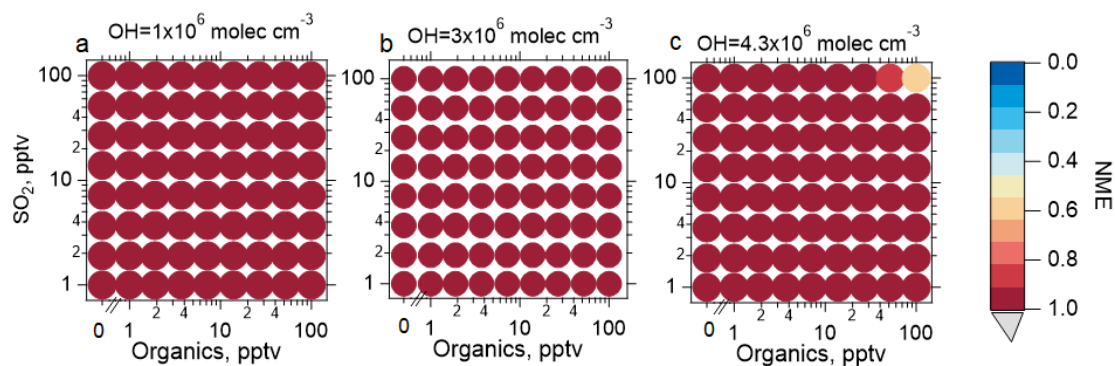
OH, molec cm ⁻³	RIC		
	Best NME	SO ₂ , pptv	Organics, pptv
1x10 ⁶	0.0565	4.3	61.6
3x10 ⁶	0.0834	1.6	23.4
4.3x10 ⁶	0.1085	1	14.4

Figure S56: The effect of the OH on the NME in TOMAS for case sd461 (ATom 2, 2017-02-04, 02:40:31-02:41:30 UTC) and RIC nucleation scheme. OH at solar zenith angle of 0° was set to 1, 3 and 4.3x10⁶ molec cm⁻³.



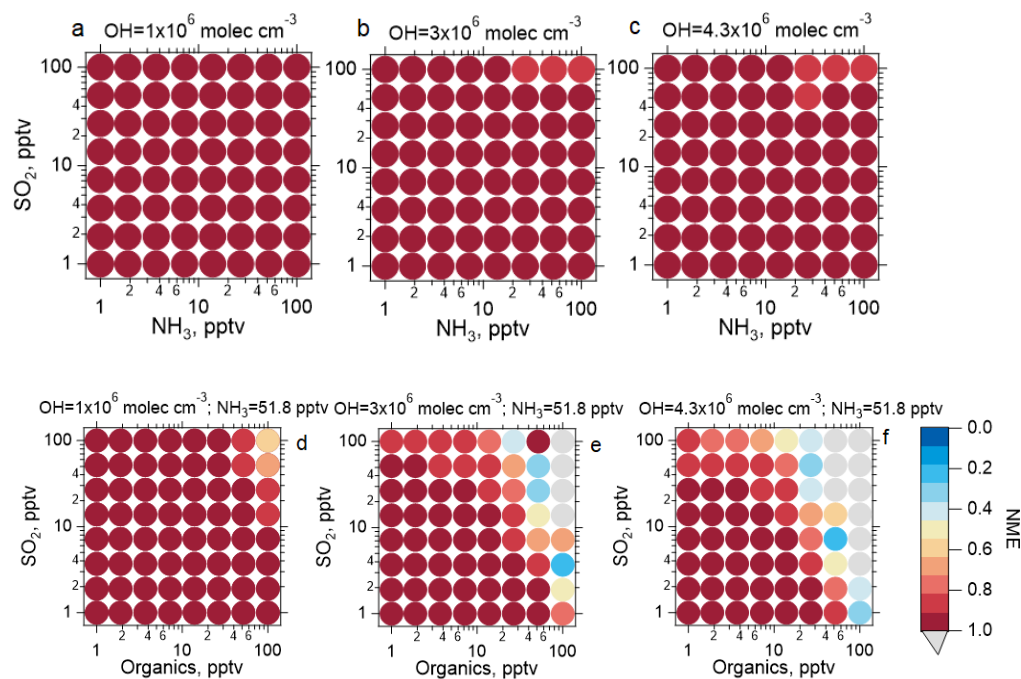
OH, molec cm ⁻³	RIC		
	Best NME	SO ₂ , pptv	Organics, pptv
1x10 ⁶	0.38	100	78.5
3x10 ⁶	0.08	23.4	100
4.3x10 ⁶	0.06	18.3	78.5

Figure S57: The effect of OH on the NME in TOMAS for case sd491 (ATom 2, 2017-02-40, 03:10:31-03:11:30 UTC) and RIC nucleation scheme. OH at solar zenith angle of 0° was set to 1, 3 and 4.3x10⁶ molec cm⁻³.



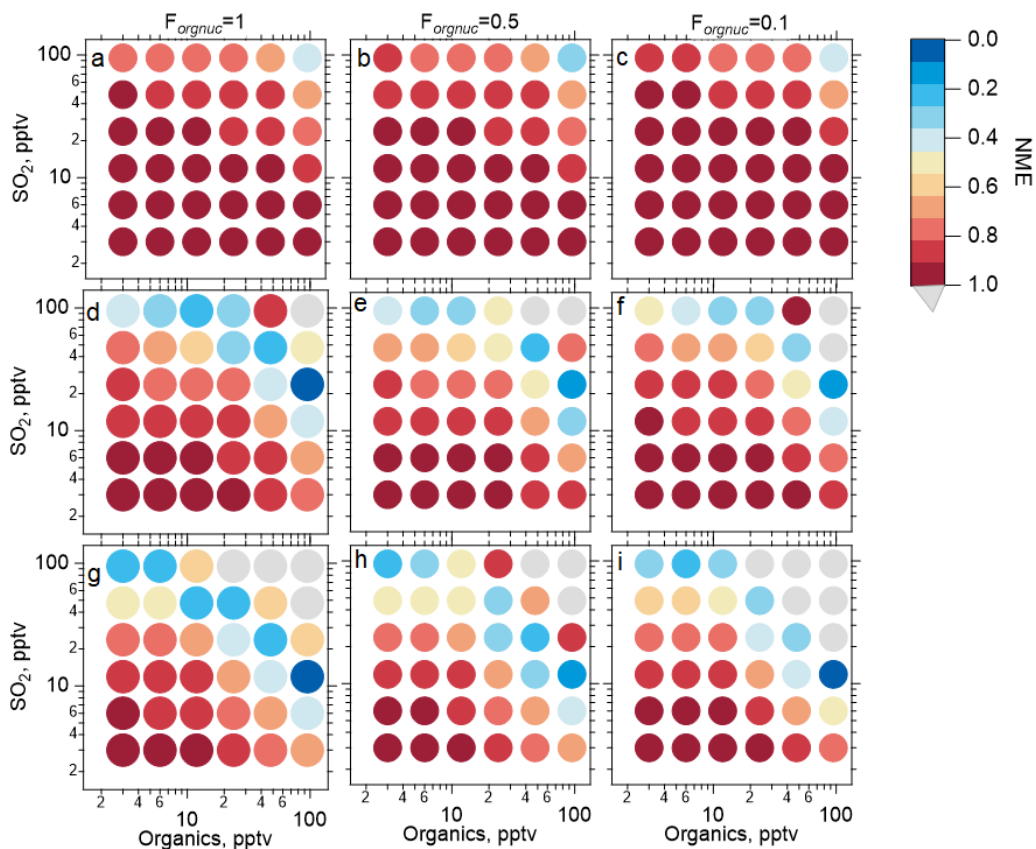
OH, molec cm ⁻³	VEHK		VEHK+org _{gr}		
	Best NME	SO ₂ , pptv	Best NME	SO ₂ , pptv	Organics, pptv
1x10 ⁶	0.957	100	0.956	1.9	100
3x10 ⁶	0.956	100	0.911	100	100
4.3x10 ⁶	0.953	100	0.622	100	100

Figure S58: The effect of OH on the NME in TOMAS for case sd491 (ATom 2, 2017-02-40, 03:10:31-03:11:30 UTC) and VEHK nucleation scheme with and without organics added for initial growth. OH at solar zenith angle of 0° was set to 1, 3 and 4.3x10⁶ molec cm⁻³.



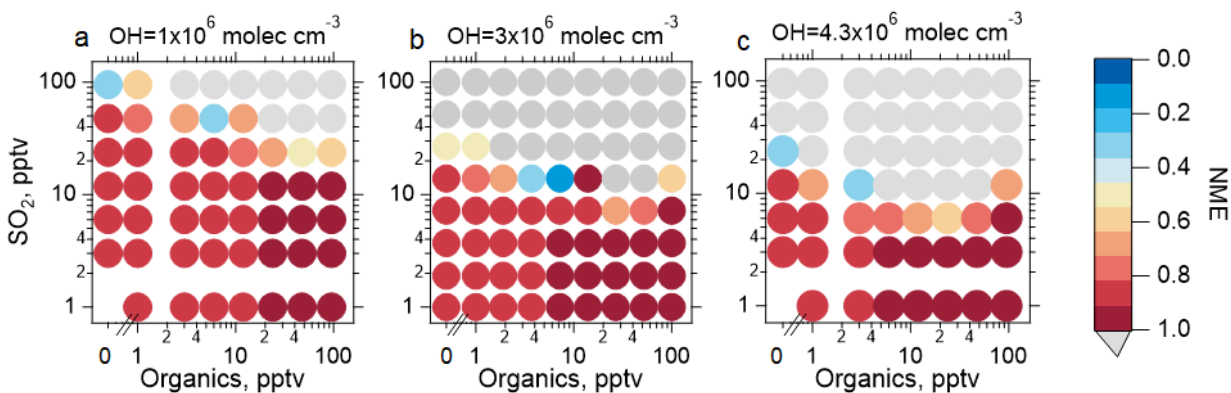
OH, molec cm ⁻³	NAPA			NAPA+org _{gr}			
	Best NME	SO ₂ , pptv	NH ₃ , pptv	Best NME	SO ₂	NH ₃ , pptv	Organics, pptv
1x10 ⁶	0.93	100	26.8	0.58	100	51.8	100
3x10 ⁶	0.89	100	26.8	0.25	3.7	51.8	100
4.3x10 ⁶	0.83	100	26.8	0.27	7.2	51.8	51.8

Figure S59: The effect of OH on the NME in TOMAS for case sd491 (ATom 2, 2017-02-40, 03:10:31-03:11:30 UTC) and NAPA nucleation scheme with and without organics added for initial growth. OH at solar zenith angle of 0° was set to 1, 3 and 4.3x10⁶ molec cm⁻³.



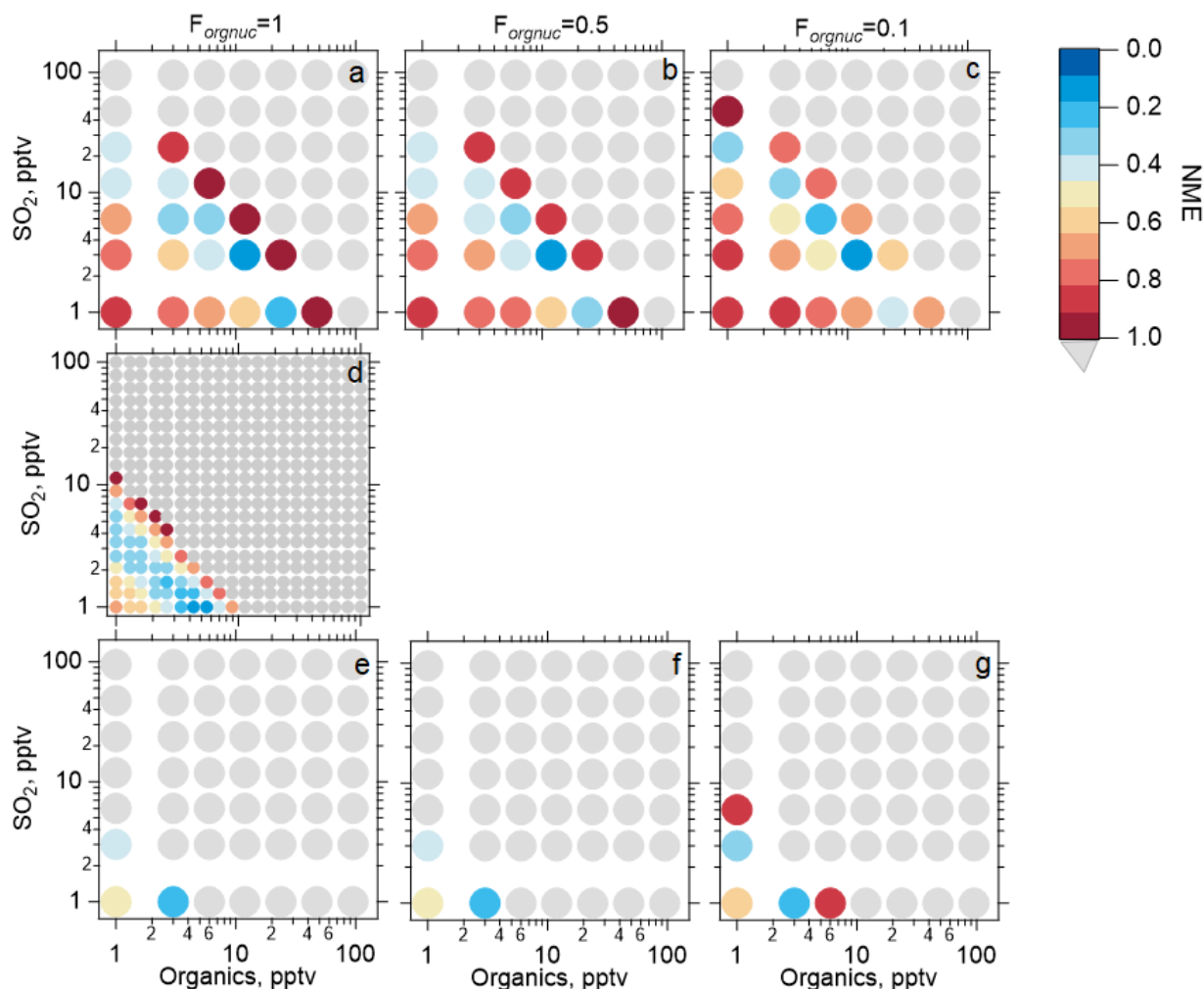
OH, molec cm ⁻³	RIC								
	F _{organuc} =1			F _{organuc} =0.5			F _{organuc} =0.1		
	Best NME	SO ₂ , pptv	Organics, pptv	Best NME	SO ₂ , pptv	Organics, pptv	Best NME	SO ₂ , pptv	Organics, pptv
1x10 ⁶	0.42	95	95	0.33	95	95	0.4	95	95
3x10 ⁶	0.09	11.9	95	0.15	23.8	95	0.18	23.8	95
4.3x10 ⁶	0.06	23.8	95	0.13	11.9	95	0.09	11.9	95

Figure S60: Example of the impact of the scaling factor ($F_{organuc}$) of organics and OH in RIC scheme and case study sd491 (ATom 2, 2017-02-40, 03:10:31-03:11:30 UTC). OH at solar zenith angle of 0° was set to 1 (a,b,c), 3 (d,e,f) and 4.3×10^6 cm⁻³ (g,h,i) time since convective influence 0.4 hr and best normalized mean error (NME) between the modeled and measured size distribution: (a,d,g) at $F_{organuc}=1$, (b,e,h) at $F_{organuc}=0.5$, (c,f,i) at $F_{organuc}=0.1$. $F_{organuc}$ represents the fraction of the condensable organic, labeled *BioOxOrg*, that may participate in nucleation by stabilizing the cluster. The color of the circles indicates the value of NME; grey circles indicate NME >1. Varying $F_{organuc}$ does not change results significantly. The best NME stays best for same initial mixing ratios of SO₂ and organics. Notice different resolution than in Figure S52 for RIC scheme.



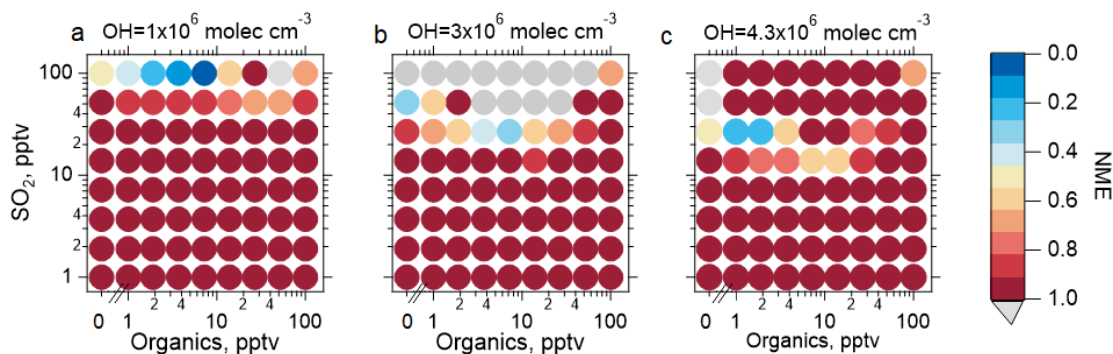
OH, molec cm ⁻³	VEHK		VEHK+org _{gr}		
	Best NME	SO ₂ , pptv	Best NME	SO ₂	Organics, pptv
1x10 ⁶	0.35	95	0.31	47.5	6
3x10 ⁶	0.52	26.8	0.16	13.9	7.2
4.3x10 ⁶	0.3	24	0.35	12	3

Figure S61: Results of simulations using the TOMAS box model and VEHK nucleation scheme with and without organics added for initial particle growth for case sd448 (ATom 2, 2017-02-04, 02:27:31-02:28:30 UTC) where OH has been varied between 1 and 4.3x10⁶ molec cm⁻³ (a-c). d) Size distribution for the corresponding best NME of each OH setting as in (a-c). Best NME results are summarized in the table. and NME results in the table. OH settings of 1 and 4x10⁶ molec cm⁻³ simulated at lower resolution. No simulations done for SO₂=1pptv and no organics for OH1 and 4.3x10⁶ molec cm⁻³.



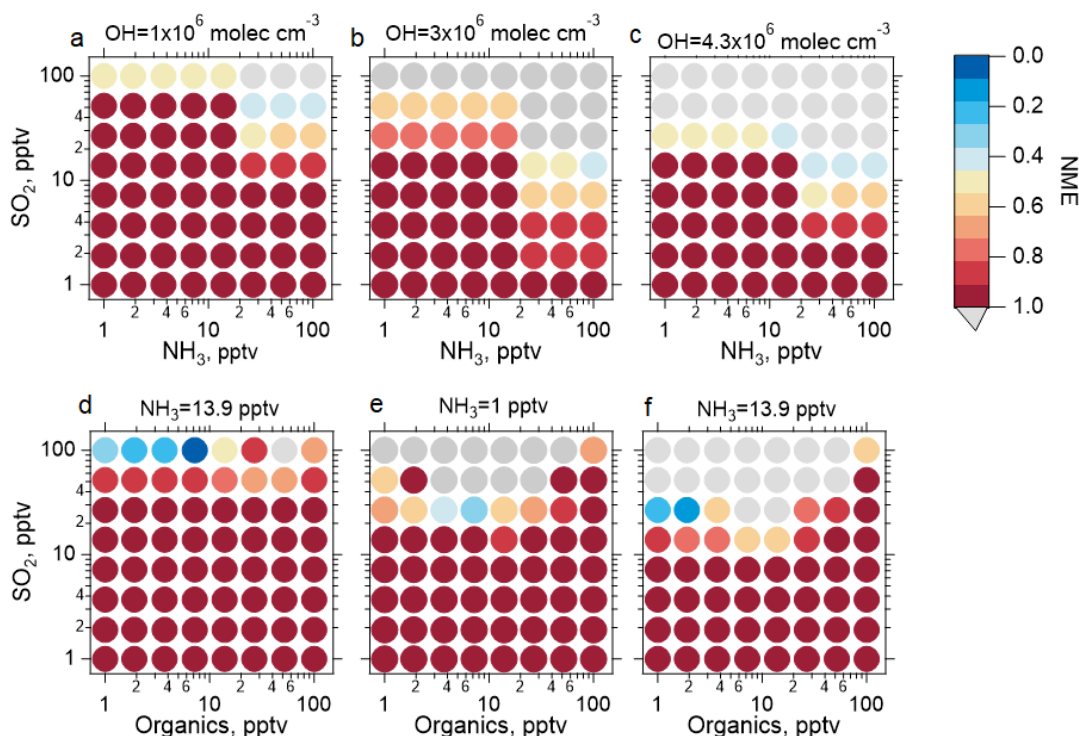
OH, molec cm^{-3}	RIC								
	$F_{organuc}=1$			$F_{organuc}=0.5$			$F_{organuc}=0.1$		
	Best NME	SO_2 , pptv	Organics, pptv	Best NME	SO_2 , pptv	Organics, pptv	Best NME	SO_2 , pptv	Organics, pptv
1×10^6	0.16	3	12	0.15	3	12	0.14	3	12
3×10^6	0.16	1	4.3	n/a	n/a	n/a	n/a	n/a	n/a
4.3×10^6	0.26	1	3	0.26	1	3	0.18	1	3

Figure S62: Example of the impact of the scaling factor ($F_{organuc}$) of organics and OH in RIC scheme and case study sd448 (ATom 2, 2017-02-04, 02:27:31-02:28:30 UTC). OH at solar zenith angle of 0° was set to 1 (a,b,c), 3 (d) and $4.3 \times 10^6 \text{ molec cm}^{-3}$ (e,f,g) time since convective influence 9.08 hrs and best normalized mean error (NME) between the modeled and measured size distribution: (a,d,e) at $F_{organuc}=1$, (b,f) at $F_{organuc}=0.5$, (c,g) at $F_{organuc}=0.1$. $F_{organuc}$ represents the fraction of the condensable organic, labeled *BioOxOrg*, that may participate in nucleation by stabilizing the cluster. The color of the circles indicates the value of NME; grey circles indicate $\text{NME} > 1$. Varying $F_{organuc}$ does not change results significantly. The NME best stays best for same initial mixing ratios of SO_2 and organics. No simulations were done for $F_{organuc}=0.5$ and $F_{organuc}=0.1$ at OH set to $3 \times 10^6 \text{ molec cm}^{-3}$.



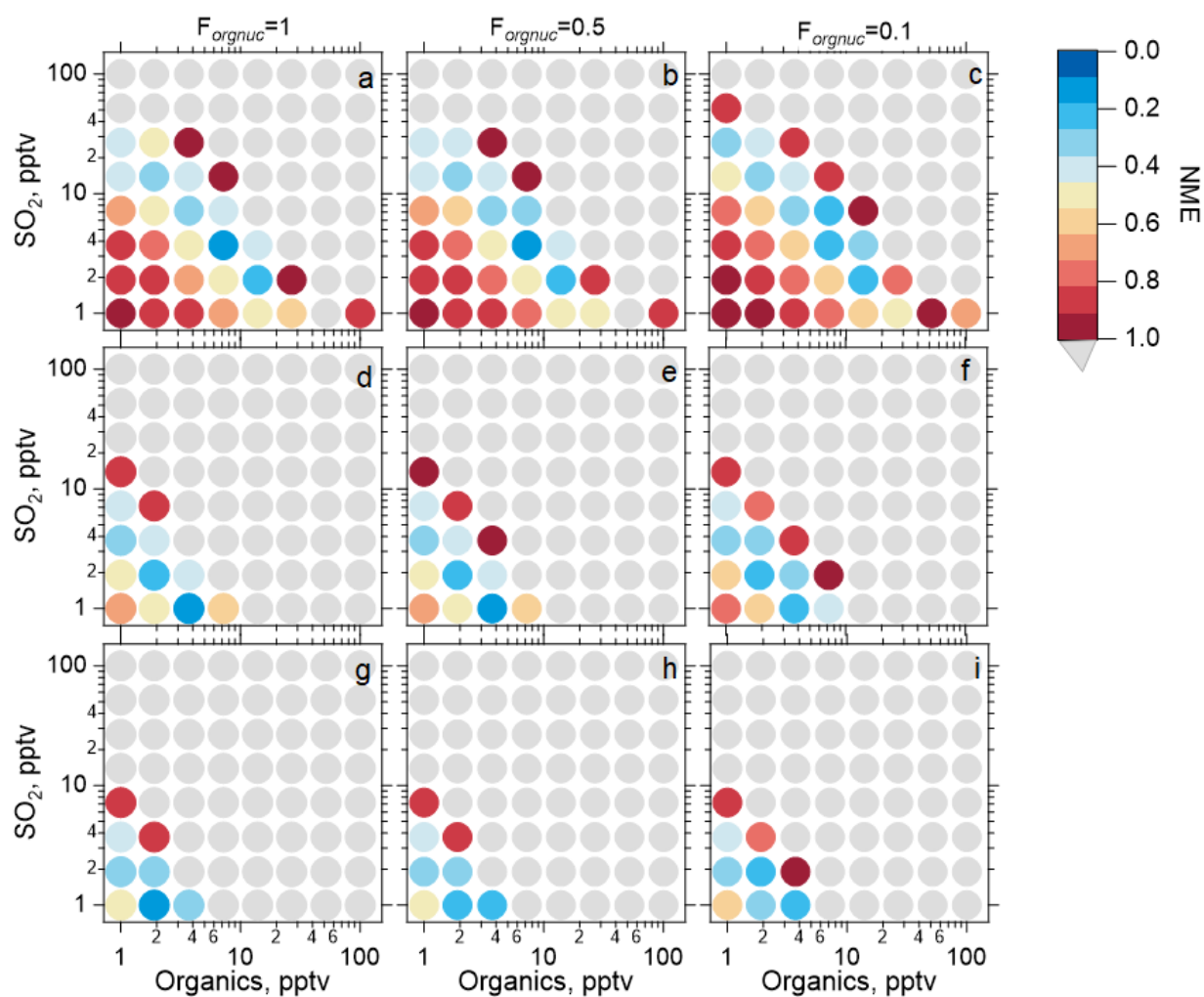
OH, molec cm ⁻³	VEHK		VEHK+org _{gr}		
	Best NME	SO ₂ , pptv	Best NME	SO ₂	Organics, pptv
1x10 ⁶	0.52	100	0.09	100	7.2
3x10 ⁶	0.35	52	0.32	27	7.2
4.3x10 ⁶	0.46	27	0.18	27	1

Figure S63: Results of simulations using the TOMAS box model and VEHK nucleation scheme with and without organics added for initial particle growth for case sd477 (ATom2, 2017-02-03, 03:05:31-03:06:30 UTC) where OH has been varied between 1 and 4.3x10⁶ molec cm⁻³ (a-c). Best NME results are summarized in the table. and NME results in the table. OH settings of 1 and 4x10⁶ molec cm⁻³ simulated at lower resolution.



OH, molec cm ⁻³	NAPA			NAPA+org _{gr}			
	Best NME	SO ₂ , pptv	NH ₃ , pptv	Best NME	SO ₂	NH ₃ , pptv	Organics, pptv
1x10 ⁶	0.42	51.8	100	0.08	100	13.9	7.2
3x10 ⁶	0.45	13.9	100	0.32	26.8	1	7.2
4.3x10 ⁶	0.42	13.9	100	0.18	26.8	13.9	1.9

Figure S64: The effect of OH on the NME in TOMAS for case sd477 (ATom 2, 2017-02-04, 02:56:31-02:57:30 UTC) and NAPA nucleation scheme with and without organics added for initial growth. OH at solar zenith angle of 0° was set to 1, 3 and 4.3x10⁶ molec cm⁻³.



OH, molec cm ⁻³	RIC								
	F _{organuc} =1			F _{organuc} =0.5			F _{organuc} =0.1		
	Best NME	SO ₂ , pptv	Organics, pptv	Best NME	SO ₂ , pptv	Organics, pptv	Best NME	SO ₂ , pptv	Organics, pptv
1x10 ⁶	0.12	3.7	7.2	0.15	3.7	7.2	0.23	7.2	7.2
3x10 ⁶	0.11	1	3.7	0.14	1	3.7	0.24	1	3.7
4.3x10 ⁶	0.16	1	1.9	0.19	1	1.9	0.21	1.9	1.9

Figure S65: Example of the impact of the scaling factor ($F_{organuc}$) of organics and OH in RIC scheme and case study sd477 (ATom 2, 2017-02-04, 02:56:31-02:57:30 UTC). OH at solar zenith angle of 0° was set to 1 (a,b,c), 3 (d,e,f) and 4.3×10^6 cm⁻³ (g,h,i) time since convective influence 10.5 hrs and best normalized mean error (NME) between the modeled and measured size distribution: (a,d,g) at $F_{organuc}=1$, (b,e,h) at $F_{organuc}=0.5$, (c,f,i) at $F_{organuc}=0.1$. $F_{organuc}$ represents the fraction of the condensable organic, labeled *BioOxOrg*, that may participate in nucleation by stabilizing the cluster. The color of the circles indicates the value of NME; grey circles indicate NME > 1. Varying $F_{organuc}$ does not change results significantly. The NME best stays best for same initial mixing ratios of SO₂ and organics.

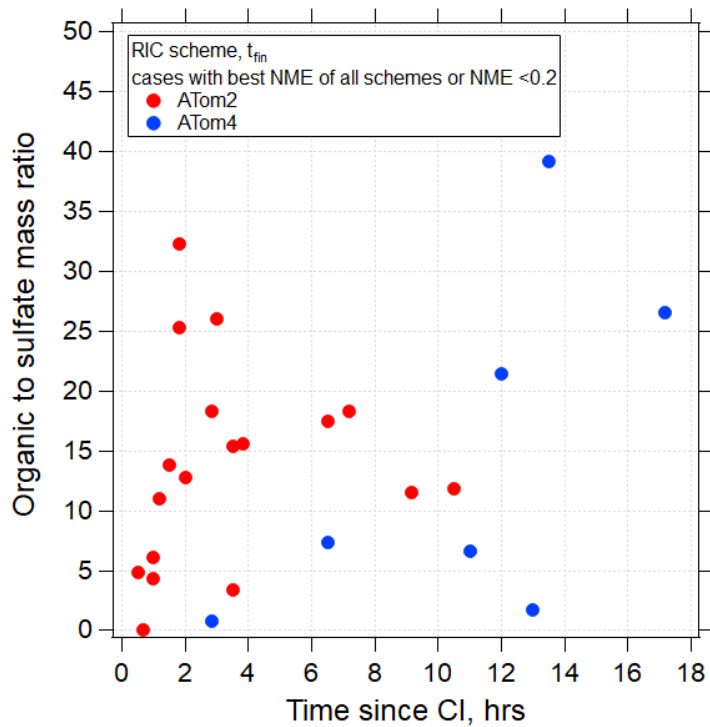


Figure S66: The simulated organic and sulfate mass ratio for particles with diameters below 12 nm for ATom-2 and -4 at the point of measurement by the aircraft (t_{fin}) is plotted to the time since convective influence (CI). TOMAS simulations were performed using RIC scheme. A comparison of the production rate of organics to sulfate suggests that the composition of small particles might be dominated by organics rather than sulfate.

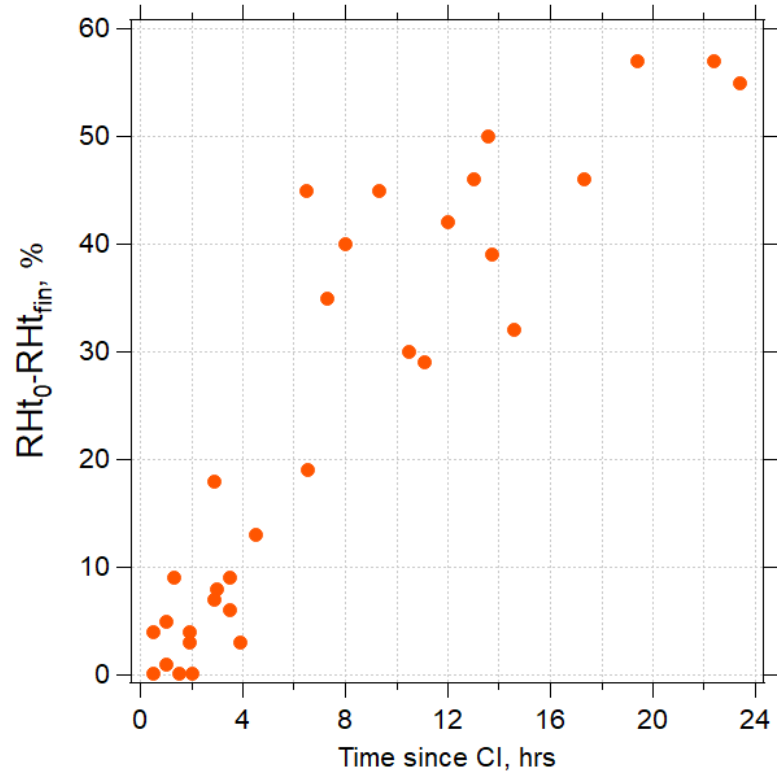


Fig.S67. The difference in (RH) along the trajectory between the trajectory location at the cloud edge (t_0) and the point of the aircraft location (t_{fin}) for 32 simulated cases.

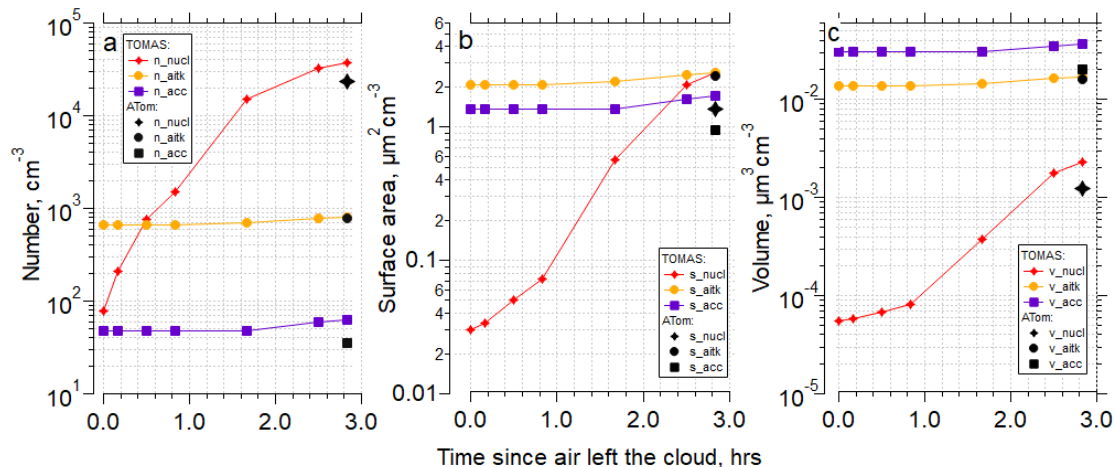


Figure S68: as in Fig. 7 but for case 461 (NME=0.08). Measured on ATom aerosol surface area is dominated by the Aitken mode (b). Initial $\text{SO}_2=1.6$ pptv, and initial organics=23.4 pptv.

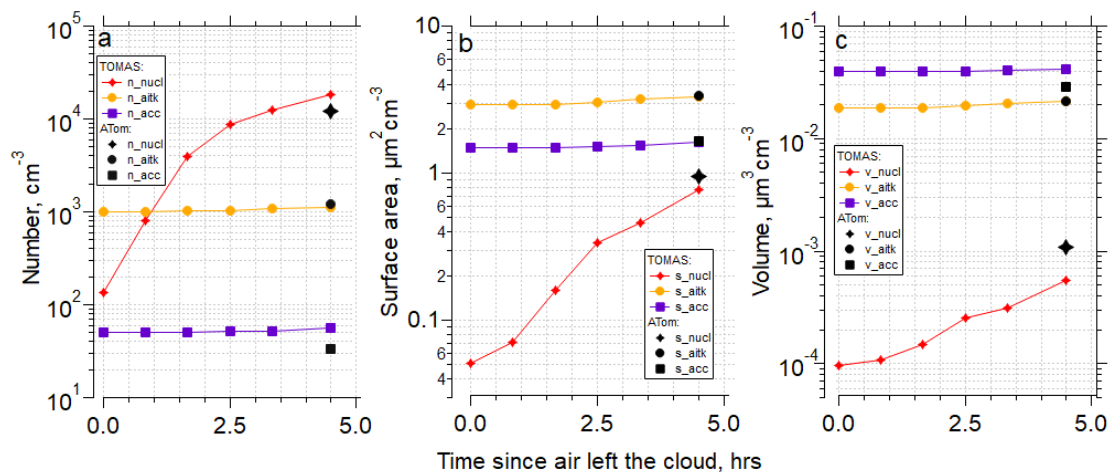


Figure S69: as in Fig. 7 above but for case 470 (NME=0.28). Measured on ATom aerosol surface area is dominated by the Aitken mode (b). Initial $\text{SO}_2=1$ pptv, and initial organics=3.4 pptv.

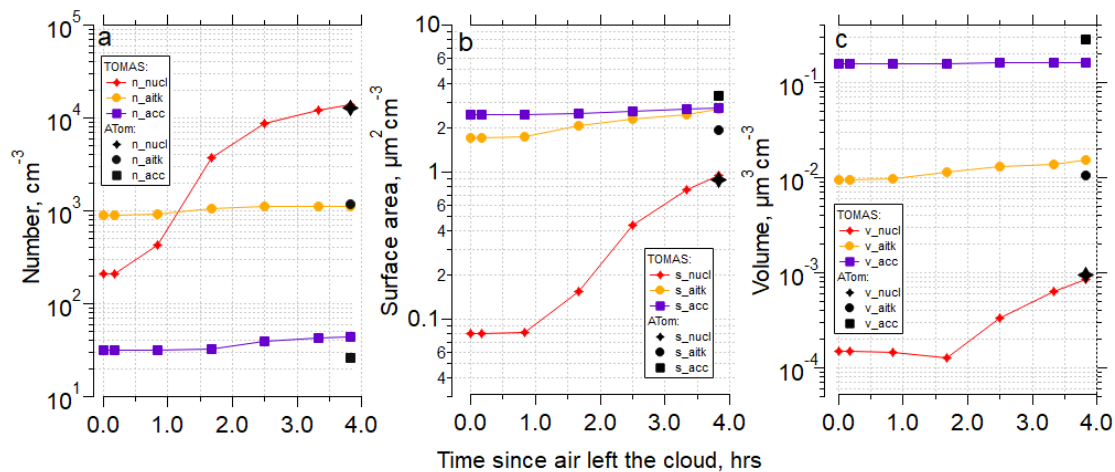


Figure S70: as in Fig. 7 but for case 530 (NME=0.13). Aerosol surface area measured on ATom is dominated by the accumulation mode (b). Initial $\text{SO}_2=1$ pptv, and initial organics=7 pptv.

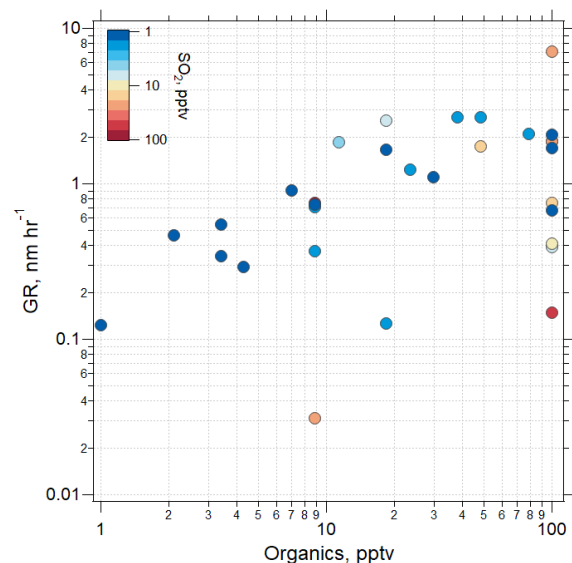


Figure S71. Growth rates calculated for simulations with SO₂ that have the lowest (best) NME for each case (32 cases in total) studied using RIC scheme. Calculation is based on the diameter of the leading edge and threshold value of $dN/d\log_{10}D_p > 10 \text{ cm}^{-3}$ in any of the size bins below 12 nm.

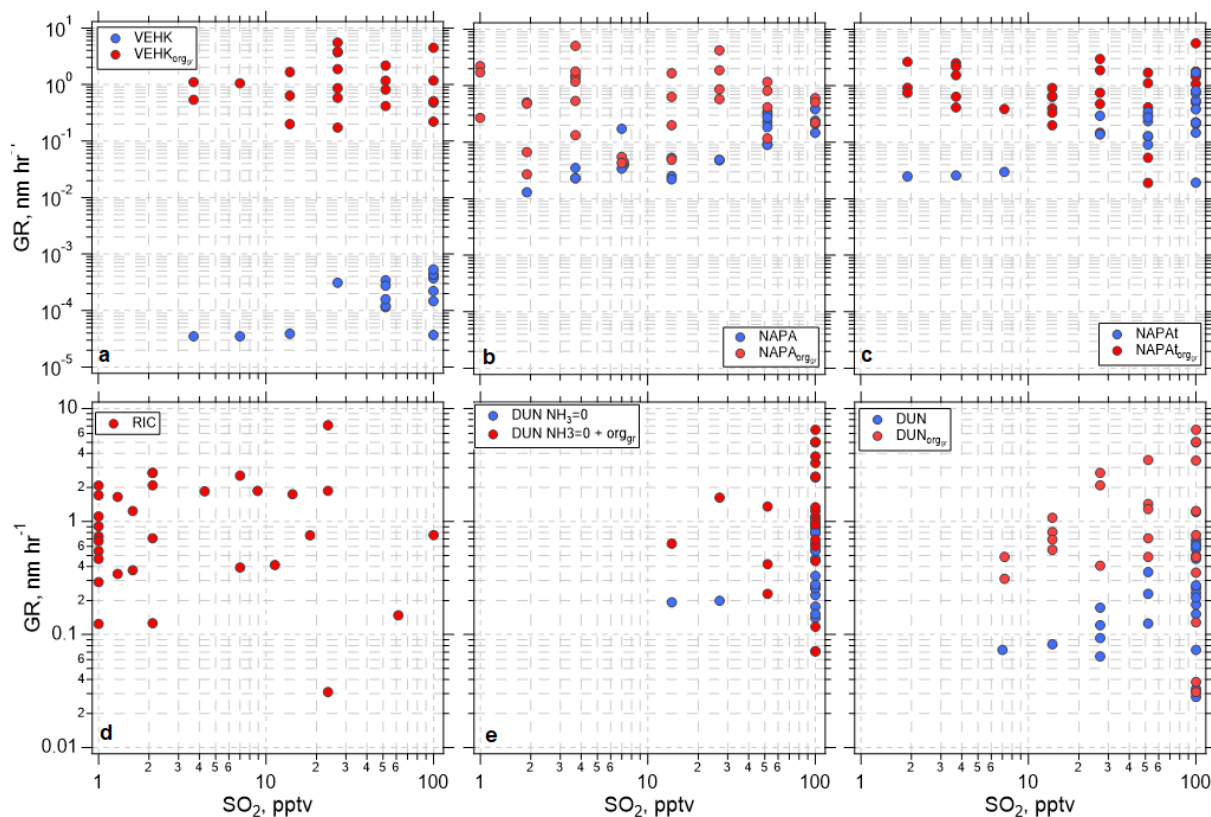


Figure S72. Growth rates calculated for the leading-edge diameter and threshold of $dN/d\log_{10}D_p > 10 \text{ cm}^{-3}$ in any of the size bins below 12 nm, for simulations with SO₂ that have the lowest (best) NME in (a) VEHK and with added organics for the initial growth of the particles, (b) NAPA and with added organics, (c) NAPAt and with added organics, (d) RIC, (e) DUN NH₃=0 and with organics added for initial growth, and (f) DUN and with organics added. Note different y-axis ranges in (a,b,c) and (d,e,f). Blue and red symbols represent simulations without and with organics added for initial growth of the particles, respectively. The RIC scheme is the only one here that includes organics both in the particle nucleation and growth.

References

- Clegg, S. L., Rard, J. A., and Pitzer, K. S.: Thermodynamic properties of 0–6 mol kg⁻¹ aqueous sulfuric acid from 273.15 to 328.15 K, *J. Chem. Soc., Faraday Trans.*, 90, 1875–1894, doi:10.1039/FT9949001875, 1994.
- Curtius J., Froyd, K.D., Lovejoy, E.R., Cluster ion thermal decomposition (I): Experimental kinetics study and ab initio calculations for HSO₄-(H₂SO₄)_x(HNO₃)_y, *J. Phys. Chem. A*, 105, 48, 10867-10873, 2001.
- Dunne, E. M., Gordon, H., Kürten, A., Almeida, J., Duplissy, J., Williamson, C., Ortega, I. K., Pringle, K. J., Adamov, A., Baltensperger, U., Barmet, P., Benduhn, F., Bianchi, F., Breitenlechner, M., Clarke, A., Curtius, J., Dommen, J., Donahue, N. M., Ehrhart, S., Flagan, R. C., Franchin, A., Guida, R., Hakala, J., Hansel, A., Heinritzi, M., Jokinen, T., Kangasluoma, J., Kirkby, J., Kulmala, M., Kupc, A., Lawler, M. J., Lehtipalo, K., Makhmutov, V., Mann, G., Mathot, S., Merikanto, J., Miettinen, P., Nenes, A., Onnela, A., Rap, A., Reddington, C. L. S., Riccobono, F., Richards, N. A. D., Rissanen, M. P., Rondo, L., Sarnela, N., Schobesberger, S., Sengupta, K., Simon, M., Sipilä, M., Smith, J. N., Stozkhov, Y., Tomé, A., Tröstl, J., Wagner, P. E., Wimmer, D., Winkler, P. M., Worsnop, D. R., and Carslaw, K. S.: Global atmospheric particle formation from CERN CLOUD measurements, *Science*, 354, 1119-1124, 10.1126/science.aaf2649, 2016.
- Froyd, K. D. and Lovejoy, E. R.: Experimental thermodynamics of cluster ions composed of H₂SO₄ and H₂O. 1. Positive Ions, *J. Phys. Chem. A*, 107, 9800–9811, 2003.
- Gao, R. S., Rosenlof, K. H., Fahey, D. W., Wennberg, P. O., Hintsä, E. J., and Hanisco, T. F.: OH in the tropical upper troposphere and its relationships to solar radiation and reactive nitrogen, *J. Atmos. Chem.*, 71, 55-64, 10.1007/s10874-014-9280-2, 2014.
- Giauque, W. F., Hornung, E. W., Kunzler, J. E., and Rubin, T. T.: The thermodynamic properties of aqueous sulfuric acid solutions and hydrates from 15 to 300 K, *Am. Chem. Soc. J.*, 82, 62–70, 1960.
- Hanson, D., and Lovejoy, E. R., Measurement of the thermodynamics of the hydrated dimer and trimer of sulfuric acid. *J. Phys. Chem. A*, 110, 9525-9528. doi:10.1021/jp062844w, 2006.
- Hodshire, A. L., Bian, Q., Ramnarine, E., Lonsdale, C. R., Alvarado, M. J., Kreidenweis, S. M., et al. (2019). More than emissions and chemistry: Fire size, dilution, and background aerosol also greatly influence near-field biomass burning aerosol aging. *J. Geophys. Res.: Atmos.*, 124, 5589–5611. <https://doi.org/10.1029/2018JD029674>, 2019.
- Kazil, J., and Lovejoy, E. R.: A semi-analytical method for calculating rates of new sulfate aerosol formation from the gas phase, *Atmos. Chem. Phys.*, 7, 3447-3459, 10.5194/acp-7-3447-2007, 2007.
- Lovejoy, E. R., Hanson, D. R., and Huey, L. G.: Kinetics and products of the gas-phase reaction of SO₃ with water, *J. Phys. Chem.*, 100, 19 911–19 916, doi:10.1021/jp962414d, 1996.
- Lovejoy, E. R., and J. Curtius, Cluster ion thermal decomposition (II): Master equation modeling in the low-pressure limit and fall-off regions—Bond energies for HSO₄(H₂SO₄)_x(HNO₃)_y, *J. Phys. Chem. A*, 105, 10,874–10,883, 2001.
- Lovejoy, E. R., Curtius, J., and Froyd, K. D.: Atmospheric ion-induced nucleation of sulfuric acid and water, *J. Geophys. Res.*, 109, 10.1029/2003jd004460, 2004.
- Napari, I., Noppel, M., Vehkamäki, H., and Kulmala, M.: Parametrization of ternary nucleation rates for H₂SO₄-NH₃-H₂O vapors, *J. Geophys. Res.*, 107, AAC 6-1-AAC 6-6, 10.1029/2002jd002132, 2002.
- O'Brien, K., The theory of cosmic-ray and high-energy solar-particle transport in the atmosphere, in *Proceedings of the 7th International Symposium on the Natural Radiation Environment*, edited by J. P. McLaughlin, S. E. Simopoulos, and F. Steinhusler, pp. 29–44, Elsevier, New York, 2005.

- Riccobono, F., Schobesberger, S., Scott, C. E., Dommen, J., Ortega, I. K., Rondo, L., Almeida, J., Amorim, A., Bianchi, F., Breitenlechner, M., David, A., Downard, A., Dunne, E. M., Duplissy, J., Ehrhart, S., Flagan, R. C., Franchin, A., Hansel, A., Junninen, H., Kajos, M., Keskinen, H., Kupc, A., Kürten, A., Kvashin, A. N., Laaksonen, A., Lehtipalo, K., Makhmutov, V., Mathot, S., Nieminen, T., Onnela, A., Petäjä, T., Praplan, A. P., Santos, F. D., Schallhart, S., Seinfeld, J. H., Sipilä, M., Spracklen, D. V., Stozhkov, Y., Stratmann, F., Tomé, A., Tsagkogeorgas, G., Vaattovaara, P., Viisanen, Y., Vrtala, A., Wagner, P. E., Weingartner, E., Wex, H., Wimmer, D., Carslaw, K. S., Curtius, J., Donahue, N. M., Kirkby, J., Kulmala, M., Worsnop, D. R., and Baltensperger, U.: Oxidation products of biogenic emissions contribute to nucleation of atmospheric particles, *Science*, 344, 717-721, 10.1126/science.1243527, 2014.
- Seinfeld, J. H., and Pandis, S. N.: *Atmospheric Chemistry and Physics: From Air Pollution to Climate Change*, (Wiley, 1998), 2006.
- Stevens, B., G. Feingold, W. R. Cotton, and R. L. Walko, 1996: Elements of the microphysical structure of numerically simulated nonprecipitating stratocumulus. *J. Atmos. Sci.*, 53, 980–1006, [https://doi.org/10.1175/1520-0469\(1996\)053<0980:EOTMSO>2.0.CO;2](https://doi.org/10.1175/1520-0469(1996)053<0980:EOTMSO>2.0.CO;2).
- Vehkamäki, H., Kulmala, M., Napari, I., Lehtinen, K. E. J., Timmreck, C., Noppel, M., and Laaksonen, A.: An improved parameterization for sulfuric acid–water nucleation rates for tropospheric and stratospheric conditions, *J. Geophys. Res.*, 107, AAC 3-1-AAC 3-10, 10.1029/2002jd002184, 2002.
- Weigel, R., Borrmann, S., Kazil, J., Minikin, A., Stohl, A., Wilson, J. C., Reeves, J. M., Kunkel, D., de Reus, M., Frey, W., Lovejoy, E. R., Volk, C. M., Viciani, S., D'Amato, F., Schiller, C., Peter, T., Schlager, H., Cairo, F., Law, K. S., Shur, G. N., Belyaev, G. V., and Curtius, J.: In situ observations of new particle formation in the tropical upper troposphere: the role of clouds and the nucleation mechanism, *Atmos. Chem. Phys.*, 11, 9983-10010, 10.5194/acp-11-9983-2011, 2011.
- Williamson, C. J., Kupc, A., Axisa, D., Bilsback, K. R., Bui, T., Campuzano-Jost, P., Dollner, M., Froyd, K. D., Hodshire, A. L., Jimenez, J. L., Kodros, J. K., Luo, G., Murphy, D. M., Nault, B. A., Ray, E. A., Weinzierl, B., Wilson, J. C., Yu, F., Yu, P., Pierce, J. R., and Brock, C. A.: A large source of cloud condensation nuclei from new particle formation in the tropics, *Nature*, 574, 399-403, 10.1038/s41586-019-1638-9, 2019.
- Yu, F., Luo, G., Nadykto, A. B., and Herb, J.: Impact of temperature dependence on the possible contribution of organics to new particle formation in the atmosphere, *Atmos. Chem. Phys.*, 17, 4997-5005, 10.5194/acp-17-4997-2017, 2017.